



Universität Hamburg

**Regeneration in peripheral and central nervous systems
after injury and application of glycomimetics
- Study in *Mus musculus* (Linnaeus, 1758) -**

**Dissertation
zur Erlangung des Grades eines Doktors der
Naturwissenschaften
- Dr. rer. nat. -**

**dem Department Biologie der Fakultät für Mathematik,
Informatik und Naturwissenschaften an der Universität
Hamburg vorgelegt**

**von Ali Mehanna
aus Beirut**

Juli 2009

Genehmigt vom Department Biologie
der Fakultät für Mathematik, Informatik und Naturwissenschaften
an der Universität Hamburg
auf Antrag von Frau Professor Dr. M. SCHACHNER
Weiterer Gutachter der Dissertation:
Herr Professor Dr. K. WIESE
Tag der Disputation: 03. Juli 2009

Hamburg, den 19. Juni 2009



Professor Dr. Jörg Ganzhorn
Leiter des Departments Biologie



Universitätsklinikum
Hamburg-Eppendorf

Zentrum für Molekulare Neurobiologie Hamburg (ZMNH)

**Diese Arbeit wurde am Institut für Biosynthese Neuraler Strukturen des
Zentrums für Molekulare Neurobiologie Hamburg (ZMNH) angefertigt.**

**Gutachter der Dissertation: Pr. Dr. Melitta Schachner
Pr. Dr. Konrad Wiese**

**Gutachter der Disputation: Pr. Dr. med. Christian Hagel
Pr. Dr. Lothar Renwrantz**

Betreuer: Dr. Andrey Irintchev



University of Connecticut Health Center
School of Medicine

Department of Neuroscience

June 01, 2009

As a native English speaker I confirm that the PhD thesis of Ali Mehanna titled "Regeneration in peripheral and central nervous systems after injury and application of glycomimetics study in *Mus musculus*" is written in correct English grammar and comprehensible style.

Sincerely,

Nicole Mayer

A handwritten signature in black ink, appearing to read "Nicole Mayer", written over the printed name.

An Equal Opportunity Employer

263 Farmington Avenue
Farmington, Connecticut 06030-3401

Telephone: (860) 679-8787

Facsimile: (860) 679-8766

web: <http://neuroscience.uchc.edu/>

Table of contents

1. SUMMARY.....	1
2. ZUSAMMENFASSUNG.....	4
3. INTRODUCTION.....	7
3.1. Structure of the nervous system.....	7
3.2. Injury and regeneration of the nervous system.....	9
3.3. Glycans and their role in regeneration.....	13
3.4. Glycomimetics.....	16
4. MATERIALS AND METHODS.....	18
4.1. Glycomimetic peptides.....	18
4.2. Animals.....	19
4.3. Femoral nerve injury and glycomimetic application.....	19
4.4. Spinal cord injury and glycomimetic infusion.....	21
4.5. Analysis of motor function.....	24
4.5.1. Femoral nerve injury.....	25
4.5.2. Spinal cord injury.....	28
4.6. Retrograde labelling through the femoral nerve and evaluation of numbers and soma size of regenerated motoneurons.....	29
4.7. Analysis of the degree of axonal myelination in the femoral nerve.....	31
4.8. Schwann cell culture.....	32
4.9. Analysis of Schwann cell processes' length <i>in vitro</i>	33
4.10. Analysis of Schwann cell proliferation <i>in vitro</i>	34
4.11. Staining of live Schwann cells.....	35
4.12. Schwann cell proliferation <i>in vivo</i>	36
4.13. Sectioning of the injured spinal cord and immunohistochemistry.....	37
4.14. Motoneuron soma size and quantification of perisomatic terminals after spinal cord injury.....	38
4.15. Quantification of motoneurons in the lumbar spinal cord after spinal cord injury.....	39
4.16. Estimation of lesion scar volume and myelin volume in the lesioned spinal cord.....	40
4.17. Analysis of axonal myelination in the injured spinal cord.....	40
4.18. Statistical analysis.....	40
5. RESULTS.....	41
5.1. Effect of glycomimetics after femoral nerve injury.....	41
5.1.1. Cyclic HNK-1 mimetic improves regeneration and functional recovery.....	41
5.1.2. Linear PSA mimetic promotes functional recovery.....	43
5.1.3. The PSA mimetic does not influence precision of motor reinnervation and motoneuron survival.....	45
5.1.4. The PSA mimetic improves the quality of axonal regeneration.....	48

5.1.5. The PSA mimetic influences shape and proliferation of Schwann cells <i>in vitro</i>	50
5.1.6. The PSA mimetic enhances Schwann cell proliferation <i>in vivo</i>	56
5.2. Effect of glycomimetics after spinal cord injury.....	58
5.2.1. Delivery of peptides to the injured spinal cord.....	58
5.2.2. Improved motor recovery after immediate post-traumatic administration of a PSA mimetic.....	59
5.2.3. Enhanced catecholaminergic, cholinergic and glutamatergic innervation in the lumbar spinal cord after PSA treatment.....	63
5.2.4. PSA treatment enhances axonal myelination rostral to the site of injury...	70
5.2.5. The therapeutic time window of the PSA mimetic is limited to acute spinal cord injury.....	72
6. DISCUSSION.....	74
6.1. Effect of glycomimetics in the femoral injury.....	74
6.1.1. Improvement of motor function by PSA mimetic.....	74
6.1.2. Mode of PSA mimetic action.....	75
6.1.3. Possible molecular mechanisms underlying the glycomimetic effects on myelination.....	77
6.2. Effect of glycomimetics after spinal cord injury.....	79
6.2.1. Improved functional outcome after PSA mimetic treatment.....	79
6.2.2. Lack of functional effects after HNK-1 glycomimetic application.....	81
6.2.3. Therapeutic time-window of the PSA glycomimetic.....	82
6.3. Conclusions	83
7. References.....	85
8. Abbreviations.....	99
9. Acknowledgements.....	100

1. Summary

In adult mammals, regeneration after injury of the central nervous system is hindered by the abundance of molecules inhibiting axonal growth which severely restrict functional recovery. In contrast to the central nervous system, peripheral nerves regenerate after injury and this ability is attributed to the growth-permissive environment provided by Schwann cells and their basal lamina. Despite this regenerative potential, however, functional recovery is often limited.

Here we pursued to promote regeneration in two models of nervous system injuries in mice, femoral nerve transection and spinal cord compression, using peptides which functionally mimic polysialic acid (PSA) and human natural killer antigen-1 (HNK-1) glycan, carbohydrate epitopes on cell recognition molecules known to promote neurite outgrowth *in vitro*.

In the femoral nerve injury paradigm, functional HNK-1 or PSA mimicking peptides or a control peptide were applied in a polyethylene tube used to surgically reconnect the severed stumps of the femoral nerve before it bifurcates into the motor and sensory branches. Using video-based motion analysis to monitor motor recovery over a 3-month post-operative period, we observed a better functional outcome in the HNK-1 and PSA mimetic-treated than in control mice receiving a control peptide or phosphate buffered saline. Retrograde tracing of regenerated motoneurons and morphometric analyses showed that accuracy of reinnervation, motoneuron survival and motoneuron soma size were enhanced with the HNK-1 mimetic treatment but not with the PSA mimetic. However, the PSA mimetic enhances remyelination of the regenerated axons distal to the injury site, indicating that effects on Schwann cells in

the denervated nerve may underlie the improved motor recovery. In line with this notion was the observation that the PSA mimetic enhanced the elongation of Schwann cell processes and Schwann cell proliferation *in vitro*, when compared with the control peptide. Moreover, Schwann cell proliferation *in vivo* was enhanced in both motor and sensory branches of the femoral nerve by application of the PSA mimetic. These effects were likely mediated by NCAM through its interaction with the fibroblast growth factor receptor (FGFR) since they were not observed when the PSA mimetic was applied to NCAM-deficient Schwann cells, and since application of two different FGFR inhibitors reduced process elongation from Schwann cells *in vitro*.

In the spinal cord injury paradigm, subdural infusions were performed with an osmotic pump over a two-week time period after low thoracic compression injury in young adult C57BL/6J mice. When applied immediately after injury, the PSA mimetic and the combination of PSA and HNK-1 mimetics, but not the HNK-1 mimetic alone, improved functional recovery as assessed by locomotor rating and video-based motion analysis over a 6-week observation period. Better outcome in PSA mimetic treated mice was associated with increased, as compared with control mice, number of cholinergic terminals on lumbar motoneurons, higher numbers of glutamatergic terminals and monoaminergic axons in the lumbar spinal cord, and increased degree of axonal myelination proximal to the injury site. Scar formation, extent of de- and re-myelination and numbers of lumbar motoneurons were not affected by the PSA or HNK-1 mimetic treatment. In contrast to immediate post-traumatic application, the PSA mimetic treatment was ineffective when initiated 3 weeks after spinal cord injury.

Our results suggest that PSA and HNK-1 mimetic peptides can be efficient therapeutic tools to promote motor recovery after peripheral and central nervous systems injuries.

2. Zusammenfassung

In adulten Säugtieren wird die Regeneration nach Verletzung des zentralen Nervensystems durch das Vorhandensein von Molekülen, die das Auswachsen von Axonen inhibieren, stark eingeschränkt. Im Gegensatz zum zentralen Nervensystem ist das periphere Nervensystem in der Lage, nach Verletzung zu regenerieren. Diese Fähigkeit wird auf die wachstumsfördernden Eigenschaften der Umgebung zurückgeführt, die von den Schwannzellen und ihrer Basallamina bereitgestellt werden. Trotz dieses regenerativen Potentials des peripheren Nervensystems ist die funktionelle Regeneration meist unvollständig.

In dieser Arbeit wurden zwei verschiedene Modelle zur Untersuchung der Regeneration des Nervensystems herangezogen: 1.) die Verletzung des Femoralnervs und 2.) die Rückenmarksläsion.

Nach der Verletzung des Femoralnervs oder des Rückenmarks wurden an der Läsionsstelle lokal Peptide eingesetzt, die funktionell Polysialinsäure (PSA) und das „human natural killer cell antigen 1“ (HNK-1) mimikrieren. Hierbei handelt es sich um Kohlenhydrat-Epitope auf Zelladhäsionsmolekülen, welche das Neuritenwachstum *in vitro* stimulieren.

In Experimenten zur Regeneration des Femoralnervs wurde entweder funktionelles HNK-1 Peptid, PSA mimikrierendes Peptid oder ein Kontrollpeptid in ein Polyethylene-Röhrchen appliziert, welches die beiden Stümpfen des zuvor verletzten Femoralnervs verbindet. Die Verletzung des Femoralnervs erfolgte vor der Verzweigung des Nervs in den motorischen und sensorischen Ast. Es wurden auf Video-Aufzeichnungen basierende Bewegungsstudien an den operierten Mäusen

durchgeführt, mit deren Hilfe die Regeneration der Tiere anhand ihrer motorischen Fähigkeiten über einen Zeitraum von 3 Monaten post-operativ untersucht werden konnte. Diese Analysen zeigten, dass Mäuse, denen das HNK-1 und das PSA Mimetikum verabreicht wurde, wesentlich besser regenerierten als solche, die das Kontrollpeptid oder gepufferte Salzlösung erhielten. Retrograde Färbung der regenerierten Motoneurone und deren morphometrische Analysen zeigten, dass in der mit HNK-1 Mimetikum behandelten Gruppe im Vergleich zum PSA Mimetikum die korrekte Reinnervierung verbessert ist, das Überleben der Motoneurone erhöht ist und die Somata von Motoneuronen vergrößert sind. Obwohl das PSA-Mimetikum keinen Effekt auf die korrekte Reinnervierung hatte, wurde durch das PSA-Mimetikum die Remyelinisierung der regenerierten Axone distal zur Verletzung deutlich verbessert. Dies weist darauf hin, dass PSA einen Einfluß auf die Remyelinisierung durch Schwannzellen im durchtrennten Nerv hat. Diese Annahme konnte durch die Beobachtung gestützt werden, dass das PSA-Mimetikum verglichen mit dem Kontrollpeptid das Auswachsen von Schwannzell-Fortsätzen und die Schwannzell-Proliferation *in vitro* verstärkt. Darüber hinaus war die Schwannzell-Proliferation auch *in vivo* sowohl im motorischen als auch im sensorischen Teil des Femoralnervs durch das PSA-Mimetikum erhöht. Diese Effekte könnten möglicherweise durch das neurale Zelladhäsionsmolekül (NCAM) und seine Interaktion mit dem Fibroblasten-Wachstumsfaktor-Rezeptor (FGFR) vermittelt werden, da die Effekte ausblieben, wenn NCAM-defiziente Schwannzellen mit dem PSA Mimetikum behandelt werden. Darüber hinaus verminderte die Zugabe von FGFR-Inhibitoren *in vitro* die Elongation der Schwannzell-Fortsätze.

In den Experimenten zur Verletzung des Rückenmarks wurde das Rückenmark junger adulter C57BL/6J Mäuse auf der Höhe der unteren Brustwirbel durch Kompression verletzt und Peptide über einen Zeitraum von zwei Wochen mittels einer osmotischen Pumpe subdural zugeführt. Über einen Zeitraum von 6 Wochen wurde die funktionelle Regeneration mittels Beobachtungen des Laufverhaltens und über auf Video-Aufnahmen basierenden Bewegungsanalysen determiniert. Wenn das PSA Mimetikum oder die Kombination aus PSA und HNK-1 Mimetikum direkt nach der Verletzung appliziert wurden, konnten diese einen positiven Effekt auf die funktionelle Regeneration ausüben. Das HNK-1 Mimetikum alleine vermittelte diesen Effekt nicht. Verglichen mit Kontrolltieren wiesen PSA Peptid behandelte Tiere eine erhöhte Anzahl von cholinergen Endungen der lumbalen Motoneurone, eine erhöhte Anzahl der glutamatergen Endungen und der monoaminergen Axone im lumbalen Rückenmark, sowie eine erhöhte Rate axonaler Myelinisierung proximal zur Verletzungsstelle auf. Die Narbenbildung, das Ausmaß an De- und Remyelinisierung und die Anzahl der lumbalen Motoneurone wurden durch die Zugabe des PSA oder HNK-1 Mimetikums nicht beeinflusst. Im Gegensatz zur Applikation direkt nach der Verletzung, hatte das PSA Mimetikum drei Wochen nach der Rückenmarksverletzung keinen Effekt. Diese Ergebnisse deuten darauf hin, dass das PSA und das HNK-1 Mimetikum ein effizientes therapeutisches Hilfsmittel sind, welches positiv auf die funktionelle Regeneration nach Verletzung des peripheren als auch des zentralen Nervensystems wirkt.

3. Introduction

3.1. Structure of the nervous system

The **nervous system** is a network of specialized cells that communicate information about an animal's surroundings and itself. It processes this information and causes reactions in other parts of the body. It is composed of neurons and other specialized cells called glia, that aid in the function of the neurons. The nervous system is divided broadly into two categories: the central nervous system which includes the brain and the spinal cord, and the peripheral nervous system which includes the somatic and autonomic nervous systems (Columbia Encyclopedia, 2003).

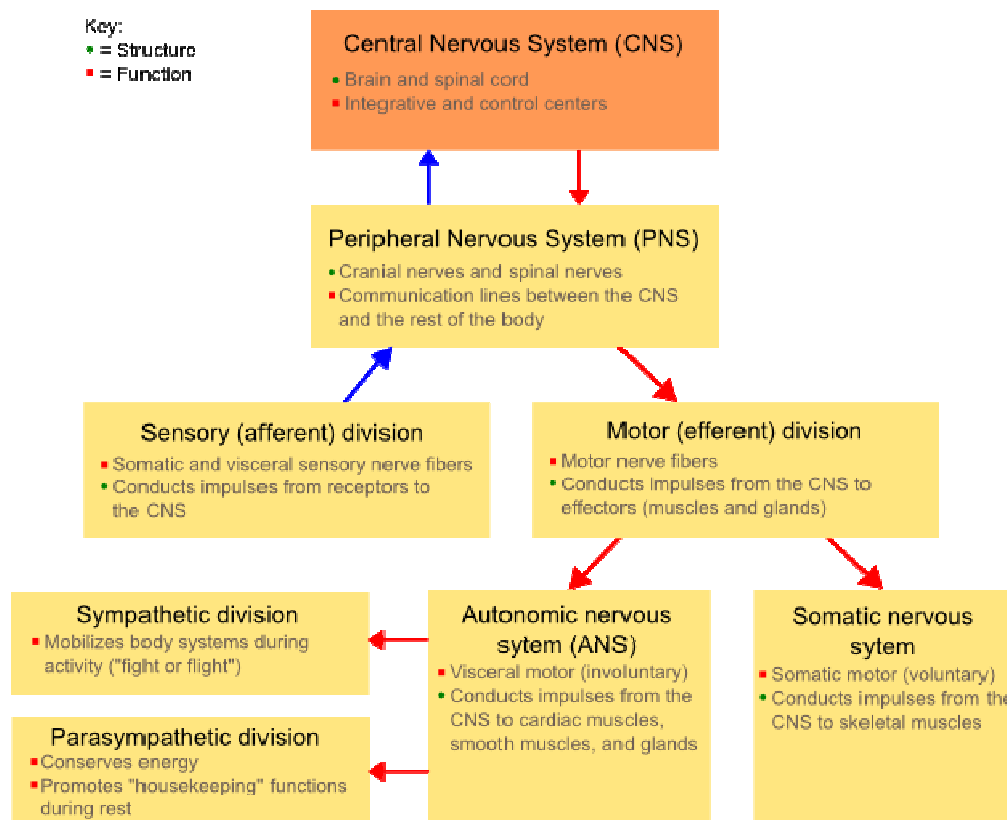
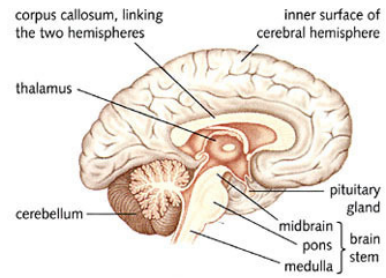
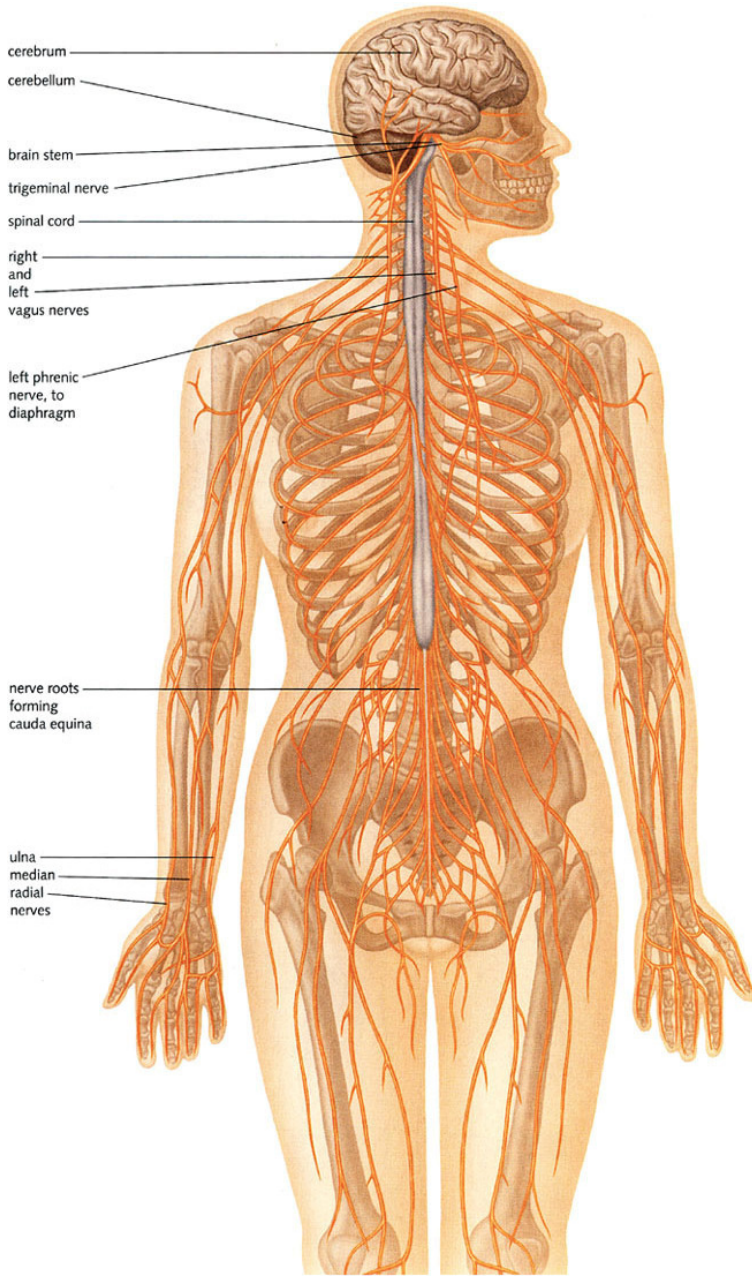
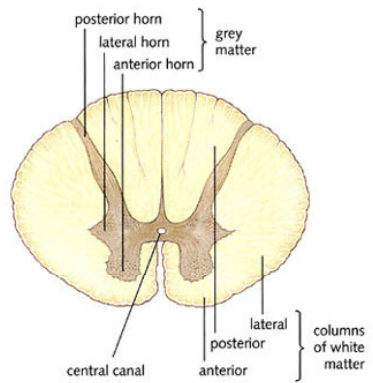


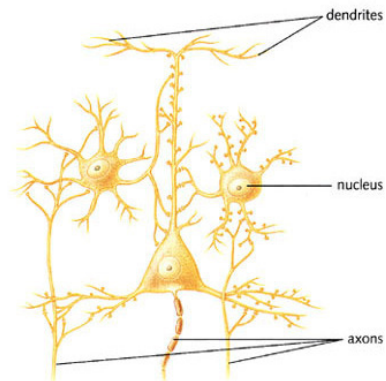
Figure 1: The major divisions of the nervous system (from Wikipedia, the free encyclopedia; based on Elaine Marieb's Human Anatomy & Physiology, 7th ed. New York; Pearson 2007).



Midline section of the brain.



Section of the spinal cord in the thoracic region.



Nerve cells.

The brain and spinal cord (central nervous system) and nerves connected to them (peripheral nervous system).

Figure 2: The central nervous system (CNS) is composed of the brain and the spinal cord, from which peripheral nerves emerge and connect the CNS to sensory receptors, muscles, glands and organs (from Wikipedia, the free encyclopedia; Laurence Garey).

3.2. Injury and regeneration of the nervous system

Injury to the nervous system results in degeneration of axons and nerve cells and loss of function. The response to injury and the ability to regenerate differ between central and peripheral nervous systems.

In the adult mammalian **central nervous system**, severed axons do not regenerate (Ramón y Cajal, 1928). Traumatic injuries lead, in addition to direct and immediate tissue damage, to ischemia and excitotoxic neuronal death (Figure 3). Within several weeks, macrophages clear the tissue debris resulting in fluid-filled cysts (Schwab, 2002). Glial cells, namely astrocytes, proliferate and release chondroitin sulphate proteoglycans (CSPG) constituting a cellular and molecular barrier for regeneration (Fawcett, 2006).

Other molecules derived from myelin as for instance NogoA, myelin-associated glycoprotein (MAG), Oligodendrocyte myelin glycoprotein (OMgp) and semaphorin4D, contribute to the regeneration failure (Schwab, 2002; Fawcett, 2006; Loers and Schachner, 2007). Overcoming the inhibitory cues and enhancing the conducive ones is an important aim in promoting functional recovery after spinal cord lesion in adult mammals including humans. Experimental studies aiming to improve regeneration after spinal cord injury have used different approaches like cellular bridges (Bunge, 2001), injecting drugs like methylprednisolone (Liu WL et al., 2008) or enzymes like chondroitinase ABC (Garcia-alías et al., 2008), transplanting stem cells (Coutts et al., 2008), injecting growth factors (Lu and Tuszynski, 2008), transplanting Schwann cell or injecting virus that overexpress polysialic acid (Papastefanaki et al., 2007; Zhang et al., 2007).

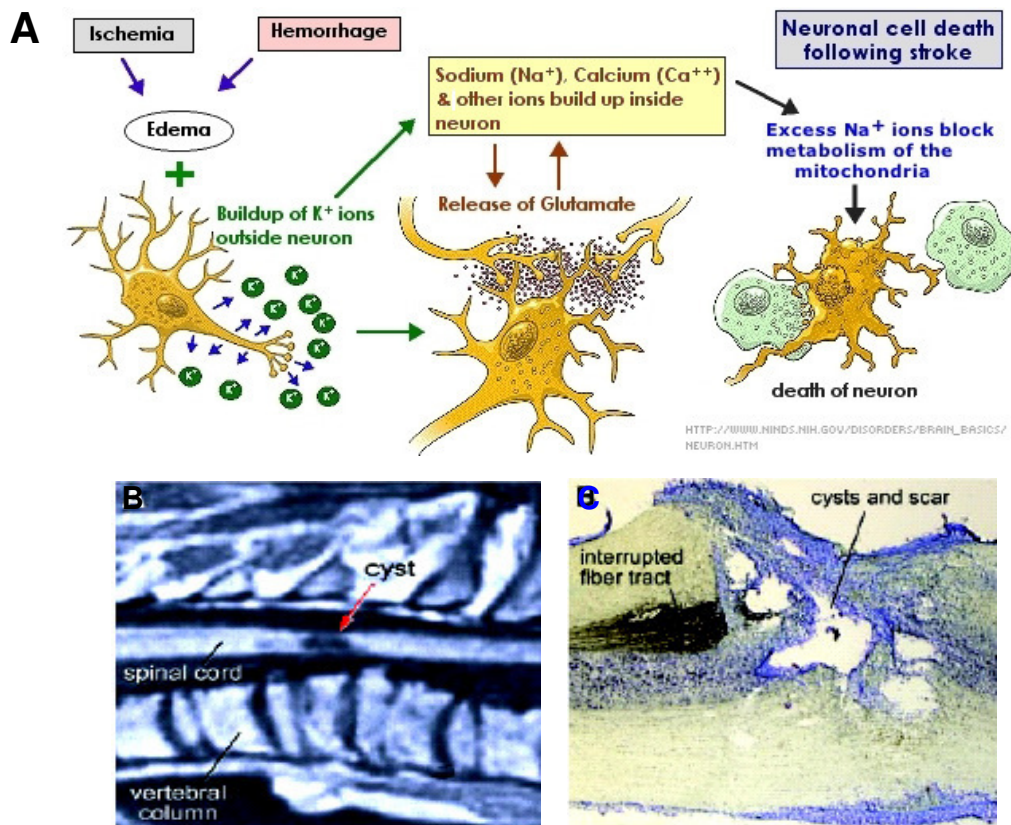


Figure 3: (A) Injury to the central nervous system leads to hemorrhage and ischemia. Lack of oxygen affects the cellular metabolism and results in loss of ionic equilibrium, which provokes excess release of glutamate and cell death by excitotoxicity. (B) Macrophages clear cell debris resulting in cysts formation. (C) Scar formation constitutes a cellular and molecular barrier for regenerating axons in the injured spinal cord (Figure A from the NINDS, National Institutes of Health; Figures B and C from Schwab, 2002).

Some researchers (Privat, 1995; Gimenez y Ribotta, 2002) propose that only a combination of 3 strategies at 3 chronological levels of postlesional intervention will be able to provide an optimal basis for successful therapeutic interventions improving functional recovery after spinal cord injury:

- 1) Neuroprotection soon after injury using pharmacological tools.
- 2) Promoting axonal regeneration by trophic factors and by acting on the glial scar.
- 3) Replacing neuronal loss by transplanting stem cells, genetically engineered cells or direct gene therapy.

Nerve fibres in the **peripheral nervous system** show a far greater capacity for regeneration than those in the central nervous system (Ide, 1996). After axonal injury, the neuron cell body becomes swollen (Figure 4) due to the activation of the nucleus and all other organelles in order to synthesize proteins necessary to reconstruct the cytoskeleton (Brunelli et al., 1990). In the proximal stump, the axons degenerate retrogradely as far as the first node of Ranvier. Within a few hours, each injured axons gives rise to several collaterals (sprouts) (Wong and Mattox, 1991). It has been proposed that this phenomenon helps maximizing the chances of each neuronal cell to reach its target organ (Terenghi, 1999). Many of these sprouts will die back later through collateral pruning (Brushart, 1993). In the distal stump, Wallerian degeneration (named after Augustus Volney Waller) starts and leads to degradation of axons and myelin, leaving behind dividing Schwann in basal lamina tubes that surrounded the original nerve fiber (Lubińska, 1977). These columns of Schwann cells surrounded by basal lamina are known as endoneurial tubes or bands of Büngner. The Schwann cell basal lamina contains molecules like laminin and fibronectin, which play a positive role in axon regeneration (Fawcett and Keynes, 1990). Despite this regenerative potential, functional recovery is often poor in both humans and laboratory animals (Fu and Gordon, 1997; Lee and Wolfe, 2000; Lundborg, 2003).

Different strategies that aim at improving the outcome of peripheral nerve injury have been tested in animal experiments, for example, electrical stimulation (Al-Majed et al., 2000a; Ahlborn et al., 2007), stem cell transplantation (Tohill and Terenghi, 2004), application of neurotrophic factors (Boyd and Gordon, 2003; Piquilloud et al., 2007),

application of antibodies against neurotrophic factors (Streppel et al., 2002) or mechanical stimulation of the target musculature (Angelov et al., 2007).

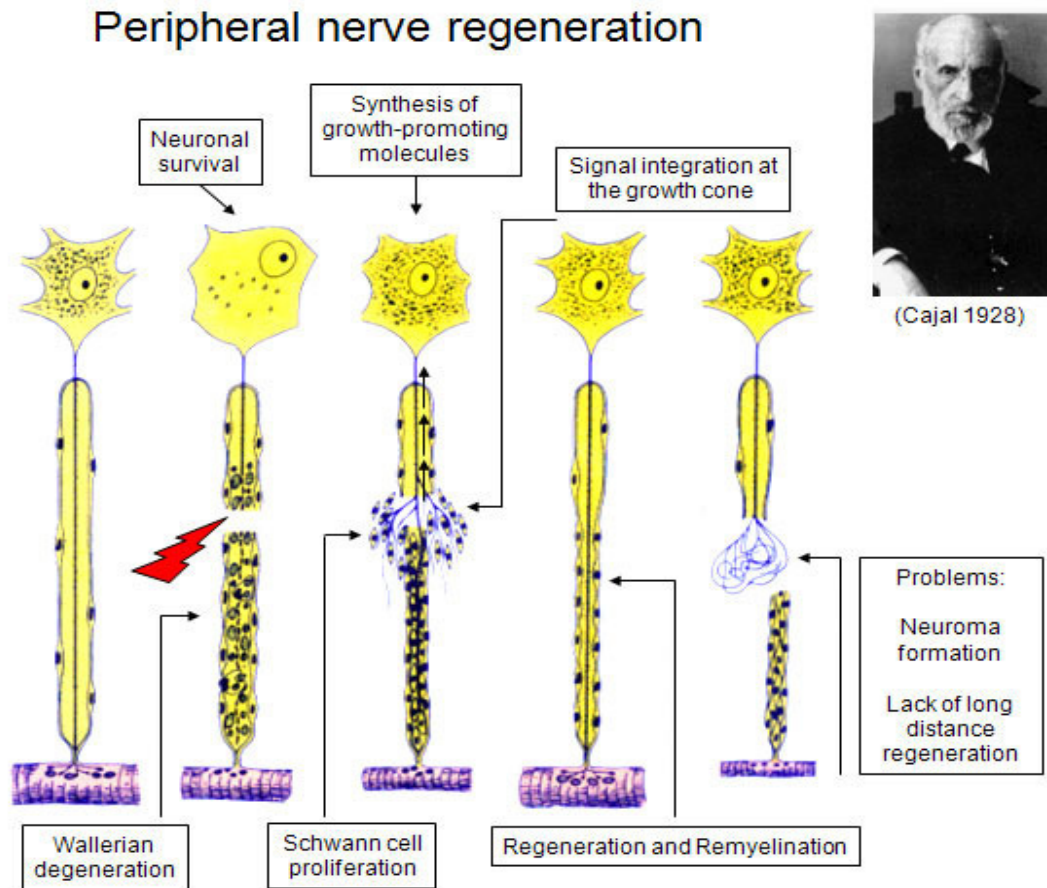


Figure 4: Injury to the peripheral nerve leads to morphological changes in the neuron, mainly swelling of the cell body and activation of the nucleus, the Golgi apparatus and the endoplasmic reticulum. Schwann cells proliferate and release neurotrophic factors contributing to axonal regeneration (Brunelli et al., 1990; Terenghi, 1999; Figure from the Division of Neuroanatomy, Innsbruck Medical University).

Despite enormous experimental efforts, efficient therapies for peripheral nerve and spinal cord injuries do not exist (Lundborg, 2003; Fawcett, 2006). An emerging approach to improve regeneration and functional outcome after injuries of the nervous system is the use of carbohydrates or their mimetic peptides, an approach to which this work was devoted.

3.3. Glycans and their role in regeneration

Glycans are chains of monosaccharides (single sugar molecules) that vary in length from a few sugars to several hundred. After the discovery of the DNA structure in 1953, biomedical research had focused on studying genes and their products (proteins), which gave rise to proteomics. However, proteomics does not describe post-translational modifications of proteins, e.g. glycosylation, which contribute decisively to their functionality (European science foundation, 2006). Nowadays, the importance of glycans for the nervous system has become better understood and widely recognized, as they are involved in development, regeneration, synaptic plasticity and diseases (Kleene and Schachner, 2004). We have been interested in the therapeutic potential of glycans for treatment of the nervous system injuries, since increasing evidence indicates that carbohydrates are of functional significance during neural repair (Kleene and Schachner, 2004; Eberhardt et al., 2006; Gravvanis et al., 2007; Papastefanaki et al., 2007). Two glycans have been chosen for our study: the human natural killer cell glycan (HNK-1), and the polysialic acid (PSA).

The **HNK-1** carbohydrate (3' sulfoglucuronyl β 1,3 galactoside) [Figure 5] is carried by different neural recognition molecules among them the myelin associated glycoprotein MAG, several laminin isoforms, amphoterin, the neural cell adhesion molecule (NCAM), L1, P0, and highly acidic glycolipids (Kruse et al., 1984, 1985; ffrench-Constant et al., 1986, Löw et al., 1994; Schachner and Martini, 1995; Kleene and Schachner, 2004). Interactions of the HNK-1 epitope with chondroitin sulfate proteoglycans enhance neuronal cell adhesion and neurite outgrowth (Miura et al., 1999). *In vivo*, HNK-1 has been associated with proper targeting of regenerating motor

axons (Martini et al., 1992; Brushart, 1993). This assumption is based on the observation that HNK-1 is upregulated specifically on the motor branch for at least 14 days after femoral nerve injury (Martini et al., 1992). Interestingly, application of HNK-1 glycomimetics (Bächle et al., 2006) has also been shown to promote PMR and functional recovery after peripheral nerve injury in adult mice (Simova et al., 2006).

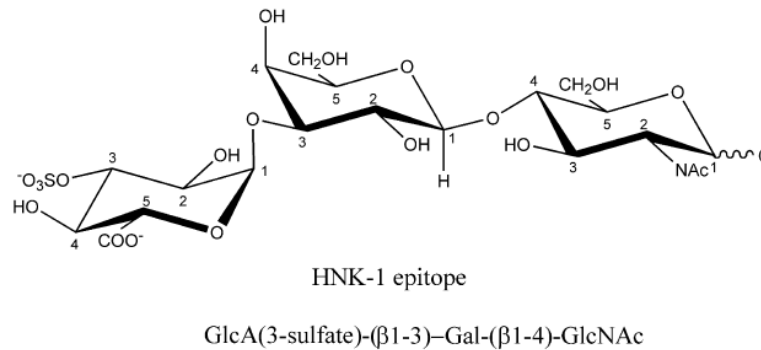


Figure 5: Structure of the HNK-1 epitope. SO_4 , sulfate; GlcA, glucuronic acid; Gal, galactose; GlcNAc, N-acetylglucosamine (Simon-Haldi et al., 2002).

PSA (α 2,8 polysialic acid) [Figure 6] is a unique glycan carried by the neural cell adhesion molecule (NCAM). NCAM exists in membrane-associated forms on neurons, glia and muscles, as well as in soluble forms in the cerebrospinal fluid (Bock et al., 1987; Olsen et al., 1993). Recently, it has been shown that neuropilin-2, a receptor for the semaphorin in neurons, is expressed on the surface of human dendritic cells and is also a PSA carrier (Curreli et al., 2007). PSA was first thought, considering its negative charges, to be an anti-adhesive molecule inhibiting NCAM function (Rutishauser et al., 1988). Later studies have shown that PSA is a positive rather than negative modulator of NCAM function, since removal of PSA from NCAM by endoneuraminidase (endo-N) was associated with an inhibition of NCAM function as

for instance inhibition of long-term potentiation (LTP), reduction of axonal growth and of intramuscular nerve branching (Doherty et al., 1990; Tang and Landmesser, 1993; Muller et al., 1996; Dityatev et al., 2004). Expressed abundantly during embryonic development, PSA is considered to be essential for neuronal and glial cell migration (Yamamoto et al., 2000; Durbec and Cremer, 2001). This expression decreases in adulthood and persists only in structures that display a high degree of functional plasticity (Rutishauser and Landmesser, 1996; Rutishauser, 2008). Interestingly, PSA is upregulated after various types of central and peripheral nervous system lesion (Covault et al., 1986; Olsen et al., 1995; Carratù et al., 1996; Rutishauser and Landmesser, 1996), and overexpression of PSA by lesion scar astrocytes or transplantation of PSA-overexpressing Schwann cells improves regeneration after spinal cord injury (El Maarouf et al., 2006; Papastefanaki et al., 2007; Zhang et al., 2007).

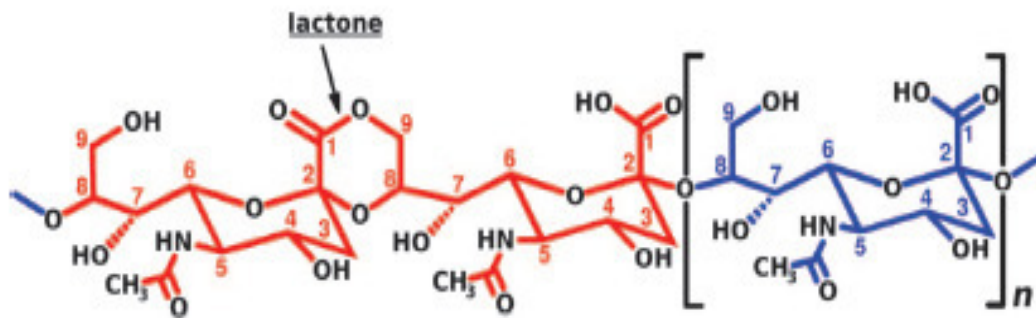


Figure 6: Chemical structure of PSA (poly- $\alpha(2 \rightarrow 8)\text{Neu5Ac}$). The numbers identify carbon positions, and n can reach 200. Blue and red are used to differentiate the two possible forms the linkage can take. At neutral pH, most $\alpha(2 \rightarrow 8)$ linkages are like the blue one, resulting in a highly flexible linear molecule. At low pH, the number of lactones increases, resulting in a rigidified structure (Azurmendi et al., 2007).

3.4. Glycomimetics

Carbohydrates are not very abundant in natural sources, and are difficult to synthesize in sufficient amount for experimental use. As a substitute, phage display techniques have been used in order to isolate peptides that functionally and/or structurally mimic the glycan of interest, and thus the name glycomimetics (Simon-Haldi et al., 2002). Mimic peptides (Figure 7) provide an elegant alternative for interfering with the interaction between complex carbohydrates and their receptors (Bächle et al., 2006).

In this study we examined whether PSA and HNK-1 mimetics, applied in two different injury models in mice (femoral nerve and spinal cord injury), would improve the functional outcome. The HNK-1 and PSA mimetics used have been well characterized. They bind with high affinity to the antibodies 412 and 735, specific antibodies against HNK-1 and PSA glycans, respectively, and promote, similar to the endogenous epitopes, axonal growth and cell survival *in vitro* (Bächle et al., 2006; Mehanna et al., 2009). After femoral nerve injury, HNK-1 and PSA mimetics enhance recovery by different modes of action. HNK-1 seems to affect motoneuron survival and precision of reinnervation (Simova et al., 2006), while PSA appears to be beneficial for remyelination (present study). In the spinal cord, we found beneficial effects for the PSA mimetic but not for the HNK-1. PSA mimetic enhances plasticity in the lumbar spinal cord, and thus functional recovery, when applied immediately after compression injury, but not when infusion was initiated in the chronic phase, at 3 weeks after injury.

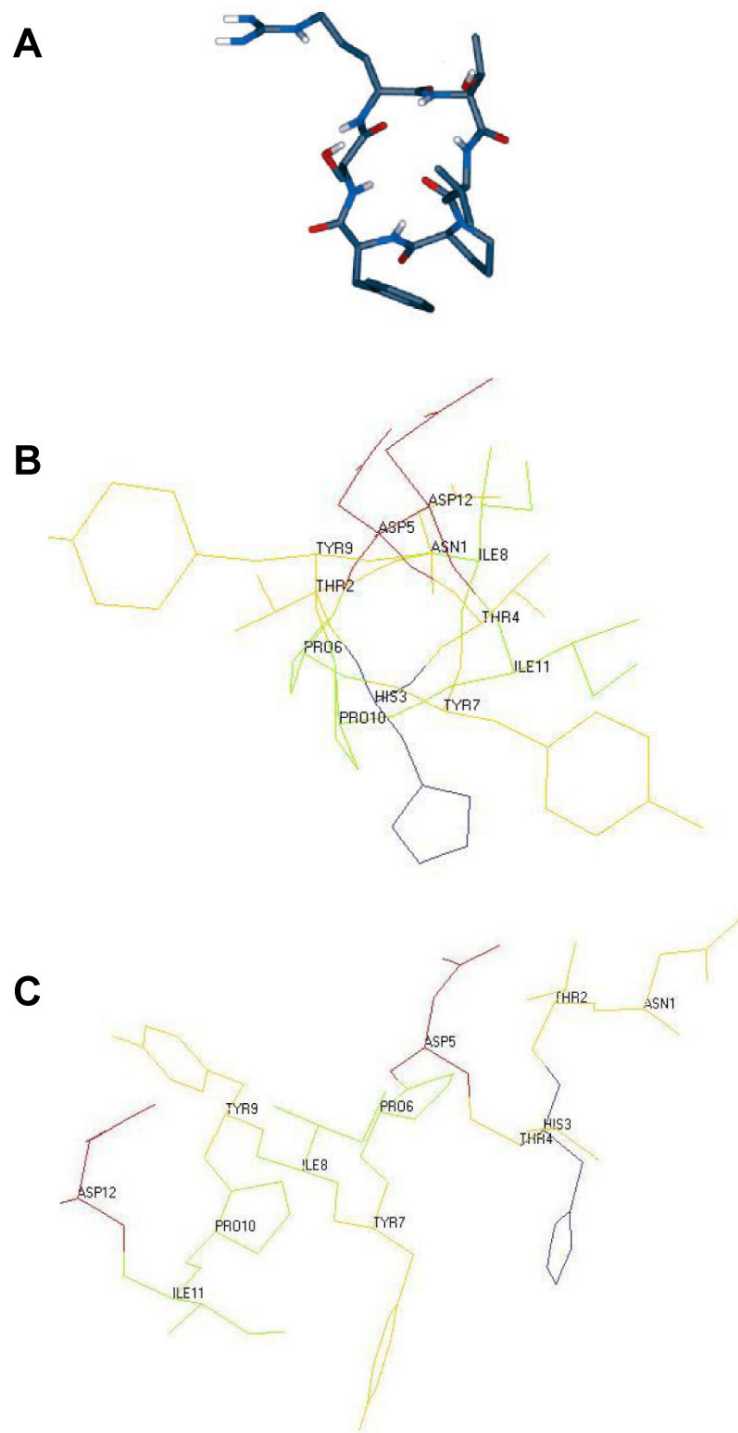


Figure 7: (A) Solution conformation of the HNK-1 mimetic *c*-(RTLPFPS) in $[D_6]DMSO$, major conformer. Blue N, red O, white H, and gray C. (B) Molecular modeled theoretical helical structure of the PSA mimetic on top view and (C) in side view. Acidic amino acids (aa): red, basic aa: blue, polar aa: yellow and non-polar aa: green (Bächle et al., 2006; Kurschat, 2006).

4. Materials and Methods

4.1. Glycomimetic peptides

Two glycomimetics were used in both the peripheral and the central nervous system injury models: the cyclic HNK-1 mimetic [sequence c-(RTL PFS), Bächle et al., 2006; Simova et al., 2006] and the linear PSA mimetic [sequence H-NTHTDPYIYPID-OH] (Mehanna et al., 2009).

The cyclic HNK-1 mimetic is derived from a linear peptide [sequence TFQLSTR TLPFS] discovered in phage display studies as a functional mimetic of the HNK-1 oligosaccharide (Simon-Haldi et al., 2002; Bächle et al., 2006). The cyclic hexapeptide shows a higher binding affinity to the HNK-1 specific antibody 412 when compared to the original linear peptide (Bächle et al., 2006; Simova et al., 2006). Moreover, survival and neurite outgrowth of murine and human motoneurons is enhanced by the HNK-1 mimetic *in vitro* (Bächle et al., 2006). A modified configuration of this peptide with the sequence c-(RtLPFS) was used as a control (scrambled peptide, SCR).

The linear PSA mimetic was also discovered in a phage display study as a functional mimetic of the PSA glycan (Kurschat, 2006). A neutral peptide with the sequence H-DSPLVPFIDFHPC-OH, served in many experiments as a control peptide (CON). A scrambled version of the PSA mimetic with the sequence H-TNYDITPPHDIYC-OH was used in some experiments as a second control.

Finally, a cyclic PSA mimetic peptide (sequence H-CSSVTAWTTGCG-NH₂, peptide1 in Torregrossa et al., 2004) was also tested in some *in vivo* and *in vitro* experiments, in order to have a double proof about the efficiency of PSA mimetics.

4.2. Animals

C57BL/6J female mice at the age of 3-4 months were obtained from the central animal facility of the Universitätsklinikum Hamburg-Eppendorf. Animals were kept under standard laboratory conditions. All experiments were conducted in accordance with the German and European Community laws on protection of experimental animals. The procedures used were approved by the responsible committee of The State of Hamburg. Numbers of animals studied in different experimental groups and at different time periods after surgery are given in the text and figures. All animal treatments, data acquisition and analyses were performed in a blinded fashion.

4.3. Femoral nerve injury and glycomimetic application

Animals were anaesthetized by intraperitoneal injections of 0.4 mg kg⁻¹ fentanyl (Fentanyl-Janssen, Janssen-Cilag GmbH, Neuss, Germany), 10 mg kg⁻¹ droperidol (Dehydrobenzperidol, OTL Pharma, Paris, France) and 5 mg kg⁻¹ diazepam (Ratiopharm, Ulm, Germany). The right femoral nerve was exposed and nerve transection performed at a distance of approximately 3 mm proximal to the bifurcation of the nerve into motor and sensory branches (Figure 8A, B). A polyethylene tubing (3 mm length, 0.58 mm inner diameter; Becton Dickinson, Heidelberg, Germany) was placed between the two nerve stumps (Figure 8C) and filled with PBS containing scaffold peptide that forms a gel matrix support (0.5% PuraMatrix Peptide Hydrogel, 3D, BD Biosciences, USA), or PBS/scaffold peptide supplemented with either control peptide, cyclic HNK-1 mimetic, linear or cyclic PSA mimicking peptides (all glycomimetics were used with a concentration of 200 µg/ml). The cut ends of the

nerve were inserted into the tube and fixed with single epineural 11-0 nylon stitches (Ethicon, Norderstedt, Germany) so that a 2 mm gap was present between the proximal and distal nerve stumps. Finally, the skin wound was closed with 6-0 sutures (Ethicon). At least eight animals were operated for each group.

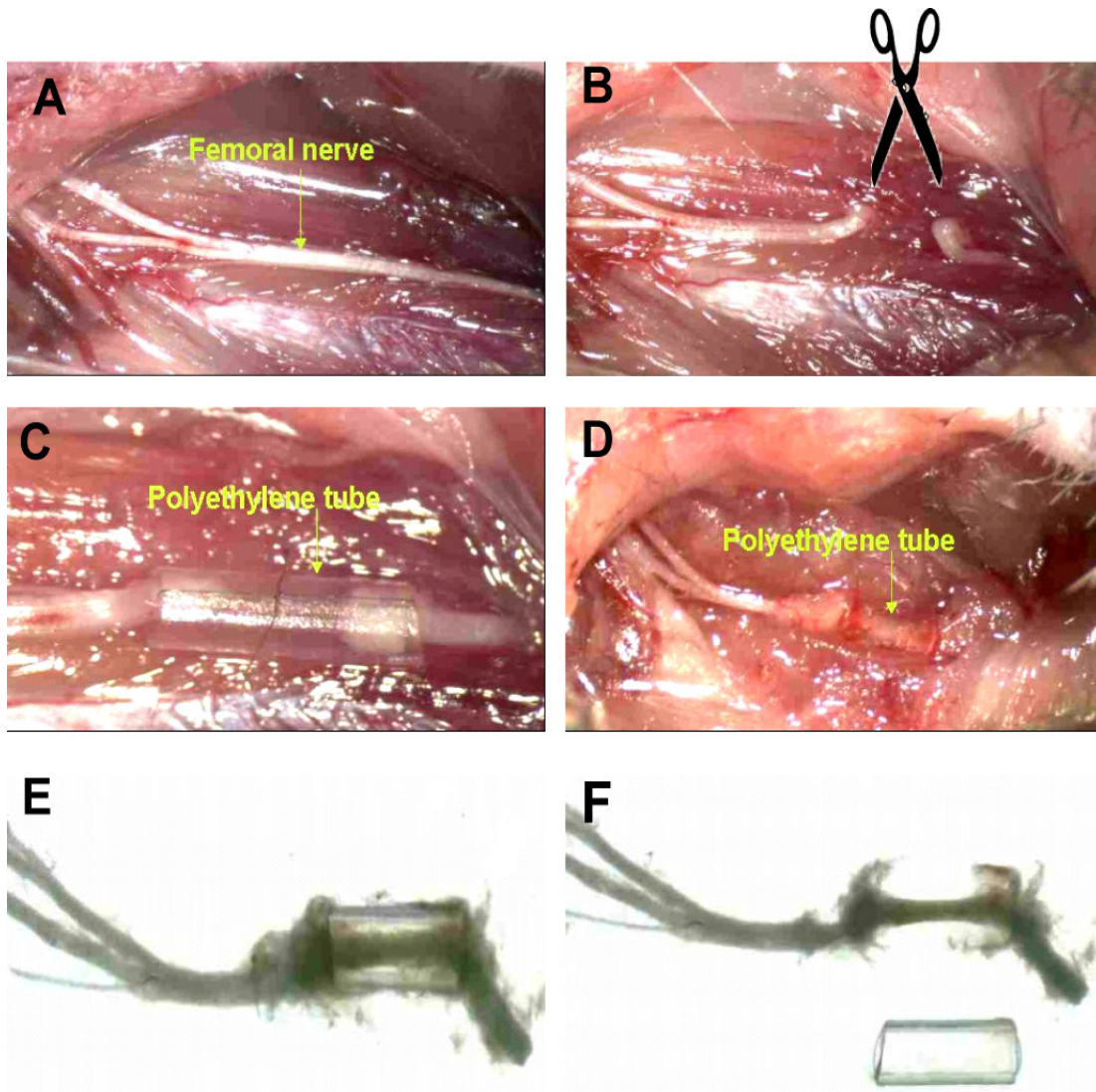


Figure 8: Femoral nerve surgery and regeneration. A: An intact femoral nerve (arrow) with its two major branches (on left hand side): the thicker quadriceps (motor) branch (upper one in A) and the thin saphenous (sensory) branch. Transection of the femoral nerve was performed proximal to the bifurcation (B) followed by surgical repair using a polyethylene tube (C). Panels D-F show the macroscopic appearance of a regenerated nerve 3 months after surgery in situ (D) and after dissection (E, F). Figures were taken with a "Stemi 2000-C Stereo Microscope" from Zeiss, with the program "Second32".

4.4. Spinal cord injury and glycomimetic infusion

Mice were anesthetized by intraperitoneal injections of ketamin and xylazin (100 mg Ketanest[®], Parke-Davis/Pfizer, Karlsruhe, Germany, and 5 mg Rompun[®], Bayer, Leverkusen, Germany, per kg body weight). Alzet osmotic pumps (model 1002, 14 days infusion, Durect, Cupertino, CA, USA) were filled with phosphate buffered saline (PBS) alone or one of the following peptides (dissolved in PBS at a concentration of 500 µg/ml): control peptide, linear PSA mimetic, cyclic HNK-1 mimetic, or combination of both mimetics. We infused glycomimetics with a high concentration of 500 µg/ml to increase the chance for the peptides to reach the lesion site, as we observed with the human Fc infusion (Figure 25). We chose 500 µg/ml because it was the highest concentration at which peptides do not precipitate when kept at 37°C for 2 weeks. Each pump was connected to a vinyl catheter (Durect). The distal tip of the catheter was stretched by hand upon fire to fit its diameter to the subdural space (< 0.4 mm). For subdural insertion of the catheter, the lumbar vertebral column was exposed and a hole between vertebrae L4-L5 was made using a needle with a 0.4 mm outer diameter. Leakage of the cerebrospinal fluid was taken as proof for penetration of the dura (Figure 9B, C). The catheter was then inserted into the hole and fixed to the surrounding tissue with a 6-0 filament (Ethicon) (Figure 9D, E, F). The pump was placed subcutaneously on the left side of the back over the thorax and the skin was closed with 6-0 nylon sutures. During the 6-week observation period, no adverse effects of the pump implantation, such as infections, paralyses or aberrant behavior, were observed.

Directly after pump implantation, laminectomy was performed at the T7-T9 level with mouse laminectomy forceps (Fine Science Tools, Heidelberg, Germany) (Figure 9H). A mouse spinal cord compression device was used to elicit compression injury (Curtis et al., 1993). Compression force (degree of closure of the forceps) and duration were controlled by an electromagnetic device: The spinal cord was maximally compressed (100%, according to the operational definition of Curtis et al., 1993) for 1 second by a time-controlled current flow through the electromagnetic device. Muscles and skin were then closed using 6-0 nylon stitches (Ethicon, Norderstedt, Germany). After the operation, mice were kept in a heated room (35°C) for several hours to prevent hypothermia and thereafter singly housed in a temperature-controlled (22°C) room with water and standard food provided ad libitum. During the postoperative time-period the bladders of the animals were manually voided twice daily.

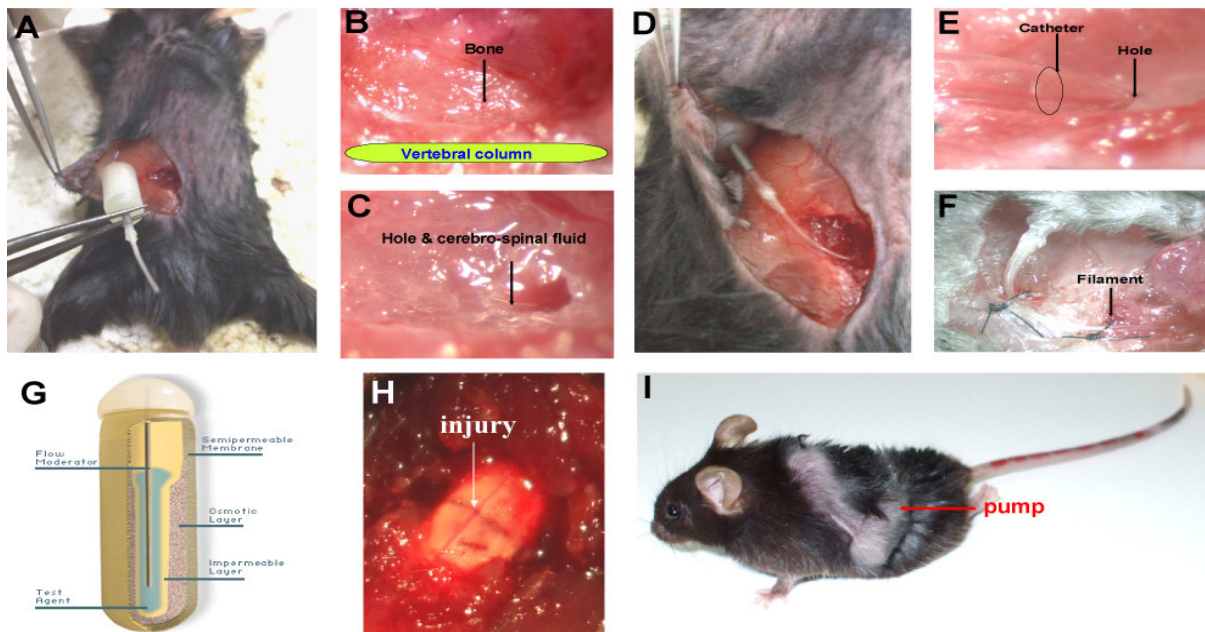


Figure 9: Different steps of the pump implantation: spinal cord exposure and perforation of the vertebral column (A-C), insertion and fixation of the catheter (D-F), structure of the pump (G), injured spinal cord (H), and mouse with pump after operation (I). Figures B, C, E and F were taken with a "Stemi 2000-C Stereo Microscope", with the program "Second32".

It is noteworthy that before starting this project, we performed pilot experiments in order to validate the placement of the catheter in the subdural space. Using magnetic resonance imaging (Figure 10, collaboration with Dr. med. Kersten Peldschus, Universitätskrankenhaus Hamburg-Eppendorf, Klinik und Poliklinik für Diagnostische und Interventionelle Radiologie), proper placement of the catheter was observed in 4 out of 4 mice studied 2 days after operation.

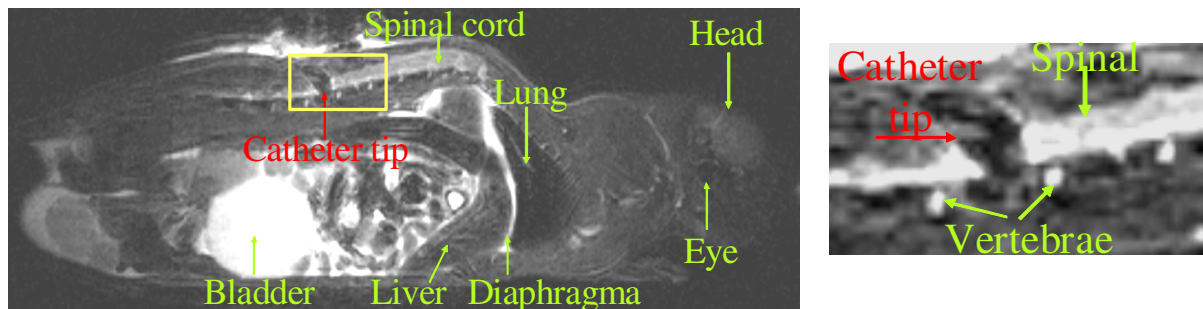


Figure 10: MRI scan of a mouse with T2 weighted sagittal section showing the catheter filled with Resovist© contrast agent. A magnified picture of the catheter tip is shown on the right side.

In addition, the fact that the catheter tip is placed in the lumbar part of the spinal cord but the injury is made at the thoracic level raised the question whether the delivered molecule can reach the injury site. To check the efficacy of the osmotic pumps, a 50 kD human Fc fragment was infused (Jackson ImmunoResearch Laboratories) at two different concentrations: 12.5 and 200 $\mu\text{g}/\text{ml}$ (Figure 25). After two weeks of infusion, spinal cords were isolated and three 5 mm-long segments from each injured spinal cord were dissected: a segment at the thoracic level with the lesion scar in the center and two segments caudally, a lumbar and a sacral one. The samples were homogenized in ice-cold buffer containing 5 mM Tris-HCl (pH 7.5), 0.32 M sucrose, 1 mM MgCl_2 , 1 mM CaCl_2 , 1 mM NaHCO_3 and protease inhibitor cocktail (Roche

Applied Science, Indianapolis, IN, USA). Proteins denatured under non-reducing conditions were subjected to SDS-PAGE and transferred onto nitrocellulose membrane (Protran, Schleicher & Schuell, Dassel, Germany). Following pretreatment in 5% non-fat dry milk powder in 0.1% Tween-20 in phosphate-buffered saline, pH 7.5 (PBS), the membranes were incubated in 5% non-fat dry milk powder in PBS containing horseradish peroxidase-conjugated anti-human Fc (1:10,000; Sigma). After washing in 0.1% Tween-20 in PBS, immunoreactivity was detected by enhanced chemiluminescence (ECL kit, Amersham Biosciences, Piscataway, NJ, USA) on Kodak Biomax X-ray film (Sigma) according to the manufacturer's instructions.

4.5. Analysis of motor function

Functional recovery was assessed by single-frame motion analysis (Irintchev et al., 2005; Apostolova et al., 2006). All experiments were performed blindly with regard to the type of treatment. Prior to operation, mice were accustomed to a classical beam-walking test. In this test, the animal walks unforced from one end of a horizontal beam (length 1000 mm, width 38 mm) towards its home cage located at the other end of the beam. For all mice, one walking trial was captured with a high-speed camera (A602fc, Basler, Ahrensburg, Germany) at 100 frames per second and stored on a personal computer in Audio Video Interleaved (AVI) format. Recordings were performed before and at different time points after injury (1, 2, 4, 8 and 12 weeks after femoral nerve injury and 1, 3 and 6 weeks after spinal cord injury). The video sequences were examined with VirtualDub software, a video capture/processing utility written by Avery Lee (free software available at <http://www.virtualdub.org>). Selected frames in which

the animals were seen in defined phases of the step cycle (see below) were used for measurements performed with UTHSCSA ImageTool 2.0 software (University of Texas, San Antonio, TX, USA, <http://ddsdx.uthscsa.edu/dig/>). The average of at least three measurements was taken for each parameter and mouse.

4.5.1. Femoral nerve injury

Three parameters were measured prior to and after nerve injury: the foot-base angle (FBA), the heels-tail angle (HTA), and the protraction length ratio (PLR). The foot-base angle, measured at toe-off position, is defined by a line dividing the sole surface into two halves and the horizontal line (Figures 11A, B). The angle is measured with respect to the medial aspect. The heels-tail angle is defined by the lines connecting the heels with the anus and measured when one leg is in the single support phase and the contralateral extremity has maximum swing altitude (Figures 11C, D). The angle is measured with respect to the dorsal aspect. Both parameters are directly related to the ability of the quadriceps muscle innervated by the motor branch of the femoral nerve to keep the knee joint extended during contralateral swing phases. As a relative measure of functional recovery at different time-points after nerve injury, we calculated the stance recovery index, by taking the average of the recovery index (RI) for the FBA and HTA. The recovery index for each angle is calculated in percent as:

$$RI = [(X_{\text{reinn}} - X_{\text{den}}) / (X_{\text{pre}} - X_{\text{den}})] \times 100,$$

where X_{pre} , X_{den} and X_{reinn} are values prior to operation, during the state of denervation (7 days after injury), and at any given time-point during reinnervation, respectively.

The third parameter, protraction length ratio, is used to evaluate voluntary movements without body weight support. To measure the PLR, the mouse was held by its tail and allowed to grasp a pencil with its fore paws. As a reaction, the mouse tries to catch the object with its hind paws and extends simultaneously both hind limbs (Figures 11E, F). In intact animals the relative length of the two extremities, as estimated by lines connecting the most distal mid-point of the extremity with the anus, is approximately equal and the PLR (ratio of the left to the right limb length) is close to 1 (Figure 11E). After denervation, the limb can not be extended maximally and the PLR increases significantly above 1 (Figure 11F).

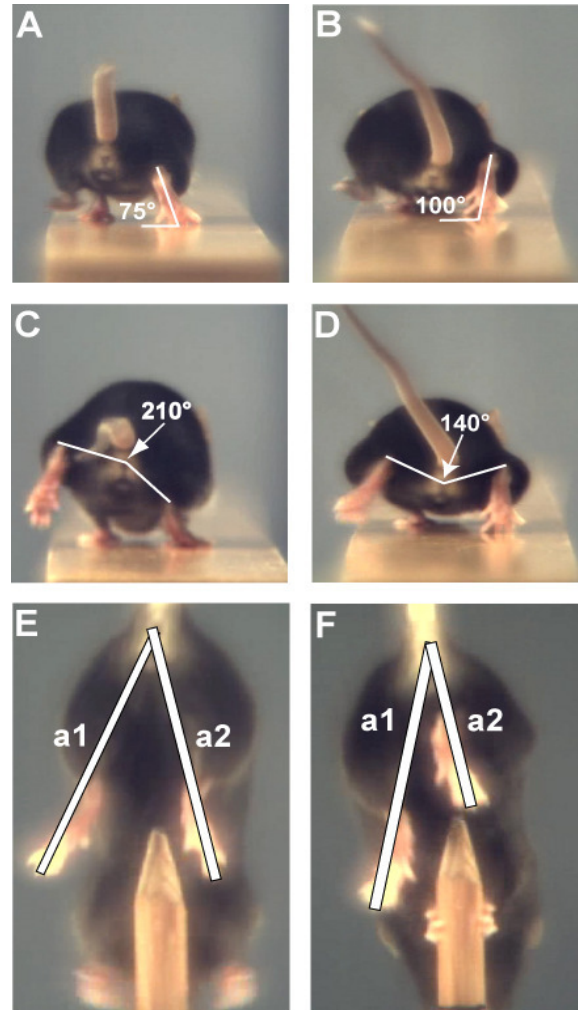


Figure 11: Analysis of motor function. Single video frames from recordings of beam walking (A-D) and voluntary movements without body weight support (“pencil” test, E, F) of C57BL/6J mice prior to (day 0, panels A, C, E) and one week after surgical repair of the right femoral nerve (B, D, F). Panels B and D show video frames in which the right paws of the mouse is at take-off position. Such frames were used for measuring the foot-base angle shown by lines drawn in the panels. Quadriceps muscle dysfunction causes an abnormal external rotation of the heel (B) resulting in a larger angle compared with the angle prior to operation (A). In panels C - D the mouse is seen at mid-stance of the right hind limb and maximum altitude of the contralateral swing. Such video frames were used to measure the heels-tail angle as shown by the lines drawn in both panels. Note the decrease of the angle after operation (D) resulting from higher position of right heel in D compared with C. Panels E – F show animals during maximal protraction of the hind extremities aiming to reach the pencil. In intact mice (E), the lengths of the left and right extremities (a1 and a2, respectively) are approximately equal and thus the ratio between these two measures (a1/a2) designated protraction length ratio is about 1. After femoral nerve injury (F), limb extension on the operated (right) side is impaired and the ratio increases ($a1 > a2$).

4.5.2. Spinal cord injury

Three parameters were measured prior to and after spinal cord injury: the foot-stepping angle, the rump-height index and the extension-flexion ratio (Apostolova et al., 2006). The foot-stepping angle is defined by a line parallel to the dorsal surface of the hindpaw and the horizontal line (Figure 12A). The angle is measured with respect to the posterior aspect at the beginning of the stance phase. In intact mice, this phase is well defined and the angle is around 25°. After spinal cord injury and severe loss of locomotor abilities, the mice drag behind their hindlimbs with dorsal paw surfaces facing the beam surface and the angle is increased to >150° (Figure 12B, C). The rump-height index is defined as height of the rump, i.e., the vertical distance from the dorsal aspect of the animal's tail base to the beam, normalized to the thickness of the beam measured along the same vertical line (Figure 12A).

The extension–flexion ratio is a numerical estimate of the animal's ability to initiate and perform voluntary movements without body weight support. Such movements require connectivity of the spinal cord to supraspinal motor control centers but, in the form evaluated here, no coordination or precision. The principle of measuring this parameter is similar to the one of the protraction length ratio mentioned above. The mouse is held by its tail and allowed to grasp a pencil with its forepaws. As a result, the mouse performs cycling flexion– extension movements with the hindlimbs (Figures 12E, F). In addition to these parameters, the recovery of ground locomotion was evaluated using the using Basso Mouse Scale (BMS, Basso et al., 2006). The overall recovery index was calculated by averaging the recovery indices of the 4 parameters

(foot-stepping angle, rump-height index, extension-flexion ratio and BMS) estimated in each animal.

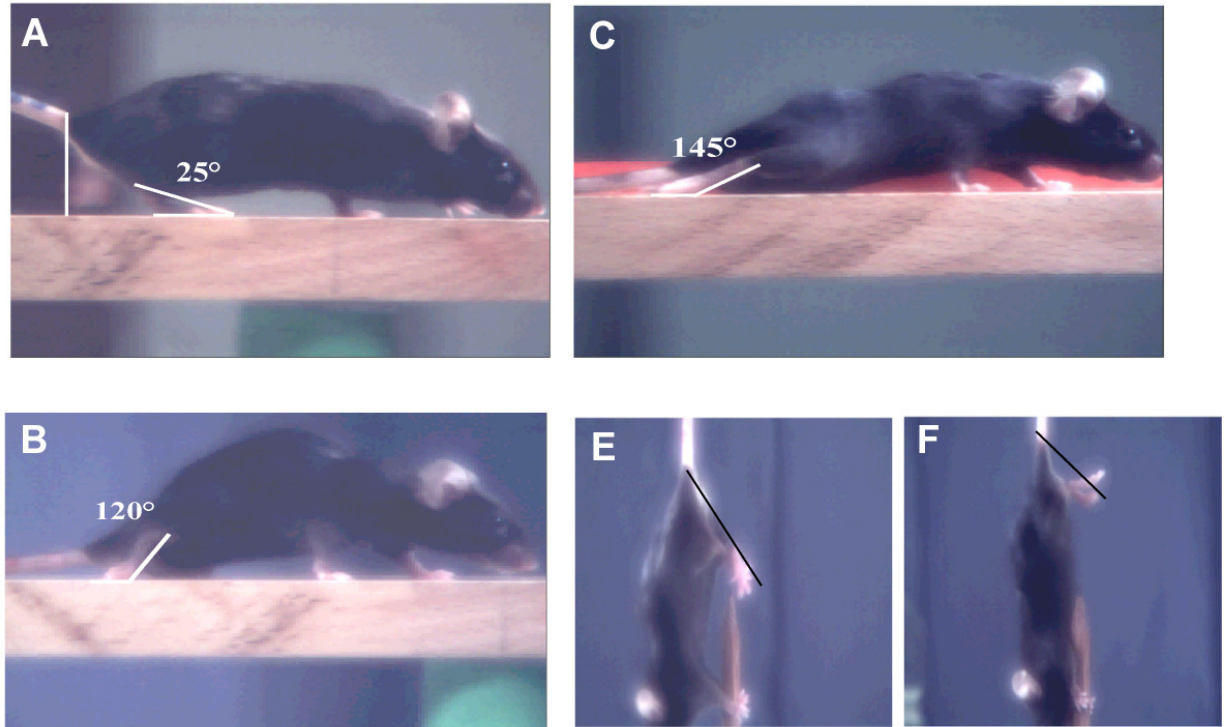


Figure 12: Single video frames showing an intact mouse (A), and PSA-treated (B) and control peptide-treated (C) mice 6 weeks after spinal cord injury. The foot-stepping angle is drawn on all three panels, A-C. The vertical line in panel A shows how the definition of the rump height. Panels E-F show extension (E) and flexion (F) of the hind limbs performed during the pencil test.

4.6. Retrograde labelling through the femoral nerve and evaluation of numbers and soma size of regenerated motoneurons

Following the last video recording, three months after injury, mice were re-operated for retrograde labelling. Under fentanyl/droperidol/diazepam anaesthesia (see above), the two nerve branches were transected approximately 5 mm distal to the bifurcation, and

two fluorescent dyes, Fast Blue (EMS-Chemie, Großumstadt, Germany) and Fluoro-Gold (Fluorochrome, Denver, CO USA), were applied to the motor and sensory branches respectively (Figure 13). One week later, mice were anaesthetized with a 16% solution of sodium pentobarbital (Narcoren, Merial, Hallbergmoos, Germany, 5 µl/g body weight) and transcardially perfused with fixative consisting of 4% formaldehyde (PFA) (Fluka, Germany) in 0.1 M sodium cacodylate buffer, pH 7.3, for 15 minutes at room temperature; 2 hours later, spinal cords and femoral nerves were dissected out and post-fixed for 24 hours at 4°C in the same solution used for perfusion.

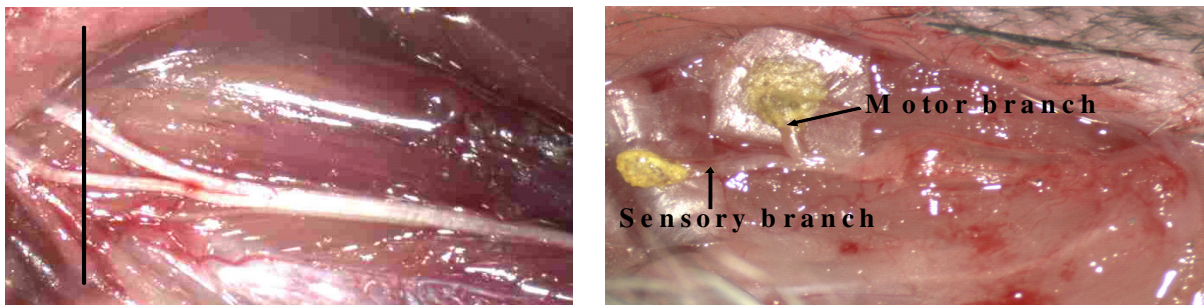


Figure 13: Retrograde labelling through the femoral nerve by application of 2 different dyes, Fast Blue to the motor branch and Fluoro-Gold to the sensory branch after transection of the branches distal to the femoral nerve bifurcation.

The lumbar part of the spinal cord was then cut transversely (serial section of 50 µm thickness) on a Leica vibratome VT1000S (Leica Instruments, Nußloch, Germany). The sections were examined under a fluorescence microscope (Axiophot 2, Zeiss, Germany) with appropriate filter sets. All cell profiles labelled with one of the dyes or with both tracers are distributed within a stack of 35 – 45 serial cross-sections. Each section, containing typically 2 – 5 labelled cell profiles, was examined using a 40x objective by focusing through the section thickness starting from the top surface. All

profiles except those visible at the top surfaces of sections were counted (Simova et al., 2006). The application of this simple stereological principle prevents double counting of labelled cells and allows an unbiased evaluation of cell numbers, which does not rely on assumptions or requires corrections. The same sections were used for measurements of soma size using the Neurolucida software (see below).

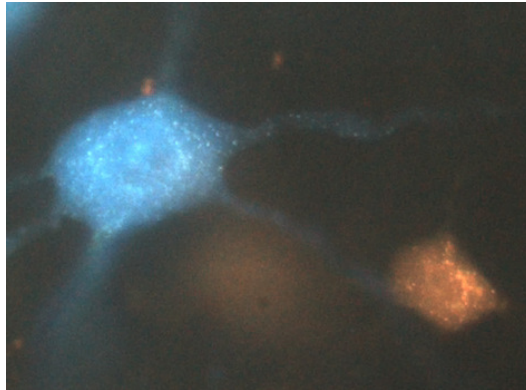


Figure 14: Cell bodies of motoneurons labelled through correctly projecting (blue) and incorrectly projecting (yellow) axons 3 months after femoral nerve injury.

4.7. Analysis of the degree of axonal myelination in the femoral nerve

After fixation with formaldehyde, femoral nerves were post-fixed in 1% osmium tetroxide in 0.1 M sodium cacodylate buffer, pH 7.3, for one hour at room temperature, dehydrated in methanol and embedded in resin at 60°C overnight. Transverse 1 µm-thick sections from the motor and sensory nerve branches were cut (Ultramicrotome, Leica) at a distance of approximately 3 mm distal to the bifurcation and stained with 1% toluidine blue/1% borax in distilled water. Total numbers of myelinated axons per nerve cross-section were estimated on an Axioskop microscope (Zeiss) equipped with a motorized stage and Neurolucida software-controlled computer system (MicroBrightField Europe, Magdeburg, Germany) using a 100x oil objective. Axonal

and nerve fibre diameters were measured in a random sample from each section. For sampling, a grid with a line spacing of 30 μm was projected into the microscope visual field using the Neurolucida software. Selection of the reference point (zero coordinates) of the grid was random. For all myelinated axons crossed by or attaching the vertical grid lines through the sections, mean orthogonal diameters of the axon (inside the myelin sheath) and of the nerve fibre (including the myelin sheath) were measured. The mean orthogonal diameter is calculated as a mean of the line connecting the two most distal points of the profile (longest axis) and the line passing through the middle of the longest axis at right angle (Irintchev et al., 1990). The degree of myelination was estimated by the ratio axon to fibre diameter (g-ratio).

4.8. Schwann cell culture

Mouse Schwann cells were isolated from peripheral nerves (sciatic and femoral nerves) and dorsal root ganglia (DRG) of 7-day-old C57BL/6J mice and nerve- and DRG-derived Schwann cells were cultured separately. Tissues were removed, washed once with ice-cooled Ham's F-12 (PAA Laboratories, Cölbe, Germany), and then incubated with 0.25% trypsin and 0.1% collagenase (Sigma-Aldrich, Steinheim, Germany) at 37°C for 30 minutes. After enzymatic digestion, tissues were washed twice with ice-cooled Ham's F-12 medium and then suspended in 1 ml Ham's F-12 medium containing 0.01% DNase (Sigma). Mechanical digestion was performed using fire-polished Pasteur pipettes, and cells were suspended in 5 ml Ham's F-12 medium, added on top of 5 ml 4% bovine serum albumin (BSA, fraction V, PAA Laboratories) cushion and centrifuged for 10 min at 4°C and 500 g. Finally, Schwann cells were

suspended in fresh pre-warmed (37°C) medium and plated on coverslips (Nunc, Roskilde, Denmark) coated with poly-L-lysine (PLL 0.01%, Sigma), or PLL coated coverslips that were additionally covered with different coatings: control peptide (100 µg/ml), PSA mimicking peptide (100 µg/ml), or laminin (10 µg/ml, Sigma). The medium used for Schwann cell culture contained DMEM high glucose/Ham's F-12 (1:1) (PAA Laboratories), 60 ng/ml progesterone (Sigma), 16 µg/ml putrescine (Sigma), 5 µg/ml insulin (Sigma), 0.4 µg/ml L-thyroxine (Sigma), 160 ng/ml sodium selenite (Sigma), 10.1 ng/ml triiodothyronine (Sigma), 38 ng/ml dexamethasone (Sigma), 100 U/ml penicillin (PAA Laboratories), 100 µg/ml streptomycin (PAA Laboratories) and 2 mM L-glutamine (PAA Laboratories).

4.9. Analysis of Schwann cell processes' length *in vitro*

Schwann cells were plated at a density of 50,000 cells/ml. Inhibitors to the fibroblast growth factor receptor (FGFR) were added to the culture 1 hour after seeding. Two inhibitors were tested, SU5402 (VWR International, Darmstadt, Germany) and PD173074 (Parke-Davis, Ann Arbor, MI, USA) at a final concentration of 50 µM and 500 nM, respectively. PD173074 exhibits a high degree of specificity towards the FGF receptor in the nanomolar range (Mohammadi et al., 1998; Niethammer et al., 2002). SU5402 also inhibits the FGF receptor tyrosine kinase, but is less specific, because it weakly affects the PDGF receptor (Mohammadi et al., 1997). L1Fc (10 µg/ml) was used in one experiment as a positive control, as L1 is known to stimulate axonal growth via FGFR (Doherty and Walsh, 1996). Twenty-four hours after seeding and incubation at 37°C, cells were fixed with 2.5% glutaraldehyde (Agar Scientific,

Stansted, UK) and stained with 1% methylen blue/toluidine blue (Sigma) in 1% borax. The length of processes was measured by using the Axiovert microscope and the AxioVision image analysis system 4.6 (Carl Zeiss MicroImaging, Göttingen, Germany). The length of all processes per cell was averaged. At least 150 cells per treatment were analyzed.

4.10. Analysis of Schwann cell proliferation in vitro

Schwann cells were plated at a density of 250,000 cells/ml onto different substrates. The cells were cultured in the presence of neuroregulin (12 ng/ml, ImmunoTools, Friesoythe, Germany). Four hours after seeding, 20 μ M BrdU (Sigma) was added to the culture. Cells were cultured for 48 hours and then fixed for immunostaining with 4 % formaldehyde in 0.1 M phosphate buffer, pH 7.3. After incubation for 30 min with 2 N HCl at 37°C, cells were washed, blocked with normal goat serum and incubated overnight with mouse primary antibody G3G4 (anti-BrdU; 1:100; Developmental Studies Hybridoma Bank, Iowa City, IA, USA). The secondary antibody, goat anti-mouse (1:200, Santa Cruz, Heidelberg, Germany), was applied for 1 h at room temperature. The coverslips were finally washed and mounted with Fluoromount-G (SouthernBiotech, Birmingham, USA).

To estimate numbers of proliferating cells, 10 photographs per treatment were taken from different areas of the coverslip using an Axiophot 2 microscope (Zeiss) and a 20x objective. Each area was photographed using phase contrast and epifluorescence. The two digital images were then overlaid using the Image J software (<http://rsbweb.nih.gov/ij/download.html>) and Image Tool 2.0 software (University of

Texas, San Antonio, TX, USA, <http://ddsdx.uthscsa.edu/dig/>) was used to count proliferating (BrdU-positive) Schwann cells and total number of Schwann cells. Schwann cells in culture have a long spindle-shaped cell body and two processes in opposite directions (Figures 20A and 21A), which makes them easily distinguishable from other contaminating cells (DRG neurons and fibroblasts). We counted approximately 1,000 cells for each experimental value.

4.11. Staining of live Schwann cells

Schwann cells were cultured on coverslips coated with poly-L-lysine (Sigma). Twenty four hours after seeding, cells were washed three times with the culture medium and incubated on ice for 20 minutes with the primary antibodies: mouse monoclonal antibody 735 (provided by R. Gerardy-Schahn) and rat monoclonal antibody H28 against NCAM (provided by V. Sytnyk), both diluted in medium containing 5% fetal bovine serum (PAA laboratories). After staining with primary antibodies, cells were washed and incubated at room temperature for 25 minutes with secondary antibodies goat anti-mouse and goat anti-rat diluted (1:200 and 1:100, respectively; Jackson ImmunoResearch, West Grove, PA, USA) in culture medium containing 5% foetal bovine serum. After washing with PBS, cells were fixed with 4% paraformaldehyde for 20 minutes at room temperature, washed again three times with PBS, and then blocked with PBS containing 5% normal goat serum and 0.2% Triton X-100 for 30 minutes at room temperature. Primary rabbit polyclonal antibody against S-100 (Schwann cell marker; Shearman and Franks, 1987) (diluted 1:500 in PBS; Dako, Glostrup, Denmark) was applied at 4°C overnight. Cells were then washed and

secondary goat anti-rabbit antibody (1:100; Jackson ImmunoResearch) was applied for one hour at room temperature. Finally cells were washed with PBS, mounted with Fluoromount-G (SouthernBiotech), and images were taken with an Olympus Fluoview 1000 microscope (Olympus, Hamburg, Germany).

4.12. Schwann cell proliferation in vivo

Three-month-old female C57BL/6J mice underwent femoral nerve transection and surgical reconstruction followed by application of either control peptide (n = 5) or PSA mimic peptide (n = 5) as described above. In addition, all mice received intraperitoneal injections of BrdU (Sigma, 200 mg/kg body weight) at day 2 and 5 after the operation. At the sixth day after injury, mice were perfused with 4% formaldehyde in cacodylate buffer, and the distal nerve stumps were removed, post-fixed overnight at 4°C and cryoprotected by overnight infiltration with sucrose (Fluka, Germany, 15% solution in cacodylate buffer, 4°C). After embedding in tissue Tek (Sakura Finetek, Zoeterwoude, NL), nerves were frozen by a 2 minute immersion into 2-methyl-butane (isopentane) precooled to -80°C and then cut on a cryostat (Leica). Transverse sections of 10 µm thickness were collected immediately distal from the level of bifurcation of the motor and sensory branch.

For immunostaining, sections were incubated in 0.1 M HCl at 60°C for 20 minutes and then rinsed three times with 50 mM glycine (Merck, Germany) for 10 minutes each. After one hour blocking with 5% normal goat serum in PBS at room temperature, sections were incubated with a mixture of rat anti-BrdU (1:200, Abcam, Cambridge, USA) and rabbit anti-S-100 (1:15000, Dako, Denmark) for 2 days at 4°C. After

washing, goat anti-rat and goat anti-rabbit IgG diluted 1:200 (Jackson ImmunoResearch, West Grove, PA, USA) were applied for 2 hours at room temperature. Sections were washed PBS, stained in bis-benzimide (nuclear staining), washed again and mounted with Fluoromount-G (SouthernBiotech). Images of the femoral nerve were taken on a Olympus Fluoview 1000 microscope with a 20x objective. Analysis of proliferating cells was performed using the Neurolucida system and a 100x oil objective. Cells that were double-labelled with S-100 and BrdU were considered as proliferating Schwann cells.

4.13. Sectioning of the injured spinal cord and immunohistochemistry

After an observation period of 6 weeks, spinal cord-injured mice were perfused and the lumbar part of the spinal cord was removed, post-fixed and embedded in Tissue Tek as mentioned above. Serial transverse or parasagittal sections were cut in a cryostat (Leica CM3050, Leica Instruments, Nussloch, Germany). Sections, 25 µm thick, were collected on SuperFrost Plus glass slides (Roth, Karlsruhe, Germany). Sampling of sections was always done in a standard sequence so that 6 sections 250 µm apart were present on each slide.

For immunohistochemistry, sections were incubated in a jar containing antigen de-masking solution (0.01M sodium citrate solution, pH 9.0), for 30 minutes at 80 °C (Jiao et al., 1999). Non-specific binding was blocked using 5% normal serum from the species in which the secondary antibody was produced, dissolved in PBS and supplemented with 0.2% Triton X-100, 0.02% sodium azide for 1 hour at room temperature (RT). Incubation with the primary antibody diluted in PBS containing 0.5% lambda-carrageenan (Sigma) and 0.02% sodium azide, was carried out for 3 days at

4°C. The following antibodies were used: goat anti-choline acetyltransferase antibody (ChAT, Chemicon, Hofheim, Germany; 1:100), rabbit anti-tyrosine hydroxylase (TH, Chemicon, 1:800), and rabbit anti-vesicular glutamate transporter 1 (Synaptic Systems, Göttingen, Germany; 1:1000), and Cy3-conjugated goat anti-rabbit and donkey anti-goat antibodies (Jackson ImmunoResearch Laboratories, Dianova, Hamburg, Germany).

After washing in PBS (3 x 15 minutes at RT), the appropriate secondary antibody, diluted 1:200 in PBS-carrageenan solution, was applied for 2 hours at RT. After a subsequent wash in PBS, cell nuclei were stained for 10 minutes at RT with bis-benzimide solution (Hoechst 33258 dye, 5 µg/ml in PBS, Sigma). Finally, the sections were washed again, mounted in anti-bleaching medium (Fluoromount G, Southern Biotechnology Associates, Biozol, Eching, Germany) and stored in the dark at 4°C. Photographic documentation was made on an LSM 510 confocal microscope (Zeiss, Oberkochen, Germany) or an Axiophot 2 microscope equipped with a digital camera AxioCam HRC and AxioVision software (Zeiss). The images were processed using Adobe Photoshop 7.0 software (Adobe Systems Inc., San Jose, California).

4.14. Motoneuron soma size and quantification of perisomatic terminals after spinal cord injury

Transverse spinal cord sections stained for ChAT or VGLUT1 were examined under a fluorescence microscope to select sections that contained motoneuron cell bodies for a distance of at least 500 µm distal from the lesion scar. Stacks of 1 µm thick images were obtained on the LSM 510 confocal microscope using a 63 x 1.5 oil immersion

objective and digital resolution of 512 x 512 pixels. One image (optical slice) per cell at the level of the largest cell body cross-sectional area was used to measure soma area, perimeter and number of perisomatic terminals. Areas and perimeters were measured using the Image Tool 2.0 software program (University of Texas, San Antonio, TX, USA). Density of ChAT⁺ terminals was calculated as number of perisomatic terminals per unit length of the cell surface. For VGLUT1⁺ terminals, densities per area in the Clarke's column, Lamina VII and ventral horns were measured by using Image J software (<http://rsbweb.nih.gov/ij/download.html>).

4.15. Quantification of motoneurons in the lumbar spinal cord after spinal cord injury

Motoneuron counts were performed using the optical dissector method on an Axioskop microscope (Zeiss) equipped with a motorized stage and NeuroLucida software-controlled computer system (MicroBrightField, Colchester, USA) (Irintchev et al., 2005; Jakovcevski et al., 2009). For each animal, 8 equidistant (250 μ m apart) transverse sections from the lumbar spinal cord stained for ChAT and nuclei were analyzed. Using the nuclear staining, the ventral horn areas on both sides of each section were outlined with the cursor of the software under low-power magnification (10x objective). All ChAT-positive motoneurons in the ventral horn motor nuclei (Rexed laminae VIII and IX) with nuclei appearing in focus within 2 to 12 μ m from the top of the section were counted using a Plan-Neofluar 40x/0.75 objective. Cell densities were calculated by dividing the cell number by the reference volume (ventral horn area x 10 μ m) and averaged per animal.

4.16. Estimation of lesion scar volume and myelin volume in the lesioned spinal cord

Spaced serial 25 μm -thick transverse sections 250 μm apart were stained with Cresyl Violet/Luxol Fast Blue and used for estimations of the scar volume and myelin volume using the Cavalieri principle. Area measurements required for volume estimation were done directly under the microscope using the Neurolucida software.

4.17. Analysis of axonal myelination in the injured spinal cord

Spinal cords were dissected from animals fixed by perfusion with formaldehyde (see above). From each specimen, 0.6 cm-long segments were cut from the lumbar and thoracic part of the spinal cord at distances of approximately 5 mm distal and proximal to the center of the lesion, respectively. Tissue was post-fixed in 1% osmium tetroxide, dehydrated and embedded in resin as mentioned above. Transverse 1 μm -thick sections were cut and stained with 1% toluidine blue/ 1% borax in distilled water, and myelination was measured in the same principle used for the femoral nerve.

4.18. Statistical analysis

All numerical data are presented as group mean values with standard errors of mean (SEM). Parametric or non-parametric tests were used for comparisons, as indicated in the text and figure legends. Analyses were performed using the SYSTAT 9 software package (SPSS, Chicago, IL, USA). The threshold value for acceptance of differences was 5%.

5. Results

5.1. Effect of glycomimetics after femoral nerve injury

5.1.1. Cyclic HNK-1 mimetic improves regeneration and functional recovery

Damage of the femoral nerve in mice induces changes in gait which can be precisely evaluated by three parameters, the heels-tail angle, the foot-base angle and the protraction length ratio, evaluated on single frames of video sequences recorded during beam walking and pencil test (Figure 11). These alterations are caused by impaired extensor function of the quadriceps muscle leading to abnormal external rotation of the ankle, high heel position at defined gate cycle phases, and weak extension of the injured limb shown in Figure 11A, B and Figure 11C, D, and Figure 11E, F respectively. We used these parameters to evaluate the effect of HNK-1 and PSA mimetics on locomotor recovery.

Application of the cyclic HNK-1 mimetic enhanced, compared with control peptide, functional recovery (Figure 15), in good correspondence with previous data obtained in our lab after application of a linear HNK-1 mimetic (Simova et al., 2006). Morphological analyses of the mice which received the linear HNK-1 mimetic, have shown enhanced precision of muscle reinnervation, enhanced motoneuron survival and soma area, and better axonal myelination in the motor branch of the femoral nerve (Simova et al., 2006).

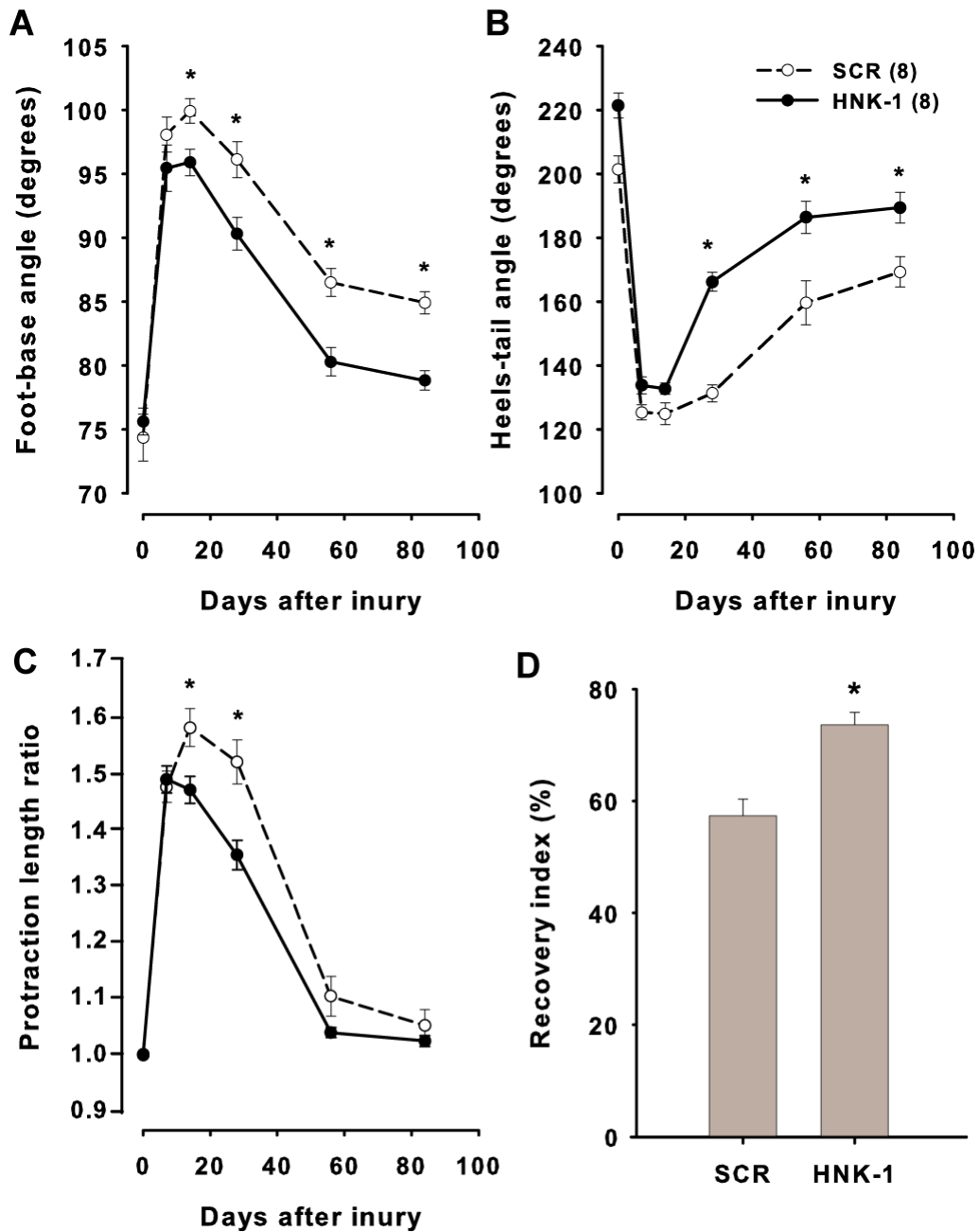


Figure 15: Time course of motor recovery after femoral nerve lesion. Shown are mean values \pm SEM of foot-base angles (A), heels-tail angles (B), and limb protraction length ratios (C) at different time-points after femoral nerve injury and application of a cyclic HNK-1 mimetic (HNK-1) or control peptide (SCR). Pre-operative values are plotted at day 0. Numbers of animals studied per group are indicated in panel B. Panel D shows the mean recovery indices \pm SEM at 3 months after injury. A recovery index of 100% indicates complete recovery. Asterisks indicate significant differences ($p < 0.05$, one-way ANOVA with Tukey's post hoc test) between the HNK-1 mimetic-treated group and the control group at the given time points.

5.1.2. Linear PSA mimetic promotes functional recovery

One week after injury, the degree of functional impairment, as evaluated by the increase of the foot-base angle (Figure 16A) and decrease of the heels-tail angle (Figure 16B) compared with the pre-operative values, was similar in three groups of mice treated with a linear PSA mimicking peptide, control peptide or vehicle (PBS). After the first week, the angles in all three groups of mice gradually returned to the pre-operative values, but recovery was incomplete even after 12 weeks (Figure 16A, B). However, improvement in PSA mimetic-treated mice was better compared with the control groups at 8 and 12 weeks after injury (Figure 16A, B; $p < 0.05$, ANOVA with Tukey's *post-hoc* test). As estimated by the stance recovery index, a measure of the individual degree of recovery calculated for both angles, the outcome of femoral nerve repair at 3 months after injury was significantly better in PSA mimetic-treated mice than in mice receiving control peptide or vehicle (Figure 16C).

To further verify that the positive functional effects of the novel linear peptide are related to its PSA mimicking properties, we also analysed locomotor recovery in a group of mice which received the previously characterized cyclic PSA mimetic peptide (peptide p1 in Torregrossa et al., 2004). As demonstrated by the time course and final degree of recovery, peptide p1 had a similar positive effect as the linear PSA mimetic (Figure 16D). Thus, the overall results show that PSA glycomimetic treatment leads to a superior functional outcome.

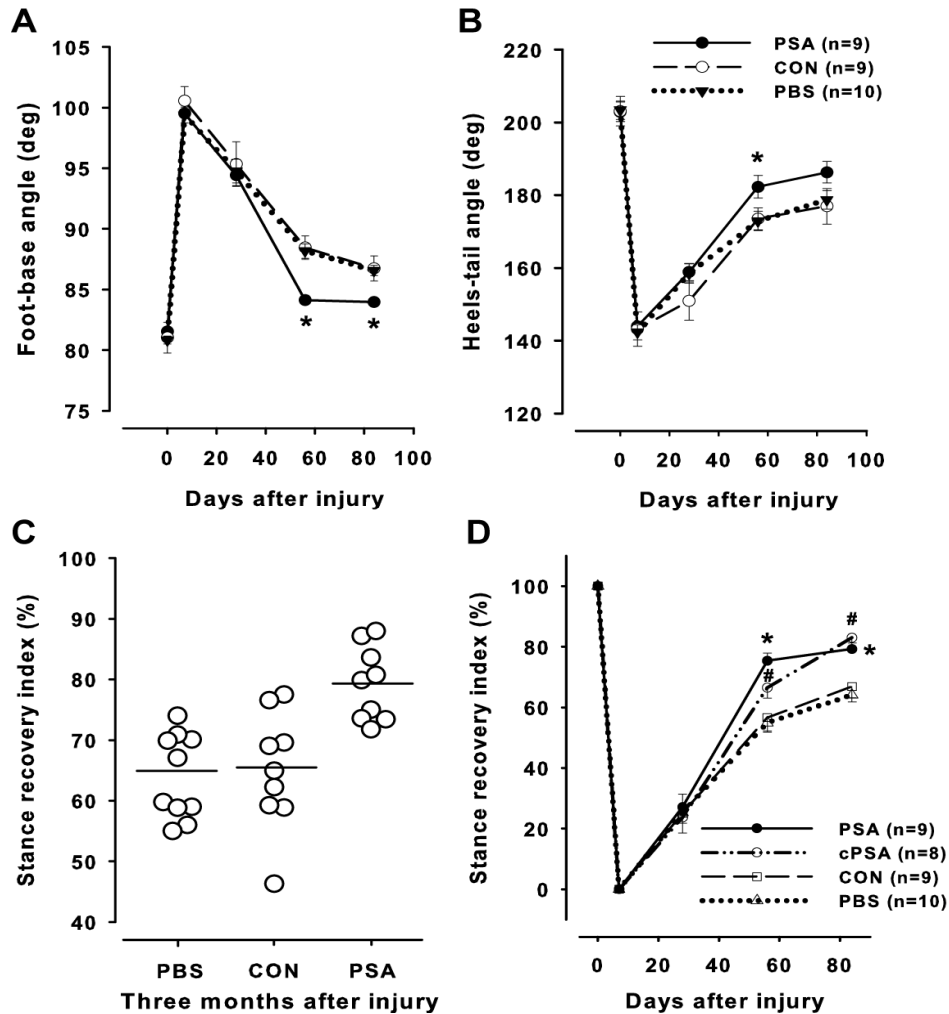


Figure 16: Time course of motor recovery after femoral nerve lesion. (A-B) Shown are mean values \pm SEM of foot-base angles (A) and heels-tail angles (B) at different time-points after femoral nerve injury and application of linear PSA mimicking peptide (PSA), control peptide (CON) or vehicle (PBS). Pre-operative values are plotted at day 0. Panel C shows individual animal values (each circle represents one mouse) and group mean values (horizontal lines) of the stance recovery index calculated for the heels-tail and the foot-base angles at three months after injury. A recovery index of 100% indicates complete recovery. Asterisks indicate significant differences ($p < 0.05$, one-way ANOVA with Tukey's post-hoc test) between the PSA mimetic-treated group and the control groups at the given time points. (D) Comparison of motor recovery in mice treated with two different PSA mimicking peptides. Shown are mean values \pm SEM of stance recovery indices at different time points after femoral nerve transection and application of linear PSA mimicking peptide (PSA), cyclic PSA mimicking peptide (cPSA), and control peptide (CON) or vehicle (PBS). Asterisk and cross-hatches indicate significant differences ($p < 0.05$, one-way ANOVA with Tukey's post-hoc test) between the PSA-treated groups and the control groups at the given time points. n indicates the number of animals operated per group.

5.1.3. The PSA mimetic does not influence precision of motor reinnervation and motoneuron survival

In search of structural correlates of the superior functional outcome after application of PSA mimetics, we performed retrograde labelling of regenerated motoneurons in the animals analyzed functionally over a three-month recovery period. The number of motoneurons back-labelled through the motor (quadriceps) or the sensory (saphenous) branch only, or through both branches of the femoral nerve, as well as the total number of labelled neurons (sum of the three previous categories) was similar in PSA mimetic-, control peptide-, or vehicle only-treated mice (Figure 17). Since numbers of retrogradely labelled motoneurons reflect the extent of motoneuron survival (de la Cruz et al., 1994; Waters et al., 1998; Asahara et al., 1999), we can conclude that treatment with the PSA mimetic did not reduce motoneuron death, a characteristic feature of the femoral nerve injury paradigm in mice (Simova et al., 2006). Also, the numbers of motoneurons projecting aberrantly to only the sensory branch were similar to those projecting correctly to the motor branch of the femoral nerve, irrespective of the treatment of the animals (Figure 17). Therefore, in all experimental groups of mice there was no preferential motor reinnervation (PMR), i.e., higher numbers of motoneurons regenerated into the appropriate motor nerve branch (Brushart, 1988). PMR was first reported in the rat femoral nerve (Brushart, 1988). The rodents' femoral nerve is a mixed nerve that arises from the lumbar part of the spinal cord and bifurcates into 2 branches: the motor branch which contains motor and sensory neurons and the cutaneous branch which contains only sensory neurons. After transection of the nerve proximally to the bifurcation, regenerating motor axons

have equal access to motor and sensory Schwann cell tubes. Nevertheless, motor axons preferentially reinnervate motor pathways. This was attributed to the upregulation of HNK-1 carbohydrate on the Schwann cell basal membrane of motor axons (Brushart, 1993). In mice, this phenomenon has also been reported (Franz et al., 2005), but it has also not been observed, in particular in inbred C57BL/6J mice that were used in this study (Robinson and Madison, 2003; Simova et al., 2006; Ahlborn et al., 2007). In conclusion, our results show that better functional recovery in PSA mimetic-treated mice cannot be attributed to better motoneuron regeneration since neither motoneuron loss was reduced nor precision of motor reinnervation was improved as compared with control mice.

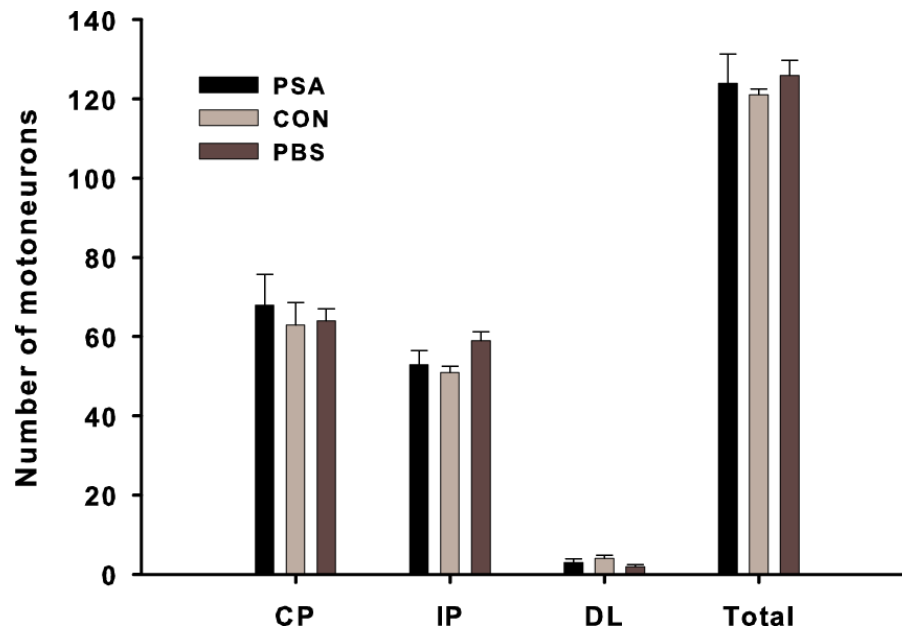


Figure 17: Analysis of regrowth of motoneuron axons after injury. Mean numbers of motoneurons (+ SEM) labelled through the motor branch (correctly projecting “CP”), through the sensory branch (incorrectly projecting “IP”), through both branches (double labelled “DL”), and the sum of neurons in the first three categories (total number “Total”) three months after femoral nerve injury and application of linear PSA mimicking peptide (PSA), control peptide (CON) or vehicle (PBS). No significant differences between group mean values were found ($p > 0.05$, one-way ANOVA with Tukey’s post-hoc test). Nine animals were studied per group.

It is known that neurons undergo atrophy after lesion to their axons (Rich et al., 1989). We have previously found significant correlations between recovery index and motoneuron size at three months after femoral nerve injury (Simova et al., 2006; Ahlborn et al., 2007). Therefore, we measured soma size of motoneurons regrowing their axons correctly and found no differences among the groups treated with PSA mimetic, control peptide or PBS (Figure 18). Similarly, no differences between experimental groups were found for soma size of motoneurons aberrantly projecting to the sensory branch of the femoral nerve (Figure 18). Therefore, we also cannot attribute better functional recovery in PSA mimetic-treated mice to larger motoneuron size, an indicator of a better functional state of regenerated motoneurons (Simova et al., 2006; Ahlborn et al., 2007).

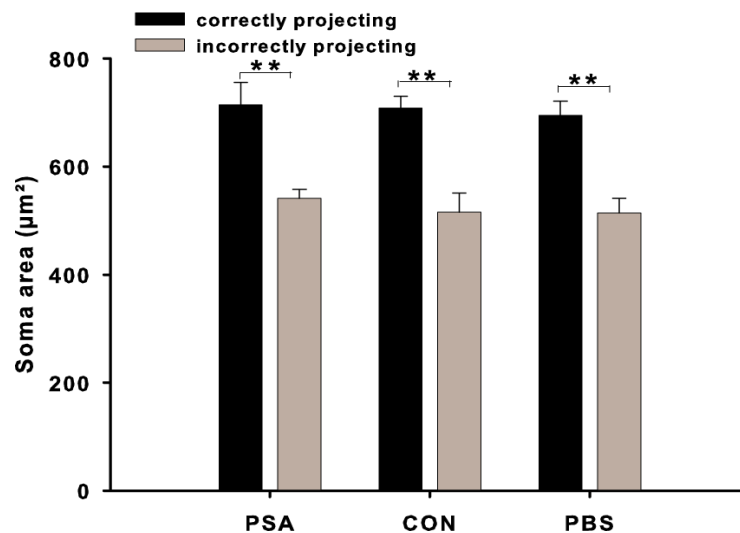


Figure 18: Analysis of soma size of regenerated motoneurons. Shown are mean values of soma area (+SEM) of correctly and incorrectly projecting motoneurons (see Fig. 5) after application of linear PSA mimicking peptide (PSA), control peptide (CON) or vehicle (PBS). No significant differences between group mean values of regrown axons for a given type of projecting neurons were found ($p > 0.05$, one-way ANOVA with Tukey's post-hoc test). However, within each animal group, correctly projecting motoneurons have significantly larger soma sizes than incorrectly projecting motoneurons (**asterisks, $p < 0.01$). Six animals were studied per group.

5.1.4. The PSA mimetic improves the quality of axonal regeneration

We next analyzed regenerated nerves morphometrically to assess axonal numbers, axonal diameters and degree of myelination. In both the motor and sensory branches of the femoral nerve, we found similar numbers of myelinated axons in PSA mimetic-treated mice and control mice three months after nerve injury (data not shown). Also, no differences among the experimental groups were found for axonal diameters (data not shown). However, a remarkable effect was found on the relative degree of myelination, evaluated by the g-ratio (axon- to fibre-diameter ratio) (Figure 19): the frequency distributions of the g-ratio in both the motor and sensory branches of PSA mimetic-treated nerves were significantly shifted towards lower values, indicating thicker myelin sheaths of the regenerated axons, compared with control mice. Importantly, as compared with intact nerves, the g-ratios in the PSA mimetic-treated motor nerve branch were normal, and even better than normal in the sensory nerve branch (Figure 19). Thus, considering all morphological results, the major effect of the PSA treatment was enhanced remyelination.

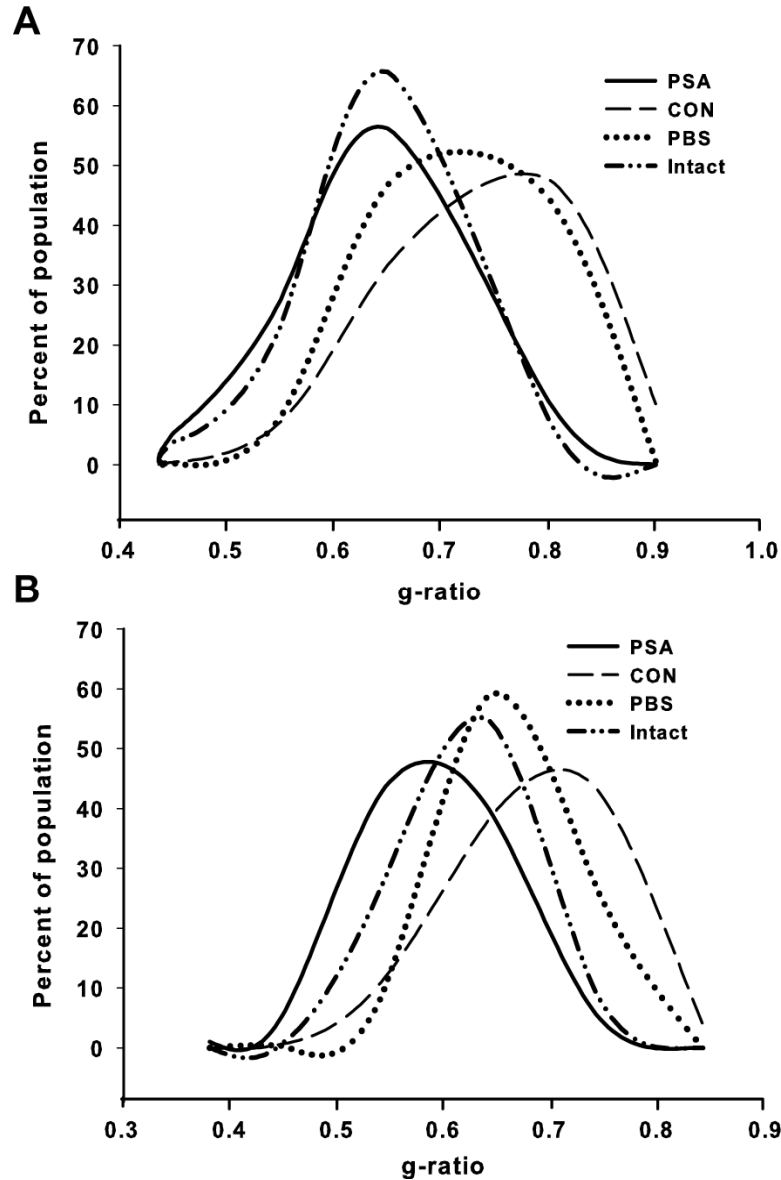


Figure 19: Analysis of myelinated nerve fibres in regenerated and intact nerves. Shown are normalized frequency distributions of g -ratios (axon/fiber diameter) in the motor (A) and sensory (B) nerve branches of the femoral nerve of intact mice ("Intact") and mice treated with linear PSA mimicking peptide (PSA), control peptide (CON) or vehicle (PBS) after femoral nerve injury. Regenerated nerves were studied three months after injury. The number of axons analyzed per nerve and nerves analyzed per animal group ranged between 60-75 and 5-6, respectively. The distribution for the PSA mimicking peptide-treated nerves is significantly different from that of the CON and PBS groups in A and from the other groups in B ($p < 0.05$, Kolmogorov-Smirnov test). Six nerves per group were used for measurements.

5.1.5. The PSA mimetic influences shape and proliferation of Schwann cells *in vitro*

The fact that the PSA mimicking peptide improved myelination *in vivo* suggested an effect on Schwann cells. To test this hypothesis, we separately cultured Schwann cells from two sources: dorsal root ganglia and sciatic/femoral nerves of early postnatal C57BL/6J mice. Morphometric analysis revealed that Schwann cells had longer processes when cultured on substrate-coated PSA mimetic compared with cultures grown on poly-L-lysine or control peptide (Figure 20B). We also checked the effect of the PSA mimetic on Schwann cell proliferation by analysis of BrdU incorporation and found that Schwann cell proliferation was enhanced by 26% in the presence of the PSA mimetic compared to the control peptide (Figure 21B). This result is in good accordance with previous observations that colominic acid enhances proliferation of Schwann cells *in vitro* (Bruns et al., 2007; Haile et al., 2007). Both effects of PSA reported here, i.e. enhanced process elongation and cell proliferation, were observed regardless from which source Schwann cells were isolated, dorsal root ganglia or peripheral nerves.

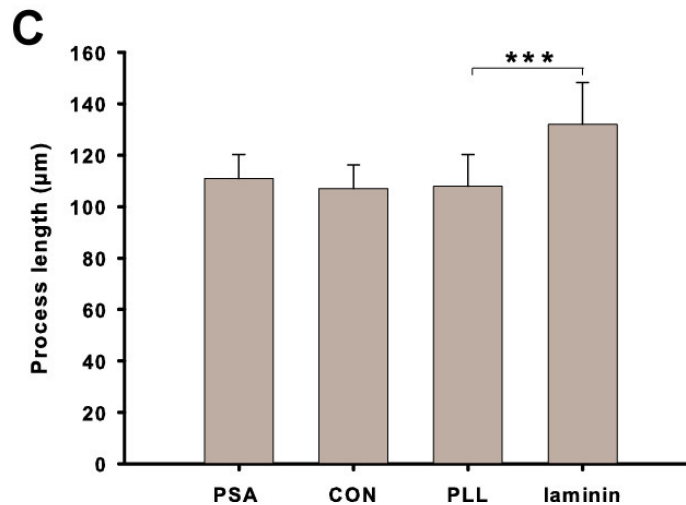
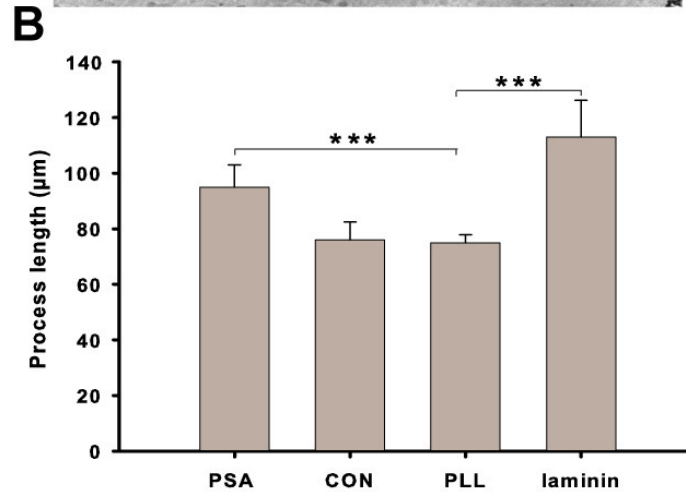
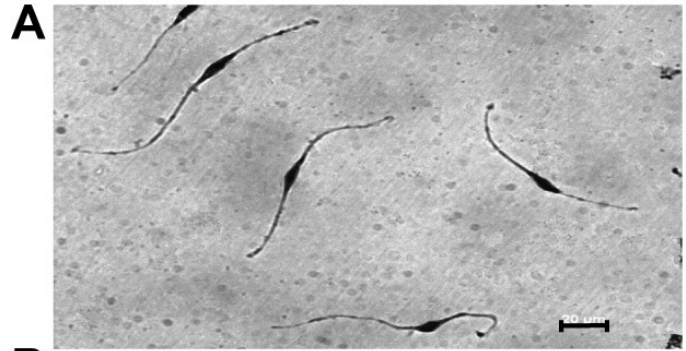


Figure 20: Analysis of Schwann cell morphology *in vitro*. (A) A micrograph of Schwann cells isolated from peripheral nerves shows their typical spindle-shaped cell bodies with two processes in opposite directions (scale bar, 20 μm). Schwann cell processes are responsible for axonal ensheathment and myelination. Linear PSA mimetic enhances process outgrowth from wild type Schwann cells (B), but not from *NCAM*^{-/-} Schwann cells (C). Poly-L-lysine (PLL) served as a negative control while laminin was used as a positive control. Data show process length in μm + SD (***)significantly different from PLL, $p < 0.001$, one-way ANOVA with Dunnett's post-hoc test).

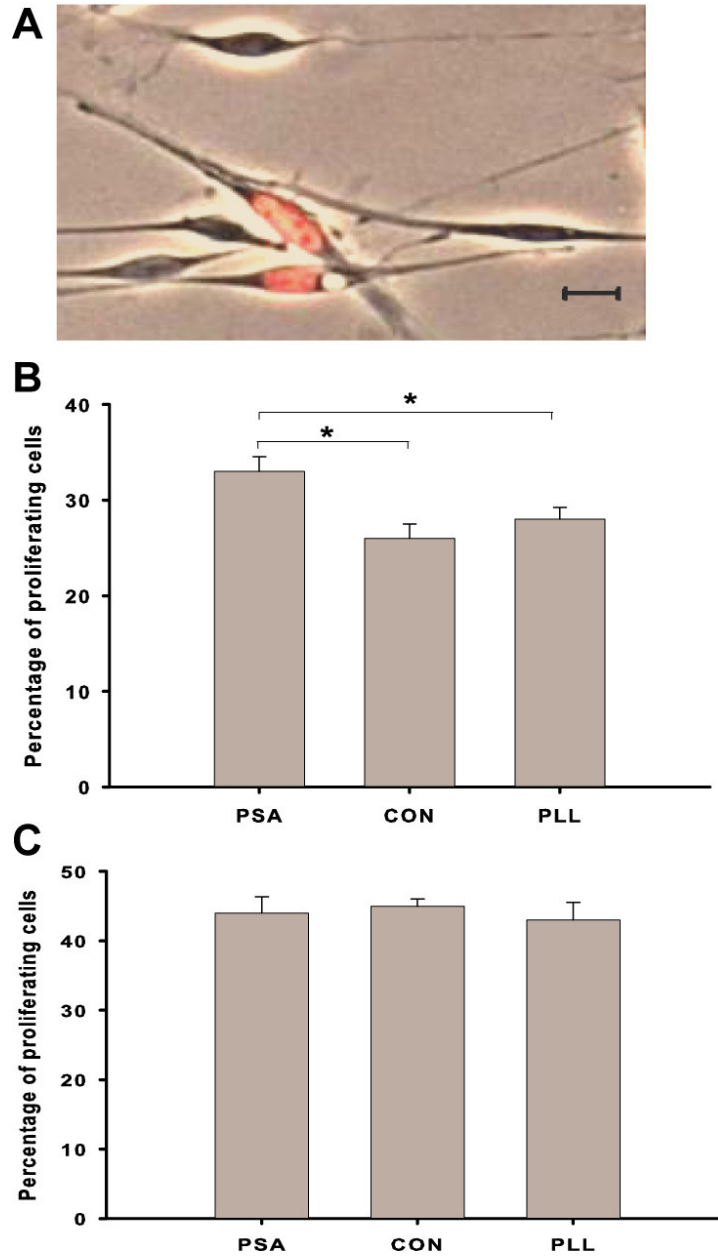


Figure 21: Analysis of Schwann cell proliferation *in vitro*. (A) Primary cultures from peripheral nerves were treated with 20 μ M BrdU, 4 hours after seeding for 48 hours to label proliferating cells. Schwann cells were identified by phase contrast microscopy as elongated bipolar cells (scale bar, 20 μ m). The number of Schwann cells with BrdU-labeled nuclei (red staining) was estimated in cultures derived from wild type (B) and NCAM-deficient mice (C) and expressed as percentage of all Schwann cells. The proportion of BrdU-labeled Schwann cells was significantly higher in cultures grown on substrate-coated PSA mimicking peptide than on control peptide (CON) or poly-L-lysine (PLL) (* $p < 0.05$, ANOVA with Tukey's post-hoc test).

To obtain insights into the cell recognition mechanism that underlies the PSA effects on cultured Schwann cells, we first tested whether these effects were dependent on the expression of NCAM, the glycoprotein carrier of PSA on the Schwann cell surface. We isolated Schwann cells from NCAM-deficient mice and tested their response to the PSA mimetic. In contrast to the wild-type cells, NCAM-deficient Schwann cells were not stimulated by the PSA mimetic. Neither process elongation (Figure 20C) nor cell proliferation (Figure 21C) was stimulated in NCAM-deficient Schwann cells. To rule out that process elongation of NCAM-deficient Schwann cells was generally impaired, cells were grown on laminin, which is known to strongly stimulate process formation. NCAM-deficient and wild-type Schwann cells showed similar process elongation (Figure 20B, C), demonstrating that NCAM-deficient Schwann cells are generally responsive to stimulatory agents. As Schwann cells express both, PSA and NCAM at the cell surface and on processes (Figure 22), the PSA mimetic acts on NCAM present at the Schwann cell surface or disrupts a PSA-dependent interaction of NCAM with itself or PSA-NCAM interaction partners. To further understand the influences of the PSA mimicking peptide on Schwann cell growth, we used inhibitors for the fibroblast growth factor receptor (FGFR), a receptor known to be involved in NCAM-dependent neuritogenesis (Doherty and Walsh, 1996). Application of two different FGFR inhibitors (PD173074 and SU5402) abolished the stimulatory effect of PSA on process elongation in wild-type Schwann cells (Figure 23A, B). Moreover, SU5402 inhibited the stimulatory effect also of L1 (Figure 23B), which is known to interact with the FGFR to stimulate neuritogenesis (Doherty and Walsh, 1996).

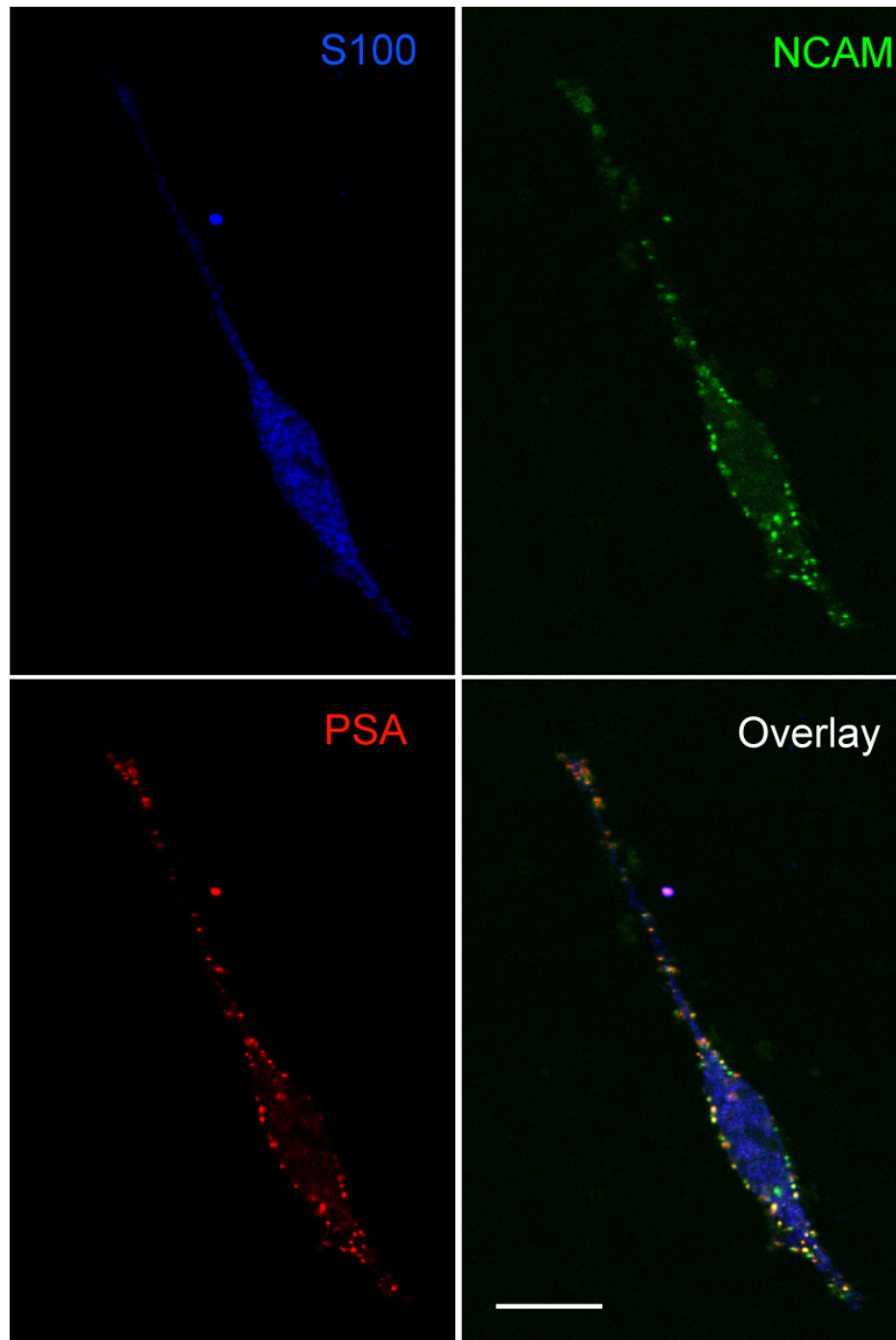


Figure 22: Immunostaining of Schwann cells for PSA and NCAM protein after 24 hours in culture. Primary cultures of Schwann cells were stained with PSA and NCAM specific monoclonal antibodies and thereafter stained with the Schwann cell specific S-100 antibody. Schwann cells express NCAM and PSA at the cell surface and on processes (scale bar, 10 μ m).

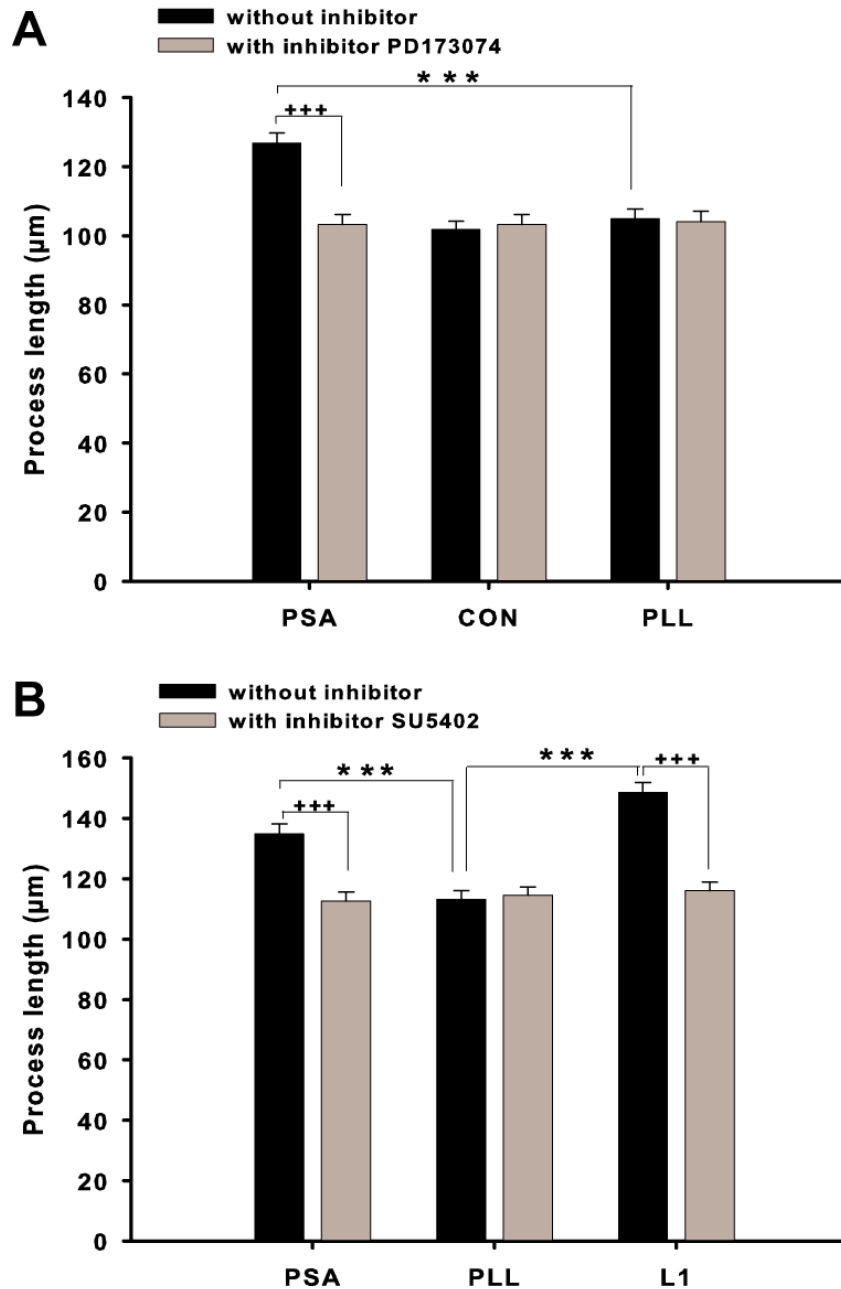


Figure 23: Analysis of Schwann cell growth in vitro after application of fibroblast growth factor receptor (FGFR) inhibitors. (A) Application of the inhibitor PD173074 significantly reduces process elongation in Schwann cells cultured on PSA mimetic coating. (B) Application of another inhibitor, SU5402, reduces the stimulatory effect on process outgrowth not only of PSA mimetic, but also of L1 which is known to stimulate neurite growth via FGFR (** $p < 0.001$, one-way ANOVA with Dunnett's post-hoc test) (+++ $p < 0.001$, t-test).

5.1.6. The PSA mimetic enhances Schwann cell proliferation *in vivo*

After determining the effect of the PSA mimetic on myelination *in vivo* and on Schwann cells *in vitro*, we examined its effect on cell proliferation *in vivo*. We estimated Schwann cell proliferation using S-100 and BrdU immunostaining of sections from the motor and sensory branch 6 days after nerve transection and application of control peptide or PSA mimetic. The analysis was performed using sections collected immediately distal to the bifurcation of the femoral nerve, i.e. at about 3-4 mm distal to the cuff containing PSA or control peptide. In both the motor and the sensory branch, we found higher numbers of S-100 cells that have incorporated BrdU, applied at day 2 and day 5 after operation, in PSA treated mice than in control treated animals (Figure 24). This finding indicates that the PSA mimetic enhances Schwann cell proliferation during the period of Wallerian degeneration and that this effect is not restricted to the immediate vicinity of the nerve cuff in which the mimetic has been applied.

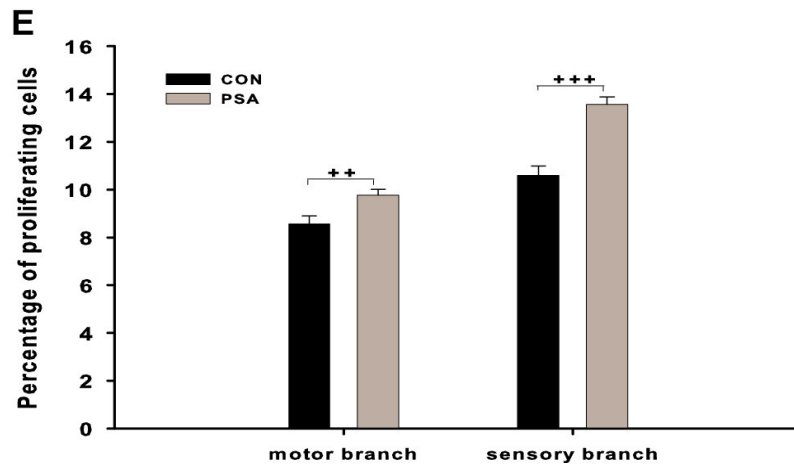
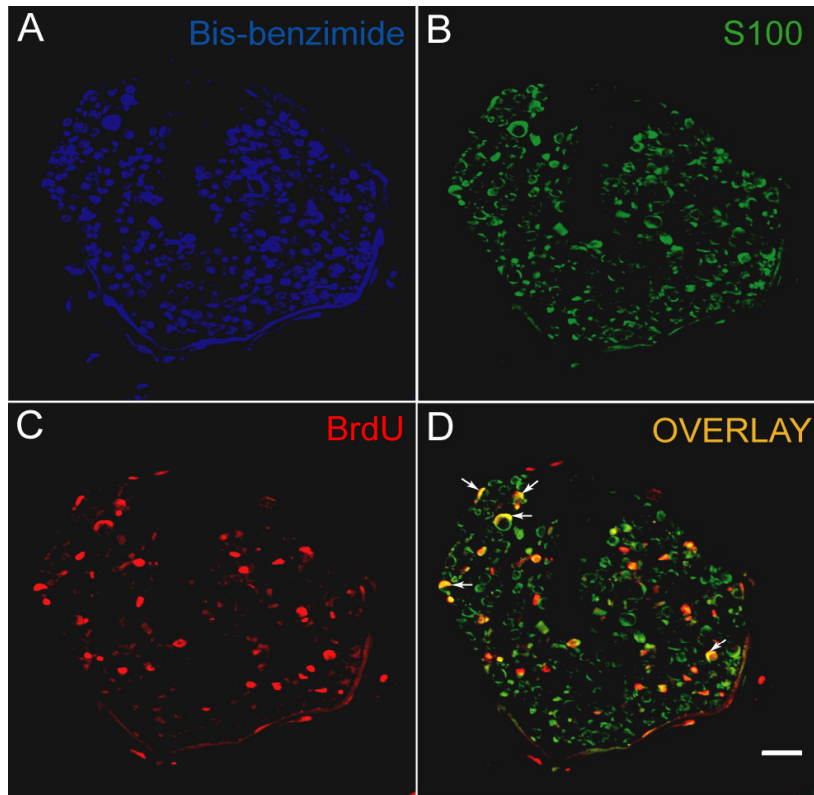


Figure 24: Analysis of Schwann cell proliferation *in vivo*. (A-D) Transverse sections from femoral nerves at and immediately distal to the level of bifurcation of the motor and sensory branch were stained with antibodies against S-100, a specific marker for Schwann cells (B), the proliferation marker BrdU (C) and with bis-benzimide to visualize cell nuclei (A). Proliferating Schwann cells were identified as S-100- and BrdU-positive cells (some indicated by arrows in the overlay of the S-100 and BrdU staining shown in panel D, scale bar, 60 μ m). (E) The percentage of proliferating Schwann cells (S-100- and BrdU-positive / S-100-positive) is significantly higher after PSA mimetic treatment as compared with control peptide (CON) ($++ p < 0.01$ and $+++ p < 0.001$, t-test).

5.2. Effect of glycomimetics after spinal cord injury

5.2.1. Delivery of peptides to the injured spinal cord

First, we analyzed the efficacy of peptide delivery to the injured spinal cord via an Alzet osmotic pump. Since glycomimetics cannot be distinguished with antibodies from the endogenous epitopes which they mimic, we infused an exogenous protein fragment, human immunoglobulin Fc, which is not expressed in the mouse spinal cord. Two weeks after compression of the thoracic spinal cord and continuous infusion of 12.5 µg/ml protein at the sacral level over this time-period, the Fc fragment was well detectable by immunoblot analysis in the sacral segments of the spinal cord (Figure 25A). At the lumbar level, Fc protein was less detectable, and no Fc was detectable in the thoracic segments, i.e. at the site of injury (Figure 25A). These observations indicated that high protein or peptide concentrations were necessary to create an efficient diffusion gradient for its remote delivery. Indeed, infusion of the Fc fragment at 200 µg/ml resulted in a more homogeneous distribution of the protein in the caudo-rostral axis, with an efficient delivery up to the thoracic spinal cord (Figure 25B). Considering these results, we applied the PSA and HNK-1 mimetics at 500 µg/ml, the highest concentration at which the peptide solutions did not form precipitates, when kept at 37°C under sterile conditions in vitro over a two-week time period.

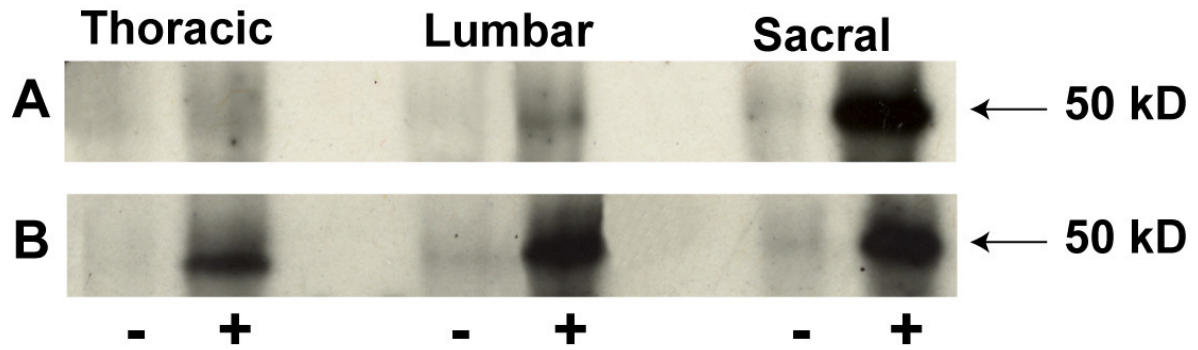


Figure 25: Efficacy of protein application to the acutely injured mouse spinal cord. Western blot analysis of thoracic, lumbar and sacral spinal cord tissue homogenates after pump application of PBS (-) or of a human IgG Fc fragment (+) into the cauda equina over a two-week time period. Lane A shows homogenates from spinal cords which received 12.5 µg/ml Fc, and lane B shows homogenates from spinal cords which received 200 µg/ml Fc. Note that a high concentration is necessary to reach the thoracic part where the lesion is performed. 40 µg of protein were loaded into each lane.

5.2.2. Improved motor recovery after immediate post-traumatic administration of a PSA mimetic

We designed four experimental groups in which either control peptide, PSA mimetic, HNK-1 mimetic or combination of PSA plus HNK-1 mimetic were applied during the first two weeks after injury. Spinal cord compression caused severe locomotor disabilities in all mice, as assessed by the BMS values at 1 week after injury (Figure 26A). Between 1 and 6 weeks, the walking abilities improved more in mice which received PSA and PSA/HNK-1 mimetics than in mice treated with control peptide or HNK-1 mimetic (Figure 26A). In addition to the BMS, we analyzed the plantar stepping ability of the animals using our previously described parameter, the foot-stepping angle (Apostolova et al., 2006). This analysis revealed, in agreement with the BMS, better recovery in the PSA and PSA/HNK-1 mimetic groups than in mice treated with

HNK-1 mimetic or control peptide at both 3 and 6 weeks after injury (Figure 26B). We further evaluated more complex motor functions than plantar stepping (Apostolova et al., 2006). Analysis of the rump-height index, a measure of the ability to support body weight during ground locomotion, showed similar, severe degree of disability at 1 week after injury and similar recovery thereafter in all experimental groups (Figure 26C). However, the ability of animals to perform voluntary movements without body weight support, estimated by the extension-flexion ratio, recovered significantly better with PSA and PSA/HNK-1 mimetic treatment than with control peptide or HNK-1 mimetic (Figure 26D). Finally, independent of treatment, numbers of correct steps made by the animals during inclined ladder climbing were reduced to almost 0 one week after injury and did not significantly improve at 3 and 6 weeks (data not shown). Overall, these results show that treatment with the PSA mimetic, alone or in combination with the HNK-1 mimetic, but not HNK-1 mimetic alone, improves the functional outcome of compression spinal cord injury compared with the control treatment. This conclusion is further validated by comparisons of overall recovery indices of individual mice from the 4 experimental groups (Figure 26E).

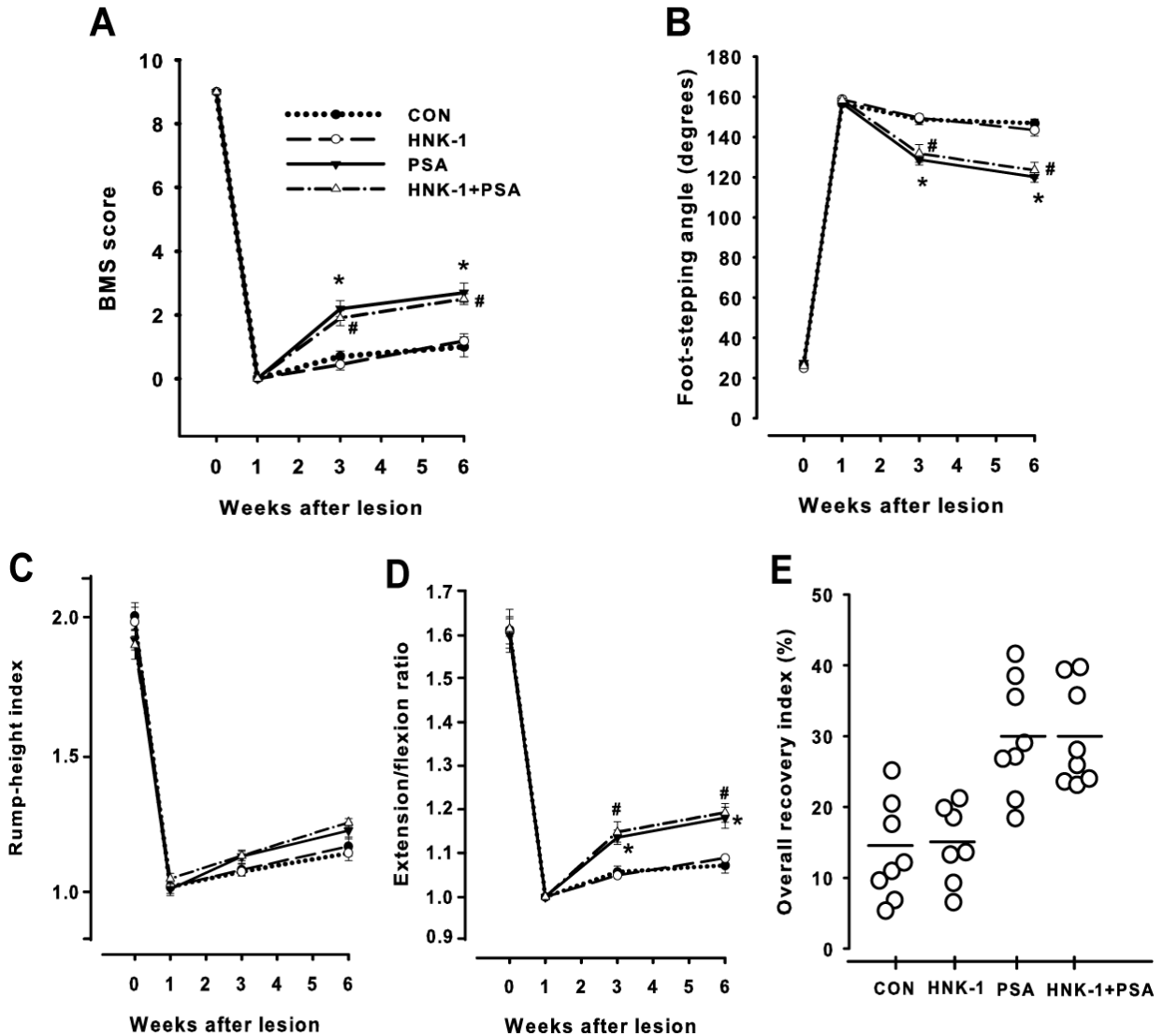


Figure 26: Analysis of motor function. Time course and degree of recovery in mice treated with PSA, HNK-1, HNK-1+PSA and control peptide (CON) after acute spinal cord injury. Shown are mean \pm SEM values of open-field locomotion (BMS) scores (A), foot-stepping angles (B), rump-height indices (C) and extension-flexion ratios (D). Asterisk and cross-hatches indicate significant differences between the mean values of the individual groups at a given time period ($p < 0.05$, one-way ANOVA for repeated measurements with Tukey's post hoc test; $n = 10$ mice per group). Panel E shows overall recovery indices in individual mice at 6 weeks after injury (each circle represents one mouse). Horizontal lines in E indicate groups' mean values. The recovery index is an individual animal estimate calculated in percent as $[(X_{7+n} - X_7) / (X_0 - X_7)] \times 100$, where X_0 , X_7 and X_{7+n} are values prior to operation, 7 days after injury, and a time-point n days after the spinal cord injury, respectively. In simpler terms, this measure estimates gain of function after the first week ($X_{7+n} - X_7$) as a fraction of the functional loss ($X_0 - X_7$) induced by the operation. An overall recovery index is the mean of the recovery indices calculated for the parameters shown in panels A-D.

Both the BMS and the numerical parameters used for our functional analysis strongly depend on the lesion severity (Kloos et al., 2005; Apostolova et al., 2006). We thus estimated lesion scar volume in control mice, as well as in mice treated with PSA and HNK-1 mimetics at 6 weeks after injury. The mean volume of the lesion scar was similar in all three groups of mice (0.14 ± 0.01 , 0.15 ± 0.02 , and 0.15 ± 0.02 mm³, in PBS, PSA and HNK-1 treated groups, respectively; $p > 0.05$, ANOVA with Tukey's post-hoc tests). We conclude that enhanced functional recovery after PSA mimetic treatment is not related to attenuated tissue scarring.

We also considered the possibility that the infused peptides might be immunogenic. To address this issue, we stained spinal cord sections from animals treated with PSA mimetic, HNK-1 mimetic or control peptide with antibodies against CD4 and CD8, markers of T-helper and T-cytotoxic lymphocytes, respectively. At six weeks after injury and initiation of the two-week peptide infusion, we found only a few lymphocytes, often apparently located in blood vessels, per spinal cord section in all groups (9.0 ± 0.7 , 9.5 ± 0.8 and 8.7 ± 0.8 in control peptide, PSA mimetic and HNK-1 mimetic treated mice, respectively (Figure 27C, $p > 0.05$, one-way ANOVA with Tukey's post hoc test). This finding indicates that the infused peptides do not cause inflammatory responses.

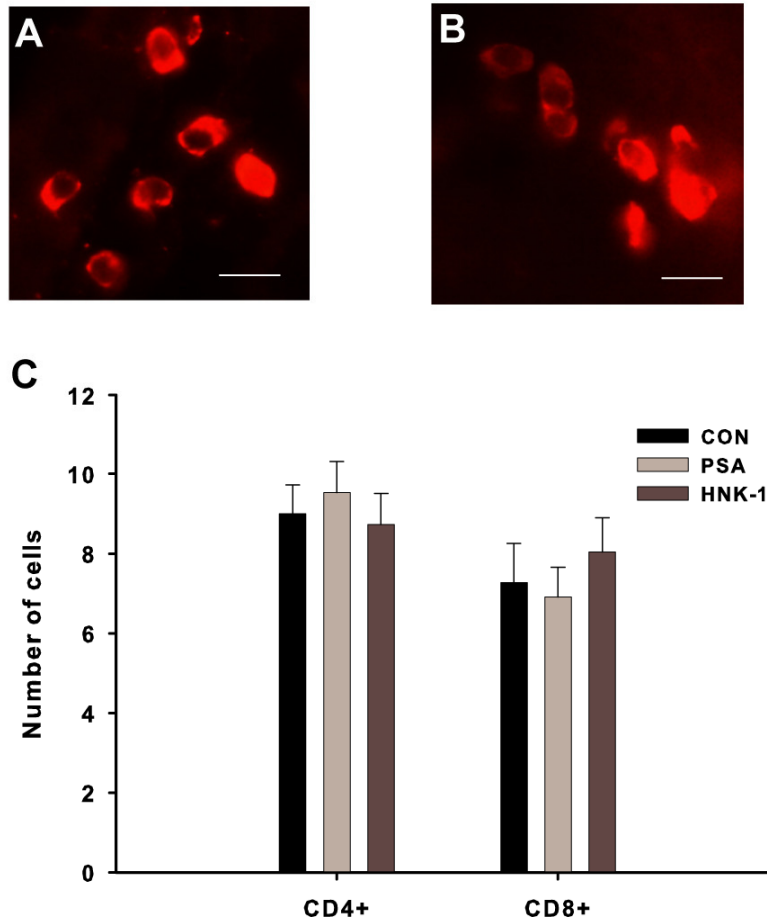


Figure 27: Analysis of the number of CD4+ and CD8+ cells in the spinal cord after infusion of control, PSA mimetic and HNK-1 mimetic. (A) and (B) show CD4+ and CD8+ cells respectively. (C) Mean values \pm SEM of CD4+ and CD8+ cells at 6 weeks after acute spinal cord injury and application of PSA mimetic, HNK-1 mimetic, and control peptide (CON) are shown. No difference in the number of immune cells was found among the groups ($p > 0.05$ one way ANOVA with Dunnett's post hoc test). $N = 5$ animals per group. Scale bar 10 μ m.

5.2.3. Enhanced catecholaminergic, cholinergic and glutamatergic innervation in the lumbar spinal cord after PSA treatment

Recovery of locomotor abilities after spinal cord injury depends on the extent of regrowth and/or sprouting of monoaminergic axons (Crutcher and Bingham, 1978;

Heckman et al., 2003; Jakovcevski et al., 2007a). To assess whether improved motor functions in PSA mimetic treated mice were related to enhanced monoaminergic innervation of the spinal cord caudal to the injury, we counted numbers of catecholaminergic (TH⁺) axons projecting beyond an arbitrarily selected border 250 μm caudally to the lesion site in spaced serial parasagittal sections 6 weeks after the injury (Figure 28A). The number of TH⁺ axons per section in PSA mimetic treated mice was significantly higher than in control peptide or HNK-1 mimetic treated animals (Figure 28B, $p < 0.01$, Wilcoxon–Mann–Whitney test). This observation indicates a more vigorous regenerative response, i.e. axonal regrowth and/or sprouting, of monoaminergic fibers in the injured spinal cord upon application of PSA mimetic which is in agreement with better recovery after PSA treatment.

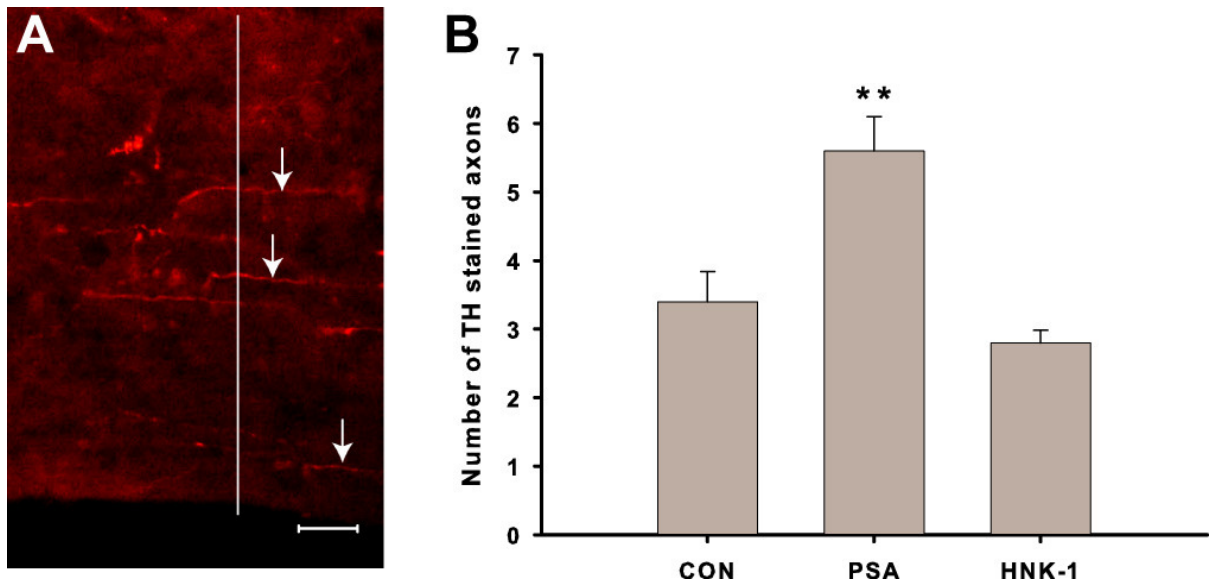


Figure 28: Analysis of the monoaminergic innervation of the lumbar spinal cord after treatment with control peptide (CON) and PSA or HNK-1 mimetics of the acutely injured mouse spinal cord. (A) Representative image of tyrosine hydroxylase (TH) staining in the lumbar spinal cord 6 weeks after injury. Noradrenergic axons are descending modulatory inputs from the brainstem. (B) Mean numbers per section of TH⁺ axons crossing an arbitrary border 250 μm caudally from the lesion site (vertical line in A) at 6 weeks after the lesion (** $p < 0.01$; $n = 5$ mice per group; Wilcoxon–Mann–Whitney test). Scale bar 20 μm.

The density of large perisomatic cholinergic (ChAT⁺) boutons, known to form C-type synapses on motoneurons associated with muscarinic type 2 receptors (Davidoff and Irintchev, 1986; Hellström et al., 2003), is strongly reduced in the lumbar spinal cord after thoracic spinal cord compression in mice (Apostolova et al., 2006, Jakovcevski et al., 2007a). Importantly, the locomotor performance assessed by the BMS score or the foot-stepping angle positively correlates with the number of these terminals 6 weeks after spinal cord injury (Jakovcevski et al., 2007a). We measured cholinergic synaptic coverage of motoneuron cell bodies in PSA mimetic, HNK-1 mimetic and control peptide treated animals (Figure 29A, B). Compared with control peptide, the number of ChAT⁺ terminals was significantly increased (+ approximately 15%) in PSA, but not in HNK-1 mimetic treated mice (Figure 29B, $p < 0.05$, one-way ANOVA with Dunnett's post-hoc test). The number of cholinergic synapses on motoneurons in the intact spinal cord is clearly higher than all the other groups (Figure 29B, $p < 0.01$, one-way ANOVA with Tukey's post-hoc test). We conclude that infusion of PSA mimetic limits synaptic loss and/or promotes reestablishment of synaptic connections to lumbar motoneurons after injury, thus positively influencing recovery of motor functions.

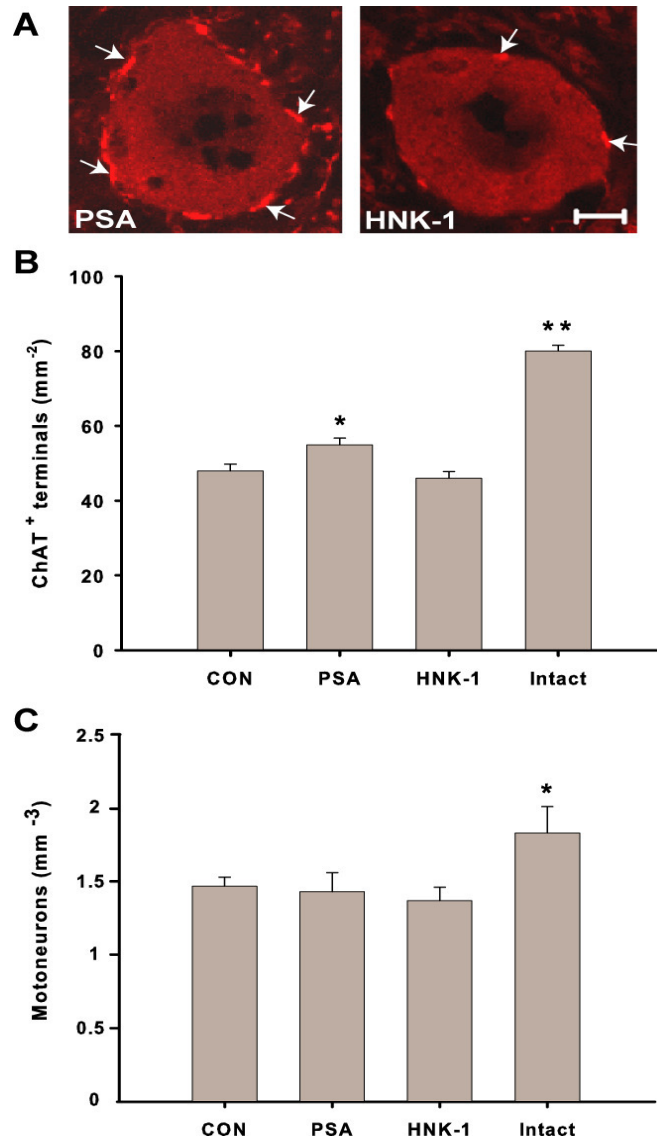


Figure 29: Analysis of cholinergic terminals and motoneuron numbers in the lumbar spinal cord caudal to the injury site after treatment with control peptide (CON), PSA or HNK-1 mimetics. (A) Individual motoneurons with ChAT⁺ perisomatic terminals indicated by arrow heads (scale bar 5 μ m). ChAT terminals are excitatory inputs from interneurons. (B) Higher numbers of cholinergic synapses were found around motoneurons of mice treated with PSA glycomimetic compared to control peptide (asterisk, $p < 0.05$, one-way ANOVA with Dunnett's post hoc test). Compared to the intact spinal cord, there was a clear loss of cholinergic synapses in all the groups after injury ($p < 0.01$, one-way ANOVA with Tukey's post-hoc test). Approximately 100 motoneurons were analyzed per group (5 animals). (C) No difference among the groups was found for motoneuron density in the lumbar spinal cord after injury and glycomimetic treatment. But interestingly, motoneuron density in intact spinal cord is significantly higher than in all the other groups, indicating motoneuron loss after injury (asterisk, $p < 0.05$, one-way ANOVA with Tukey's post hoc test).

To evaluate whether the glycomimetics used in this study influence cell survival, we analyzed motoneuron densities in the lumbar spinal cord and found no differences between mice treated with PSA mimetic, HNK-1 mimetic or control peptide (Figure 29C). However there was a significant reduction of motoneuron density in all groups compared to intact spinal cord, indicating motoneuron loss after injury ($p < 0.05$, one-way ANOVA with Tukey's *post hoc* test). As for motoneuron soma size, no effect of PSA or HNK-1 mimetics, as compared with control treatment, was found (data not shown). These findings indicate that different outcomes of spinal cord injury in PSA and HNK-1 mimetic treated mice cannot be related to different, positive or adverse, effects on motoneurons.

The degree of locomotor recovery after spinal cord injury is largely determined by preservation and functionality of primary afferent inputs (Dietz, 2002; Lavrov et al., 2008). We were, therefore, interested whether spinal cord connectivity is altered in mimetic-treated mice compared with controls. We analyzed VGLUT1⁺ synaptic terminals, which are derived from medium- to large-sized neurons in the dorsal root ganglia and convey mechano- and proprioceptive information to the spinal cord (Brumovsky et al., 2007). We selected three areas for analysis in which VGLUT1⁺ terminal densities were prominent: Clarke's column which receives proprioceptive information, an adjacent part of lamina VII, a lamina in the spinal cord containing, among other neurons, last-order interneurons, i.e., innervating motoneurons, and the motoneuron region, lamina IX, where proprio- and mechanoreceptors form contacts predominantly on motoneuron dendrites (Figure 30A). We analyzed VGLUT1⁺ terminal density at the end-point of our study, 6 weeks after injury. In mice treated with control,

PSA and HNK-1 peptides there was no difference in density of VGLUT1⁺ terminals in Clarke's column, but in lamina VII the density was increased after treatment with both PSA and HNK-1 mimicking peptides (Figure 30B). Additionally, after treatment with HNK-1 peptide there was a small but significant increase in the density of VGLUT1⁺ terminals in lamina IX, around motoneurons, compared with both control and PSA mimetic-treated animals. This treatment-related difference indicates that glycomimetic infusion results in an area-specific increase in afferent inputs to the injured spinal cord. Interestingly, values of glutamatergic density in intact spinal cord show that spinal cord injury leads to a significant loss of glutamatergic synapses in Laminae VII and IX but not in the Clarke's column (* $p < 0.05$ and *** $p < 0.001$, one-way ANOVA with Tukey's *post hoc* test).

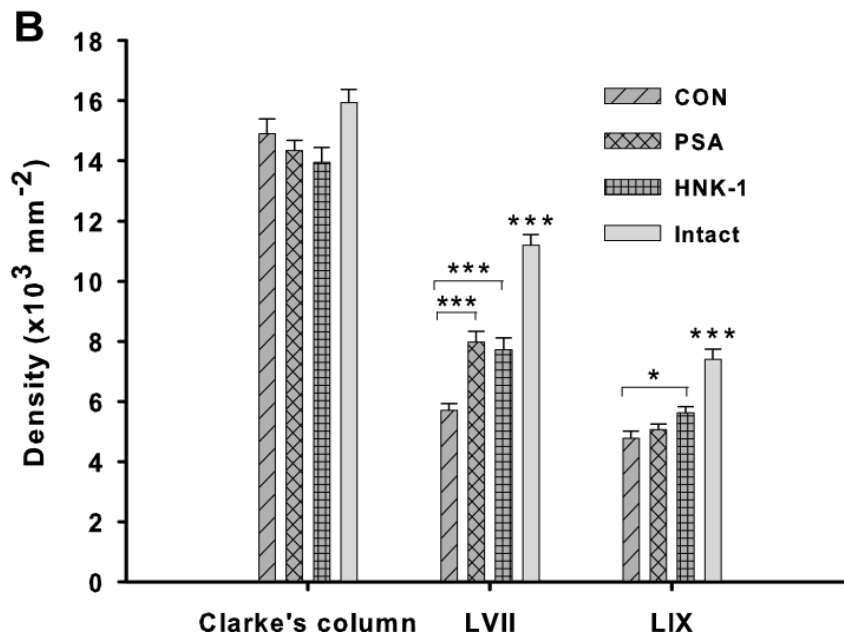
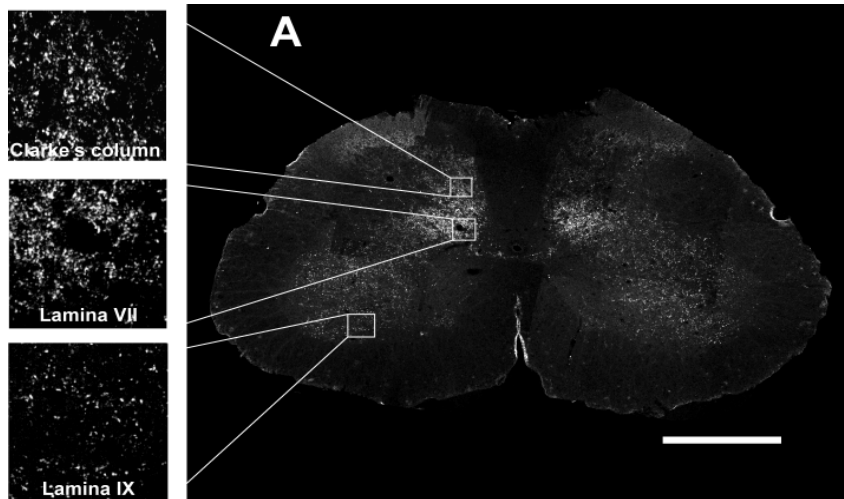


Figure 30: Analysis of VGLUT1 terminal densities in the lumbar spinal cord after injury and treatment with control peptide (CON) and PSA or HNK-1 mimetics. (A) Representative image of a VGLUT1 stained spinal cord (scale bar 200 μm). Glutamate is an excitatory neurotransmitter released in the spinal cord by upper motoneurons and some interneurons.

(B) Density (means + SEM) of VGLUT1⁺ terminals in spinal cords of control, PSA and HNK-1 peptide treated mice, measured in three different areas: Clarke's column, lamina VII and lamina IX (see (A)). Compared with control mice, more glutamatergic synapses were found in lamina VII in both PSA and HNK-1 treated mice, and in lamina IX after HNK-1 treatment (* $p < 0.05$ and *** $p < 0.001$, one-way ANOVA with Dunnett's post hoc test). In the intact spinal cord, glutamatergic density is significantly higher than in all the other groups in Laminae VII and IX but not in the Clarke's column (* $p < 0.05$ and *** $p < 0.001$, one-way ANOVA with Tukey's post hoc test). $N = 5$ animals per group.

5.2.4. PSA treatment enhances axonal myelination rostral to the site of injury

PSA plays an important role in primary myelination and remyelination (Charles et al., 2000, 2002; Jakovcevski et al., 2007b; Papastefanaki et al., 2007). Also the PSA mimetic used here has a beneficial effect on axonal remyelination as recently shown in a peripheral nerve lesion model in mice (Mehanna et al., 2009). Since spinal cord injury is associated with considerable demyelination, we hypothesized that the beneficial effect of the PSA mimetic on motor recovery after spinal cord injury could be mediated by promotion of CNS myelination. We stained serial horizontal sections of spinal cords treated with PSA mimetic, HNK-1 mimetic and control peptide with Luxol Fast Blue. Analysis of the areas occupied by Luxol Fast Blue-positive structures within the borders 5 mm rostral to 5 mm caudal from the lesion site was similar in the three experimental groups (data not shown), indicating that superior functional recovery was not related to better remyelination or reduced demyelination in the PSA mimetic-treated group. In accordance with this notion, a more refined analysis of the degree of axonal myelination by measuring g-ratios (axon-to-fiber diameters of individual axons) in semi-thin sections from the ventral white matter in the lumbar spinal cord revealed no differences among the animal groups (data not shown). However, the PSA mimetic showed a considerable effect on the relative degree of myelination proximal to the injury site. While the g-ratios in control peptide treated mice were increased (indicating worse myelination) compared with uninjured mice, the frequency distribution of the g-ratios were near-normal in PSA mimetic and, interestingly, also in HNK-1 mimetic treated animals (Figure 31).

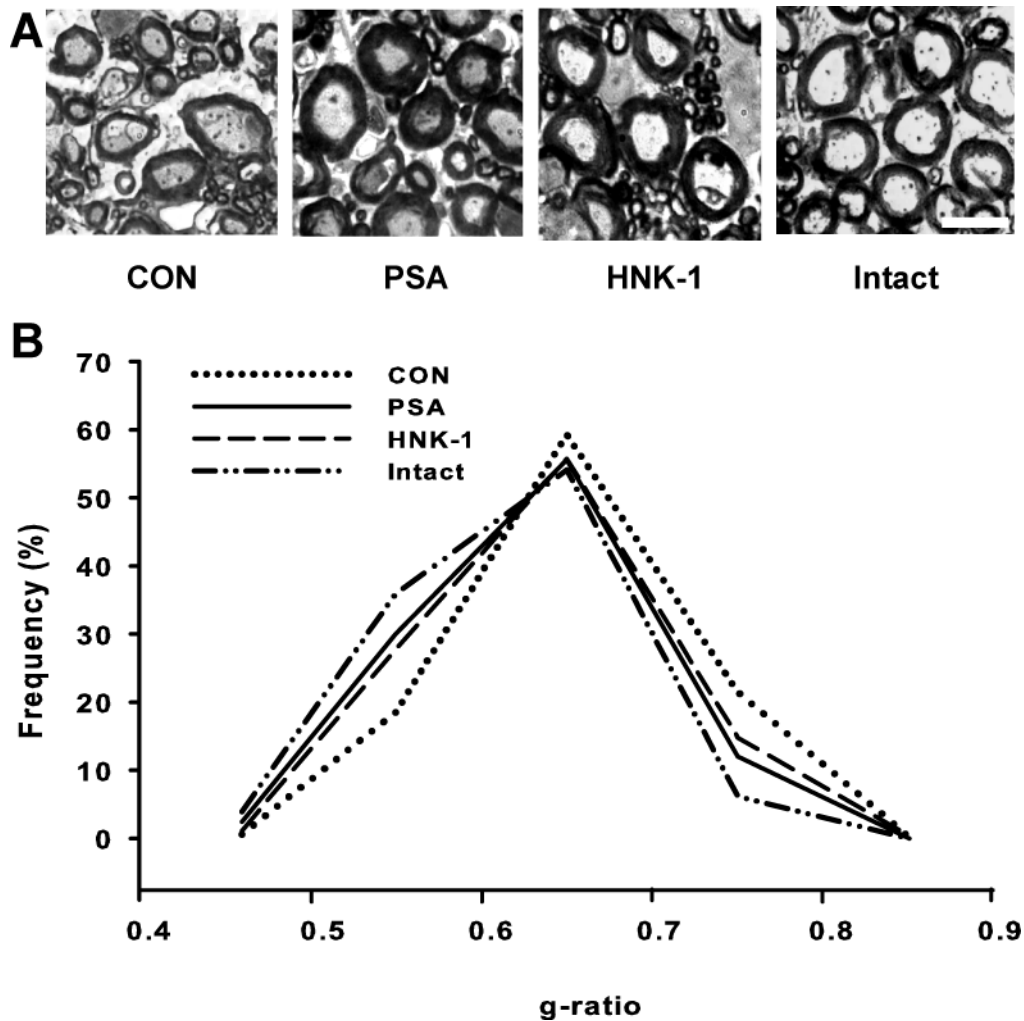


Figure 31: Analysis of axonal myelination proximal to the spinal cord injury. (A) Representative images of axons from spinal cords of mice treated with control peptide (CON), PSA mimetic, HNK-1 mimetic, as well as from intact mice are shown (scale bar 3 μ m). (B) Frequency distributions of g-ratios in the four groups. Animals treated with PSA and HNK-1 mimetics have significantly better myelination compared with control peptide as shown by the shift to lower g-ratio values ($p < 0.05$, Kolmogorov-Smirnov test). Five animals and approximately 500 axons were analyzed per group.

The overall results do not allow the conclusion that the PSA mimetic has a direct effect on axonal myelination. The improvement observed most distally to the site of PSA mimetic application, i.e. rostral to the injury site at mid-thoracic level, might be a secondary phenomenon related to better preservation and/or regeneration of axons

above the lesion site, which would then be more prone to myelination. Nevertheless, better axonal myelination rostral to the injury may contribute to better functional recovery after PSA mimetic application.

5.2.5. The therapeutic time window of the PSA mimetic is limited to acute spinal cord injury

Considering that PSA mimetic application immediately after injury leads to enhanced recovery of locomotor function, we tested whether a similar beneficial outcome could be achieved when PSA is applied three weeks after spinal cord injury. At this time point the cellular consequences of injury, such as scar formation, and most of the spontaneous locomotor recovery in C57BL/6J mice have been reached (Basso et al., 2006; Apostolova et al., 2006; Jakovcevski et al., 2007a), but in the lumbar spinal cord caudal from the lesion site some tissue remodeling is still active (Lee et al., 2009). We infused PSA mimetic, HNK-1 mimetic, control peptide or vehicle (PBS) to different groups of C57BL/6 mice 3 weeks after lesion and analyzed locomotor recovery in a way similar to that used for acute application. No differences among the groups were found for any of the parameters measured (Figure 32A-D). This finding suggests that PSA mimetic treatment is effective only when initiated during the acute phase of spinal cord injury.

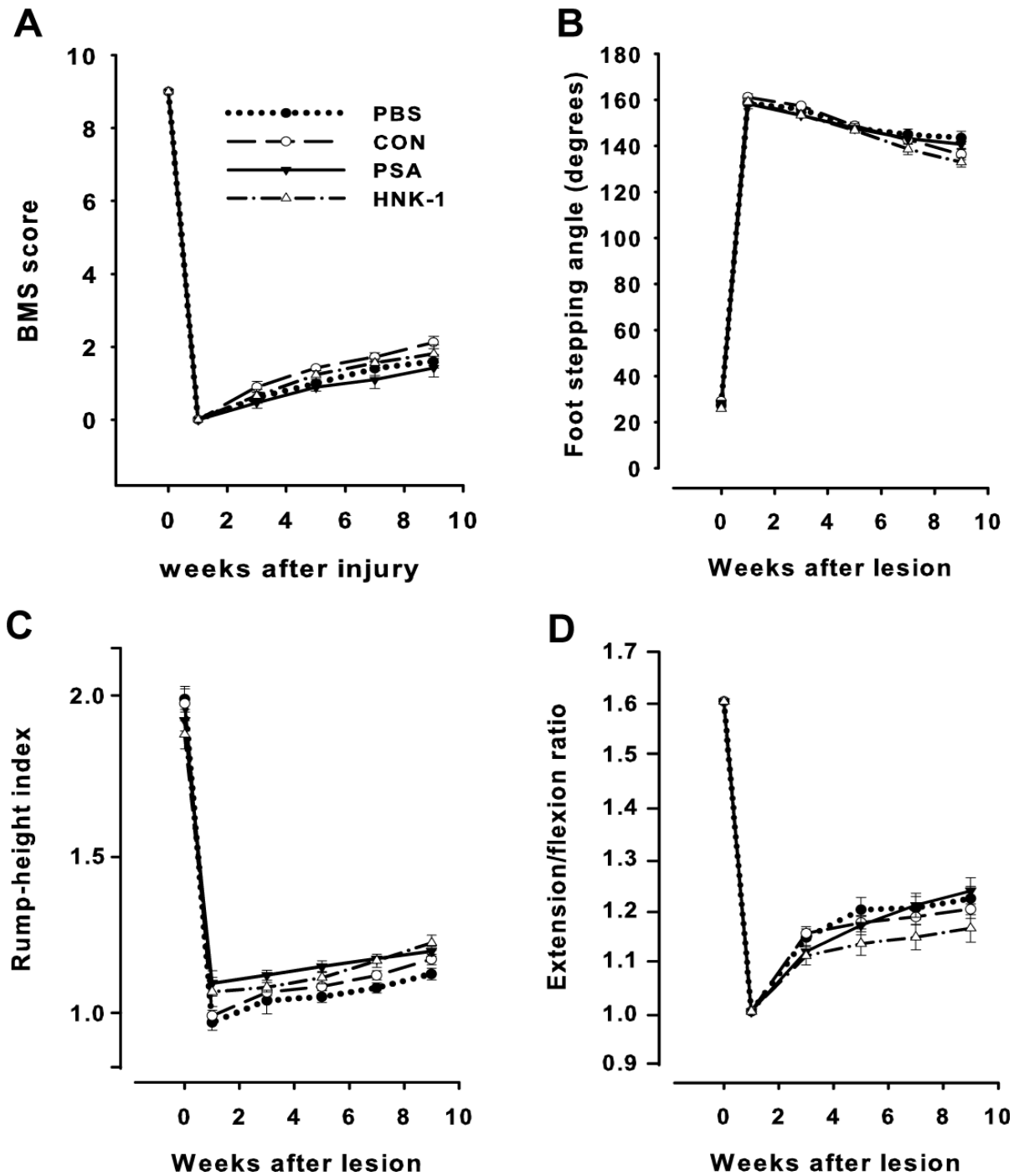


Figure 32: Analysis of motor functions after glycomimetic application to chronically injured spinal cord. Time course and degree of recovery in mice in which treatment with PBS, control peptide (CON), HNK-1 or PSA mimetics was initiated at 3 weeks after injury. Shown are mean \pm SEM values of open-field locomotion (BMS) scores (A), foot-stepping angles (B), rump-height indices (C) and extension-flexion ratios (D). No differences among the groups were found at any time-point studied ($p > 0.05$, one-way ANOVA for repeated measurements with Tukey's post hoc test; $n = 10$ mice per group).

6. Discussion

6.1. Effect of glycomimetics in the femoral injury

This study provides first evidence that PSA mimicking peptides are beneficial agents for treatment of peripheral nerve injuries. After a single application of the mimetics performed during surgical reconstruction of the injured femoral nerve of adult C57BL/6J mice, we observed strongly improved axonal remyelination and enhanced functional outcome as measured by recovery of locomotor behaviour. As indicated by results of cell culture experiments, the likely mechanism underlying these effects is NCAM-mediated stimulation of Schwann cell process elongation and proliferation.

6.1.1. Improvement of motor function by PSA mimetic

We attribute the observed effects to the structural similarity of the mimicking peptides with the PSA glycan itself and thus to PSA related functional effects. Lack of effects of a control peptide with undetectable binding to the monoclonal PSA antibody 735 indicates PSA-induced specificity. More importantly, both a linear and a cyclic PSA mimicking peptide of different amino acid sequences, but high affinities for the PSA antibodies 735 (linear peptide) and MenB (cyclic peptide), were effective. The evidence for better recovery of function was obtained using an objective video-based analysis of parameters directly related to the quadriceps muscle function that has proved to be reliable and sensitive (Irintchev et al., 2005; Eberhardt et al., 2006; Simova et al., 2006; Ahlborn et al., 2007). Therefore, better recovery of functional parameters after glycomimetic treatment, observed in two independent experiments using different PSA mimetics, shows that functional improvement is related to the

treatment. We have observed similar positive effects on recovery after femoral nerve lesion in mice using HNK-1 mimicking peptides (Simova et al., 2006). The time course of improvement is similar for the HNK-1 and PSA mimetics, with positive effects becoming apparent later, i.e. at 2-3 months after injury and treatment. Based on results of the morphological analyses, HNK-1 effects were attributed to trophic support of the regenerating motoneurons indicated by reduced motoneuron death and increased motoneuron soma size and diameters of regenerated axons. Such trophic effects were not observed with the PSA mimetics. The only marked structural effect of the PSA mimetic treatment was better remyelination, and this effect was more pronounced than the one achieved by HNK-1 mimetic application. Therefore, the question arises whether better remyelination alone can explain enhanced motor recovery. We believe that this explanation is plausible since reduced remyelination has been considered as a major factor limiting recovery after peripheral nerve lesions (Smith and Hall, 1980; Chen et al., 2007). Thus these observations not only on improved locomotor recovery, but also improved remyelination after injury are of interest from a therapeutic point of view.

6.1.2. Mode of PSA mimetic action

Another issue is how a single intra-operative application of a peptide can produce late-appearing and long-lasting effects. Although a fibrin coat is formed around a nerve-guide chamber after 24 to 48 hours preventing leakage of the guide's contents (Hekimian et al., 1995) and a gel-forming matrix was used to immobilize the PSA mimetic, its local availability is most likely limited to hours or at best days, because of

degradation by peptidases originating from the damaged tissue and infiltrating proteolytically active immune cells. We favor the explanation that the PSA mimetic causes priming of the injured femoral nerve, both at and around the lesion site, in the sense that early cellular and molecular responses to injury are modulated so that the subsequent regeneration process is favorably influenced over weeks. Considering our *in vitro* and *in vivo* data on the enhanced proliferation and process elongation by Schwann cells, we propose that the PSA mimetic stimulates the early response of these cells to injury *in vivo*. Schwann cells play a critical role during regeneration. They provide mechanical and trophic support for axonal growth. After injury, myelin debris as well as macrophages that invade the lesion site induce Schwann cell proliferation (Fawcett and Keynes, 1990). These proliferating cells produce neurotrophic factors (e.g. NGF, GDNF) that are vital for the process of axonal regeneration (Mirsky et al., 2002). Schwann cell proliferation induced by PSA mimetic should then be beneficial for regeneration. In addition, the enhanced elongation of Schwann cell processes with PSA mimetic may also be beneficial since these processes are responsible for axonal ensheathment and myelination (Allt, 1972).

The idea of priming the nerve by PSA mimetic, at and around the lesion site, is supported by previous observations of long-lasting positive effects after a single intra-operative application of an HNK-1 mimicking peptide to the severed femoral nerve of adult mice (Simova et al., 2006). In this case, we proposed that priming is achieved by activation of the RAGE (receptor for advanced glycation end-products) signaling pathway (Chou et al., 2004). Another example for long-lasting effects of a short-term post-operative treatment is brief low-frequency electrical stimulation (1 hour, 20 Hz) of

the proximal nerve stump of the femoral nerve immediately after nerve transection and surgical repair. This treatment significantly shortens the period of asynchronous -and staggered over weeks- axonal regrowth after femoral nerve lesion in rats (Al Majed et al., 2000a; Brushart et al., 2002) and accelerated functional recovery after femoral nerve lesion in mice (Ahlborn et al., 2007). These beneficial effects are associated with an accelerated and enhanced up-regulation in expression of brain-derived neurotrophic factor (BDNF) and its tyrosine kinase B (TrkB) receptor in motoneurons which results from the depolarization of motoneuron cell bodies during the one-hour stimulation period (Al Majed et al., 2000b, 2004).

6.1.3. Possible molecular mechanisms underlying the glycomimetic effects on myelination

What are the mechanisms by which priming by PSA mimetics functions? PSA is associated with NCAM (Bock, 1987; Olsen et al., 1993) and was first considered, because of its negative charges, to be anti-adhesive resulting in inhibition of NCAM functions (Rutishauser et al., 1988). Later on it was shown that PSA is a positive modulator of NCAM function, since specific removal of PSA from NCAM by endoneuraminidase N is associated with an inhibition of NCAM function as for instance inhibition of LTP and reduction of axonal growth (Doherty et al., 1990; Lüthi et al., 1994; Muller et al., 1996). Based on the interpretation of Walsh and Doherty (1997), PSA modulates NCAM function by inhibiting the *cis*-interactions of NCAM in the plane of the plasma membrane, thus preventing the formation of stable, signal-transducing NCAM clusters at the cell surface. This would make more NCAM

available for *trans*-interactions (for instance with NCAM, L1 and proteoglycans), which would promote axonal growth and synaptic plasticity. Considering these properties of PSA, we propose that the observed effects of PSA mimetics *in vivo* and *in vitro* are due to PSA interactions with PSA-NCAM on Schwann cells or to disruption of inhibitory PSA-NCAM/receptor interactions. This notion is supported by the fact that Schwann cells of NCAM^{-/-} mice did not respond, in contrast to wild-type cells, to PSA mimetic stimulation *in vitro*. An interaction of the PSA mimetic with PSA-NCAM could lead to the activation of NCAM signalling pathways, which involve a tyrosine kinase receptor, fibroblast growth factor receptor (FGFR) (Doherty and Walsh, 1996; Walsh and Doherty, 1997; Kolkova et al., 2000; Kiselyov et al., 2003). FGFRs are likely mediators of the effects of PSA mimetics as they are activated by NCAM, expressed on Schwann cells (Grothe et al., 2001) and involved in myelination through the phosphatidylinositol-3-kinase (PI3K) pathways (Ogata et al., 2004). Activation of PI3K-Akt pathways in Schwann cells increases myelination in Schwann cell/DRG neuron co-cultures and allogenic nerve graft experiments *in vivo* (Ogata et al., 2004). Moreover, expression of FGFRs by Schwann cells is increased after sciatic nerve injury (Grothe et al., 2001), and FGFR-3-deficient mice display reduced myelin thickness compared to wild type controls (Jungnickel et al., 2004). Our finding that application of two different inhibitors of the FGFRs lead to reduction of process outgrowth from Schwann cells cultured in presence of the PSA mimetic strongly supports the idea of an NCAM/FRGR mediated mechanism of PSA mimetic action.

6.2. Effect of glycomimetics after spinal cord injury

This study demonstrates the feasibility, safety and efficacy of a PSA glycomimetic as a therapeutic means for spinal cord injury in an animal model. We also show that the therapeutic time-window of this treatment is limited to the acute post-traumatic phase. The positive functional effects of the mimetic appear to be achieved by endorsement of plasticity in the spinal cord.

6.2.1. Improved functional outcome after PSA mimetic treatment

Previous studies have shown that exogenous PSA is beneficial for spinal cord regeneration. Viral-mediated overexpression of PSA enhances the regrowth of severed corticospinal and sensory axons (El Maarouf et al., 2006; Zhang et al., 2007). Grafting of Schwann cells engineered to overexpress PSA in the injured spinal cord promotes functional recovery (Papastefanaki et al., 2007). The use of peptides that mimic PSA, as evaluated in this study, offers a more direct, clinically feasible opportunity than gene- and cell-based approaches. Large amounts of peptide can readily be synthesized and subdural chronic application in humans is practicable. The application of peptides appears safe as no chronic T cell responses were observed and motoneuron numbers, tissue scarring and demyelination were not negatively affected.

PSA glycomimetic application improved two aspects of motor performance in injured mice: walking and voluntary movements without body weight support. The latter finding is of special interest from a clinical point of view. Walking is controlled in a highly automated way by the spinal cord via central pattern generators and local

reflex pathways. After injury, even with a complete transection, high levels of functional recovery of stepping can be achieved in adult mammals by training the autonomic functions of the spinal cord (Edgerton et al., 2004; Fouad and Pearson, 2004). In contrast, functionally meaningful voluntary movements, for example target-oriented limb movements, are primarily under supraspinal control and the extent of trainability of the neuronal circuitries controlling such motor skills remains to be further exploited (Hallett, 2007; Kloosterman et al, 2009).

At the cellular level, we found several effects of the PSA mimetic which can explain the enhanced functional outcome. As compared with control peptide, more perisomatic cholinergic terminals were preserved on lumbar motoneurons, higher numbers of glutamatergic terminals were present in lamina VII of the spinal gray matter, and the monoaminergic innervation of the lumbar spinal cord was enhanced after PSA glycomimetic treatment. These phenomena can be interpreted as signs of enhanced axonal sprouting and synaptic maintenance/re-shuffling, i.e. augmented structural plasticity in the injured spinal cord. This notion is consistent with the view that plasticity of neuronal circuitries determines the outcome of spinal cord injury (Edgerton et al., 2004; Frigon and Rossignol, 2006) and with the plasticity-promoting properties of PSA (Kleene and Schachner, 2004; Rutishauser, 2008). PSA is a cell-surface glycan with a large hydration volume that modulates the distance, and thus contacts between cells. This regulation in a “slippery eel”, non-receptor fashion, influences different developmental mechanisms including growth and targeting of axons. Endogenous PSA is carried by the membrane-associated and soluble forms of the neural cell adhesion molecule (Bock et al., 1987; Olsen et al., 1993; Hildebrandt et

al., 2007; Rutishauser, 2008), as well as by neuropilin-2 (Curreli et al., 2007) which limits its actions to cells expressing these molecules. In contrast, application of a soluble exogenous PSA, or its functional mimetic, is not prone to this limitation and more wide-spread effects can be expected. In addition to a receptor independent mode of action, the PSA mimetic may be effective by influencing its endogenous carrier, NCAM. PSA is a positive modulator of NCAM function since its removal from NCAM is associated with an inhibition of NCAM functions like enhancement of long-term potentiation, axonal growth, synaptic plasticity, and learning and memory (Doherty et al., 1990; Becker et al., 1996; Muller et al., 1996; Dityatev et al., 2004; Stoenica et al., 2006). Interactions of the PSA mimetic with PSA-NCAM may stimulate regeneration-promoting NCAM functions and/or disrupt inhibitory PSA-NCAM/receptor interactions. In support of this notion is our recent finding that the PSA mimetic influences elongation of Schwann cell processes via a NCAM/fibroblast growth factor receptor-mediated mechanism (Mehanna et al., 2009).

6.2.2. Lack of functional effects after HNK-1 glycomimetic application

We have previously observed that both the HNK-1 and the PSA mimetics used in this study efficiently promote recovery of function after peripheral nerve injury (Simova et al., 2006; Mehanna et al., 2009). In light of these observations and the positive effects of the PSA mimetic reported here, the lack of an effect of the HNK-1 mimetic on locomotor function was unexpected. HNK-1, similar to PSA, promotes synaptic plasticity in the central nervous system (Kleene and Schachner, 2004; Dityatev and Schachner, 2006) and here we found evidence for a positive influence of the HNK-1

mimetic on glutamatergic synapses. Similar to the PSA mimetic, the HNK-1 mimetic also improved myelination in the proximal part of the lesioned spinal cord. However, other important PSA mimetic effects like enhancement of the monoaminergic innervation in the lumbar spinal cord and the cholinergic synaptic coverage of motoneurons, previously found to be associated with better recovery (Apostolova et al., 2006; Jakovcevski et al., 2007a), were not observed. Therefore, we must assume that the inefficacy of the HNK-1 mimetic is related to inability to influence major determinants of functional recovery, i.e. to cause rearrangements in the lumbar spinal cord circuitries, specifically cholinergic input to motoneurons and monoaminergic axons sprouting caudal to the lesion site. It is noteworthy, however, that our functional test systems are not able to reveal more finely tuned changes in locomotion. In addition to this simple notion, however, we have to consider that the HNK-1 epitope is carried by a larger number, as compared with PSA, of molecules such as MAG, L1, amphoterin, NCAM, P0, glycolipids (Kleene and Schachner, 2004). It is possible that HNK-1 mimetic interactions with different molecules have different molecular and cellular consequences, both positive and negative, which are counterbalanced in a way to produce no effect. It is also noteworthy that we found no adverse effects of the HNK-1 mimetic and testing of its efficacy in other injury paradigms is warranted.

6.2.3. Therapeutic time-window of the PSA glycomimetic

Based on our morphological evidence, we propose that enhanced plasticity underlies better functional outcome after PSA mimetic application in the acute phase of spinal cord injury. However, plasticity in both humans and laboratory animals is not restricted

to the acute phase (Little et al., 1999). For example, using the same paradigm, we recently showed that spontaneous functional recovery and alterations in motoneuron connectivity and excitability occur to a high degree between the 6th and the 12th week after injury (Lee et al., 2009). Therefore, it appears surprising that we found no effect when the PSA mimetic was applied after the third post-operative week. One explanation is that, despite long-term progression, most of the spontaneous and crucial functional recovery in mice occurs within the first 3 weeks after spinal cord compression (Apostolova et al., 2006; Jakovcevski et al., 2007a; Lee et al., 2009). Thus, drug-induced positive functional effects at later stages of spinal cord regeneration might be difficult to measure. In addition, it is possible that a longer observation time-period after pump application is required to observe PSA effects three weeks after injury. This notion and the fact that spontaneous recovery in larger mammals and humans is slower than in the mouse, make us believe that application of PSA at a chronic stage in other injury paradigms or clinical settings could be effective.

6.3. Conclusions

These results show that PSA is involved in processes that go beyond its classical role as an anti-adhesive epitope and reveal a promising therapeutic potential of PSA mimetics for peripheral nerve and spinal cord injury. PSA and NCAM mimicking peptides diffuse well in the brain and spinal cord of adult mammals (Cambon et al., 2004; Florian et al., 2006; present study). Therefore, and considering the effects on myelination and synaptic plasticity observed in this study, it is conceivable that such

mimics would be efficient therapeutic agents to treat patients with other disorders like demyelinating and degenerative diseases. These results also warrant further experiments with PSA and HNK-1 mimetics, for example in larger laboratory animals, aiming to translate this approach into clinical practice. This notion is strongly encouraged by positive results achieved in an independent study using a different PSA mimetic and a different injury paradigm (dorsal hemisection) in mice (Marino et al., 2009).

7. References

- Ahlborn P, Schachner M, Irintchev A. *One hour electrical stimulation accelerates functional recovery after femoral nerve repair*. Exp Neurol 2007; 208: 137-44.
- Allt G. *An ultrastructural analysis of remyelination following segmental demyelination*. Acta Neuropathol 1972; 22: 333-44.
- Al-Majed AA, Neumann CM, Brushart TM, Gordon T. *Brief electrical stimulation promotes the speed and accuracy of motor axonal regeneration*. J Neurosci 2000a; 20: 2602-8.
- Al-Majed AA, Brushart TM, Gordon T. *Electrical stimulation accelerates and increases expression of BDNF and trkB mRNA in regenerating rat femoral motoneurons*. Eur J Neurosci 2000b; 12: 4381-90.
- Al-Majed AA, Tam SL, Gordon T. *Electrical stimulation accelerates and enhances expression of regeneration-associated genes in regenerating rat femoral motoneurons*. Cell Mol Neurobiol 2004; 24: 379-402.
- Angelov DN, Ceynowa M, Guntinas-Lichius O, Streppel M, Grosheva M, Kiryakova SI, et al. *Mechanical stimulation of paralyzed vibrissal muscles following facial nerve injury in adult rat promotes full recovery of whisking*. Neurobiol Dis 2007; 26: 229-42.
- Apostolova I, Irintchev A, Schachner M. *Tenascin-R restricts posttraumatic remodeling of motoneuron innervation and functional recovery after spinal cord injury in adult mice*. J Neurosci 2006; 26: 7849-7859.
- Asahara T, Lin M, Kumazawa Y, Takeo K, Akamine T, Nishimura Y, et al. *Long-term observation on the changes of somatotopy in the facial nucleus after nerve suture in the cat: morphological studies using retrograde labeling*. Brain Res Bull 1999; 49: 195-202.
- Azurmendi HF, Vionnet J, Wrightson L, Trinh LB, Shiloach J, Freedberg DI. *Extracellular structure of polysialic acid explored by on cell solution NMR*. Proc Natl Acad Sci U S A 2007; 104: 11557-61.
- Basso DM, Fisher LC, Anderson AJ, Jakeman LB, McTigue DM, Popovich PG. *Basso Mouse Scale for locomotion detects differences in recovery after spinal cord injury in five common mouse strains*. J Neurotrauma 2006; 23: 635-659.

- Bächle D, Loers G, Guthöhrlein EW, Schachner M, Sewald N. *Glycomimetic cyclic peptides stimulate neurite outgrowth*. *Angew Chem Int Ed Engl* 2006; 45: 6582-6585.
- Bear MF, Connors BW, Paradiso MA. *Neuroscience: Exploring the Brain*. Baltimore: Lippincott. 2001 ISBN 0-7817-3944-6.
- Becker CG, Artola A, Gerardy-Schahn R, Becker T, Welzl H, Schachner M. *The polysialic acid modification of the neural cell adhesion molecule is involved in spatial learning and hippocampal long-term potentiation*. *J Neurosci Res* 1996; 45: 143-52.
- Bock E, Edvardsen K, Gibson A, Linnemann D, Lyles JM, Nybroe O. *Characterization of soluble forms of NCAM*. *FEBS Lett* 1987; 225: 33-6.
- Boyd JG, Gordon T. *Glial cell line-derived neurotrophic factor and brain-derived neurotrophic factor sustain the axonal regeneration of chronically axotomized motoneurons in vivo*. *Exp Neurol* 2003; 183: 610-9.
- Brumovsky P, Watanabe M, Hökfelt T. *Expression of the vesicular glutamate transporters-1 and -2 in adult mouse dorsal root ganglia and spinal cord and their regulation by nerve injury*. *Neuroscience* 2007; 147: 469-490.
- Brunelli G, Brunelli F. *Strategy and timing of peripheral nerve surgery*. *Neurosurg Rev*. 1990; 13: 95-102.
- Bruns S, Stark Y, Röker S, Wieland M, Dräger G, Kirschning A, et al. *Collagen biomaterial doped with colominic acid for cell culture applications with regard to peripheral nerve repair*. *J Biotechnol* 2007; 131: 335-45.
- Brushart TM. *Preferential reinnervation of motor nerves by regenerating motor axons*. *J Neurosci* 1988; 8: 1026-31.
- Brushart TM. *Motor axons preferentially reinnervate motor pathways*. *J Neurosci* 1993; 13: 2730-8.
- Brushart TM, Hoffman PN, Royall RM, Murinson BB, Witzel C, Gordon T. *Electrical stimulation promotes motoneuron regeneration without increasing its speed or conditioning the neuron*. *J Neurosci* 2002; 22: 6631-8.
- Bunge MB. *Bridging areas of injury in the spinal cord*. *Neuroscientist*. 2001; 7: 325-39.

- Cambon K, Hansen SM, Venero C, Herrero AI, Skibo G, Berezin V, et al. *A synthetic neural cell adhesion molecule mimetic peptide promotes synaptogenesis, enhances presynaptic function, and facilitates memory consolidation.* J Neurosci 2004; 24: 4197-204.
- Carratù MR, Steardo L, Cuomo V. *Role of polysialic acid in peripheral myelinated axons.* Microsc Res Tech 1996; 34: 489-91.
- Charles P, Hernandez MP, Stankoff B, Aigrot MS, Colin C, Rougon G, Zalc B, Lubetzki C. *Negative regulation of central nervous system myelination by polysialylated-neural cell adhesion molecule.* Proc Natl Acad Sci U S A 2000; 97: 7585–7590.
- Charles P, Reynolds R, Seilhean D, Rougon G, Aigrot MS, Niezgodka A, Zalc B, Lubetzki C. *Re-expression of PSA-NCAM by demyelinated axons: an inhibitor of remyelination in multiple sclerosis?* Brain 2002; 125: 1972–1979.
- Chen ZL, Yu WM, Strickland S. *Peripheral regeneration.* Annu Rev Neurosci 2007; 30: 209-33.
- Chen J., Lee H.J., Jakovcevski I., Shah R., Loers G., Liu H-Y, Meiners S, Irintchev A, Schachner M. *Tenascin C is beneficial for spinal cord regeneration.* 2009 submitted.
- Chizuka I. *Peripheral nerve regeneration.* Neuroscience Research 1996; 25: 101-121.
- Chou DK, Zhang J, Smith FI, McCaffery P, Jungalwala FB. *Developmental expression of receptor for advanced glycation end products (RAGE), amphotericin and sulfoglucuronyl (HNK-1) carbohydrate in mouse cerebellum and their role in neurite outgrowth and cell migration.* J Neurochem 2004 Sep; 90: 1389-401.
- Columbia Encyclopedia. *Nervous System*; Columbia University Press, 6th edition 2003.
- Coutts M, Keirstead HS. *Stem cells for the treatment of spinal cord injury.* Exp Neurol. 2008; 209: 368-77.
- Covault J, Merlie JP, Goridis C, Sanes JR. *Molecular forms of N-CAM and its RNA in developing and denervated skeletal muscle.* J Cell Biol 1986; 102: 731-9.
- Crutcher KA, Bingham WG Jr. *Descending monoaminergic pathways in the primate spinal cord.* Am J Anat 1978; 153: 159-164.

- Curreli S, Arany Z, Gerardy-Schahn R, Mann D, Stamatou NM. *Polysialylated neuropilin-2 is expressed on the surface of human dendritic cells and modulates dendritic cell-T lymphocyte interactions*. J Biol Chem 2007; 282: 30346-56.
- Curtis R, Green D, Lindsay RM, Wilkin GP. *Up-regulation of GAP-43 and growth of axons in rat spinal cord after compression injury*. J Neurocytol 1993; 22: 51-64.
- Davidoff MS, Irintchev AP. *Acetylcholinesterase activity and type C synapses in the hypoglossal, facial and spinal-cord motor nuclei of rats. An electron-microscope study*. Histochemistry 1986; 84: 515-524.
- De Carlos JA, Borrell J. *A historical reflection of the contributions of Cajal and Golgi to the foundations of neuroscience*. Brain research reviews 2007; 55: 8-16.
- De la Cruz RR, Pastor AM, Delgado-García JM. *Effects of target depletion on adult mammalian central neurons: morphological correlates*. Neuroscience 1994; 58: 59-79.
- Dietz V. *Proprioception and locomotor disorders*. Nat Rev Neurosci 2002; 3: 781-790.
- Dityatev A, Dityateva G, Sytnyk V, Delling M, Toni N, Nikonenko I, Muller D, Schachner M. *Polysialylated neural cell adhesion molecule promotes remodeling and formation of hippocampal synapses*. J Neurosci 2004; 24: 9372-82.
- Dityatev A, Schachner M. *The extracellular matrix and synapses*. Cell Tissue Res 2006; 326: 647-654.
- Doherty P, Cohen J, Walsh FS. *Neurite outgrowth in response to transfected N-CAM changes during development and is modulated by polysialic acid*. Neuron 1990; 5: 209-19.
- Doherty P, Walsh FS. *CAM-FGF receptor interactions: A model for axonal growth*. Mol Cell Neurosci 1996; 8: 99-111.
- Durbec P, Cremer H. *Revisiting the function of PSA-NCAM in the nervous system*. Mol Neurobiol 2001; 24 :53-64.
- Eberhardt KA, Irintchev A, Al-Majed AA, Simova O, Brushart TM, Gordon T, et al. *BDNF/TrkB signaling regulates HNK-1 carbohydrate expression in regenerating*

- motor nerves and promotes functional recovery after peripheral nerve repair. Exp Neurol* 2006; 198: 500-10.
- Edgerton VR, Tillakaratne NJ, Bigbee AJ, de Leon RD, Roy RR. *Plasticity of the spinal neural circuitry after injury. Annu Rev Neurosci* 2004; 27: 145-167.
- El Maarouf A, Petridis AK, Rutishauser U. *Use of polysialic acid in repair of the central nervous system. Proc Natl Acad Sci U S A* 2006; 103: 16989-16994.
- European Science Foundation Policy Briefing N27. *Structural Medicine: The Importance of Glycomics for Health and Disease*. July 2006.
- Fan X, Gelman BB. *Schwann cell nerve growth factor receptor expression during initiation of remyelination. J Neurosci Res* 1992; 31: 58-67.
- Fawcett JW, Keynes RJ. *Peripheral nerve regeneration. Annu Rev Neurosci* 1990; 13: 43-60.
- Fawcett JW. *Overcoming inhibition in the damaged spinal cord. J Neurotrauma* 2006; 23: 371-83.
- French-Constant C, Miller RH, Kruse J, Schachner M, Raff MC. *Molecular specialization of astrocyte processes at nodes of Ranvier in rat optic nerve. J Cell Biol* 1986; 102: 844-52.
- Finger S. *Origins of Neuroscience*, New York: Oxford University Press, 1994.
- Florian C, Foltz J, Norreel JC, Rougon G, Rouillet P. *Post-training intrahippocampal injection of synthetic poly-alpha-2,8-sialic acid-neural cell adhesion molecule mimetic peptide improves spatial long-term performance in mice. Learn Mem* 2006; 13: 335-41.
- Fouad K, Pearson K. *Restoring walking after spinal cord injury. Prog Neurobiol* 2004; 73: 107-126.
- Franz CK, Rutishauser U, Rafuse VF. *Polysialylated neural cell adhesion molecule is necessary for selective targeting of regenerating motor neurons. J Neurosci* 2005; 25: 2081-91.
- Franz CK, Rutishauser U, Rafuse VF. *Intrinsic neuronal properties control selective targeting of regenerating motoneurons. Brain* 2008; 131: 1492-505.
- Frigon A, Rossignol S. *Functional plasticity following spinal cord lesions. Prog Brain Res* 2006; 157: 231-260.

- Frosch M, Görden I, Boulnois GJ, Timmis KN, Bitter-Suermann D. *NZB mouse system for production of monoclonal antibodies to weak bacterial antigens: isolation of an IgG antibody to the polysaccharide capsules of Escherichia coli K1 and group B meningococci*. Proc Natl Acad Sci U S A 1985; 82: 1194-8.
- Fu SY, Gordon T. *The cellular and molecular basis of peripheral nerve regeneration*. Mol Neurobiol 1997; 14: 67-116.
- García-Alías G, Lin R, Akrimi SF, Story D, Bradbury EJ, Fawcett JW. *Therapeutic time window for the application of chondroitinase ABC after spinal cord injury*. Exp Neurol. 2008; 210: 331-8.
- Giménez y Ribotta M, Gaviria M, Menet V, Privat A. *Strategies for regeneration and repair in spinal cord traumatic injury*. Prog Brain Res 2002; 137: 191-212.
- Gravvanis AI, Lavdas AA, Papalois A, Tsoutsos DA, Matsas R. *The beneficial effect of genetically engineered Schwann cells with enhanced motility in peripheral nerve regeneration: review*. Acta Neurochir Suppl 2007; 100: 51-6.
- Greenblatt, SH. *Phrenology in the science and culture of the 19th century*. Neurosurgery 1995; 37: 790-805.
- Grothe C, Meisinger C, Claus P. *In vivo expression and localization of the fibroblast growth factor system in the intact and lesioned rat peripheral nerve and spinal ganglia*. J Comp Neurol 2001; 434: 342-57.
- Haile Y, Haastert K, Cesnulevicius K, Stummeyer K, Timmer M, Berski S, et al. *Culturing of glial and neuronal cells on polysialic acid*. Biomaterials 2007; 28: 1163-73.
- Hallett M. *Volitional control of movement: the physiology of free will*. Clin Neurophysiol 2007; 118: 1179-1192.
- Heckman CJ, Lee RH, Brownstone RM. *Hyperexcitable dendrites in motoneurons and their neuromodulatory control during motor behavior*. Trends Neurosci 2003; 26: 688-95.
- Hekimian KJ, Seckel BR, Bryan DJ, Wang KK, Chakalis DP, Bailey A. *Continuous alteration of the internal milieu of a nerve-guide chamber using an osmotic pump and internal exhaust system*. J Reconstr Microsurg 1995; 11: 93-8.

- Hellström J, Oliveira AL, Meister B, Cullheim S. *Large cholinergic nerve terminals on subsets of motoneurons and their relation to muscarinic receptor type 2*. J Comp Neurol 2003; 460: 476-486.
- Hildebrandt H, Mühlhoff M, Weinhold B, Gerardy-Schahn R. *Dissecting polysialic acid and NCAM functions in brain development*. J Neurochem 2007; 103: 56-64.
- Irintchev A, Draguhn A, Wernig A. *Reinnervation and recovery of mouse soleus muscle after long-term denervation*. Neuroscience 1990; 39: 231-43.
- Irintchev A, Simova O, Eberhardt KA, Morellini F, Schachner M. *Impacts of lesion severity and tyrosine kinase receptor B deficiency on functional outcome of femoral nerve injury assessed by a novel single-frame motion analysis in mice*. Eur J Neurosci 2005; 22: 802-8.
- Irintchev A, Rollenhagen A, Troncoso E, Kiss JZ, Schachner M. *Structural and functional aberrations in the cerebral cortex of tenascin-C deficient mice*. Cereb Cortex 2005; 15: 950-962.
- Jakovcevski I, Siering J, Hargus G, Karl N, Hoelters L, Djogo N, Yin S, Zecevic N, Schachner M, Irintchev A. *Close homologue of adhesion molecule L1 promotes survival of Purkinje and granule cells and granule cell migration during murine cerebellar development*. J Comp Neurol 2009; 513: 496-510.
- Jakovcevski I, Wu J, Karl N, Leshchyn's'ka I, Sytnyk V, Chen J, Irintchev A, Schachner M. *Glial scar expression of CHL1, the close homolog of the adhesion molecule L1, limits recovery after spinal cord injury*. J Neurosci 2007a; 27: 7222-7233.
- Jakovcevski I, Mo Z, Zecevic N. *Down-regulation of the axonal polysialic acid-neural cell adhesion molecule expression coincides with the onset of myelination in the human fetal forebrain*. Neuroscience 2007b; 149: 328-337.
- Jiao Y, Sun Z, Lee T, Fusco FR, Kimble TD, Meade CA, Cuthbertson S, Reiner A. *A simple and sensitive antigen retrieval method for free-floating and slide-mounted tissue sections*. J Neurosci 1999; Methods 93: 149-162.
- Jungnickel J, Gransalke K, Timmer M, Grothe C. *Fibroblast growth factor receptor 3 signaling regulates injury-related effects in the peripheral nervous system*. Mol Cell Neurosci 2004; 25: 21-9.

- Kandel E, Schwartz J, Jessel T. *Principles of Neural Science* 4th ed. 2000, eds. McGraw-Hill:New York, NY.
- Kiselyov VV, Skladchikova G, Hinsby AM, Jensen PH, Kulahin N, Soroka V, et al. *Structural basis for a direct interaction between FGFR1 and NCAM and evidence for a regulatory role of ATP*. *Structure* 2003; 11: 691-701.
- Kleene R, Schachner M. *Glycans and neural cell interactions*. *Nat Rev Neurosci* 2004; 5: 195-208.
- Kloos AD, Fisher LC, Detloff MR, Hassenzahl DL, Basso DM. *Stepwise motor and all-or-none sensory recovery is associated with nonlinear sparing after incremental spinal cord injury in rats*. *Exp Neurol* 2005; 191: 251-265.
- Kloosterman MG, Snoek GJ, Jannink MJ. *Systematic review of the effects of exercise therapy on the upper extremity of patients with spinal-cord injury*. *Spinal Cord* 2009; 47: 196-203.
- Kolkova K, Novitskaya V, Pedersen N, Berezin V, Bock E. *Neural cell adhesion molecule-stimulated neurite outgrowth depends on activation of protein kinase C and the Ras-mitogen-activated protein kinase pathway*. *J Neurosci* 2000; 20: 2238-46.
- Kruse J, Mailhammer R, Wernecke H, Faissner A, Sommer I, Goridis C, et al. *Neural cell adhesion molecules and myelin-associated glycoprotein share a common carbohydrate moiety recognized by monoclonal antibodies L2 and HNK-1*. *Nature* 1984; 311: 153-5.
- Kruse J, Keilhauer G, Faissner A, Timpl R, Schachner M. *The J1 glycoprotein--a novel nervous system cell adhesion molecule of the L2/HNK-1 family*. *Nature* 1985; 316: 146-8.
- Kurschat Nina. *Analysis of the Epitope of the L1-Antibody 324 and Search for a Polysialic Acid Peptide Mimetic via Phage Display*. Masterstudiengang Molecular Life Science, Universität zu Lübeck, 2006.
- Lavrov I, Courtine G, Dy CJ, van den Brand R, Fong AJ, Gerasimenko Y, Zhong H, Roy RR, Edgerton VR. *Facilitation of stepping with epidural stimulation in spinal rats: role of sensory input*. *J Neurosci* 2008; 28: 7774-7780.

- Lee HJ, Jakovcevski I, Radonjic N, Hoelters L, Schachner M, Irintchev A. *Better functional outcome of compression spinal cord injury in mice is associated with enhanced H-reflex responses.* Exp Neurol 2009; 216: 365-374.
- Lee SK, Wolfe SW. *Peripheral nerve injury and repair.* J Am Acad Orthop Surg 2000; 8: 243-252.
- Little JW, Ditunno JF Jr, Stiens SA, Harris RM. *Incomplete spinal cord injury: neuronal mechanisms of motor recovery and hyperreflexia.* Arch Phys Med Rehabil 1999; 80: 587-599.
- Liu WL, Lee YH, Tsai SY, Hsu CY, Sun YY, Yang LY, Tsai SH, Yang WC. *Methylprednisolone inhibits the expression of glial fibrillary acidic protein and chondroitin sulfate proteoglycans in reactivated astrocytes.* Glia. 2008; 56: 1390-400.
- Loers G, Schachner M. *Recognition molecules and neural repair.* J Neurochem 2007; 101: 865-882.
- Löw K, Orberger G, Schmitz B, Martini R, Schachner M. *The L2/HNK-1 carbohydrate is carried by the myelin associated glycoprotein and sulphated glucuronyl glycolipids in muscle but not cutaneous nerves of adult mice.* Eur J Neurosci 1994; 6: 1773-81.
- Lu P, Tuszynski MH. *Growth factors and combinatorial therapies for CNS regeneration.* Exp Neurol. 2008; 209: 313-20.
- Lubińska L. *Early course of Wallerian degeneration in myelinated fibres of the rat phrenic nerve.* Brain Res 1977; 130: 47-63.
- Lundborg G.: *Richard P. Bunge memorial lecture. Nerve injury and repair--a challenge to the plastic brain.* J Peripher Nerv Syst 2003; 8: 209-26.
- Lüthi A, Laurent JP, Figurov A, Muller D, Schachner M. *Hippocampal long-term potentiation and neural cell adhesion molecules L1 and NCAM.* Nature 1994; 372: 777-9.
- Marino P, Norreel JC, Schachner M, Rougon G, Amoureux MC. *A polysialic acid mimetic peptide promotes functional recovery in a mouse model of spinal cord injury.* Exp Neurol 2009 May 13. [Epub ahead of print].

- Martin-Araguz A, Bustamante-Martinez C, Fernandez-Armayor Ajo V, Moreno-Martinez JM. "Neuroscience in al-Andalus and its influence on medieval scholastic medicine", *Revista de neurología* 2002; 34: 877-892.
- Martini R, Xin Y, Schmitz B, Schachner M. *The L2/HNK-1 Carbohydrate Epitope is Involved in the Preferential Outgrowth of Motor Neurons on Ventral Roots and Motor Nerves*. *Eur J Neurosci* 1992; 4: 628-639.
- Mehanna A, Mishra B, Kurschat N, Schulze C, Bian S, Loers G, Irintchev A, Schachner M. *Polysialic acid glycomimetics promote myelination and functional recovery after peripheral nerve injury in mice*. *Brain* 2009; 132: 1449-62.
- Miles GB, Hartley R, Todd AJ, Brownstone RM. *Spinal cholinergic interneurons regulate the excitability of motoneurons during locomotion*. *Proc Natl Acad Sci USA* 2007; 104: 2448-2453.
- Mirsky R, Jessen KR, Brennan A, Parkinson D, Dong Z, Meier C, Parmantier E, Lawson D. *Schwann cells as regulators of nerve development*. *J Physiol Paris* 2002; 96: 17-24.
- Miura R, Aspberg A, Ethell IM, Hagihara K, Schnaar RL, Ruoslahti E, Yamaguchi Y. *The proteoglycan lectin domain binds sulfated cell surface glycolipids and promotes cell adhesion*. *J Biol Chem* 1999; 274: 11431-11438.
- Mohammadi M, McMahon G, Sun L, Tang C, Hirth P, Yeh BK, Hubbard SR, Schlessinger J. *Structures of the tyrosine kinase domain of fibroblast growth factor receptor in complex with inhibitors*. *Science* 1997; 276: 955–60.
- Mohammadi M, Froum S, Hamby JM, Schroeder MC, Panek RL, Lu GH, Eliseenkova AV, Green D, Schlessinger J, Hubbard SR. *Crystal structure of an angiogenesis inhibitor bound to the FGF receptor tyrosine kinase domain*. *EMBO J* 1998; 17: 5896–5904.
- Muller D, Wang C, Skibo G, Toni N, Cremer H, Calaora V, Rougon G, Kiss JZ. *PSA-NCAM is required for activity-induced synaptic plasticity*. *Neuron* 1996; 17: 413-422.
- Niethammer P, Delling M, Sytnyk V, Dityatev A, Fukami K, Schachner M. *Cosignaling of NCAM via lipid rafts and the FGF receptor is required for neuritogenesis*. *J Cell Biol* 2002; 157: 521–32.

- Ogata T, Iijima S, Hoshikawa S, Miura T, Yamamoto S, Oda H, et al. *Opposing extracellular signal-regulated kinase and Akt pathways control Schwann cell myelination*. J Neurosci 2004; 24: 6724-32.
- Olsen M, Krog L, Edvardsen K, Skovgaard LT, Bock E. *Intact transmembrane isoforms of the neural cell adhesion molecule are released from the plasma membrane*. Biochem J 1993; 295: 833-40.
- Olsen M, Zuber C, Roth J, Linnemann D, Bock E. *The ability to re-express polysialylated NCAM in soleus muscle after denervation is reduced in aged rats compared to young adult rats*. Int J Dev Neurosci 1995; 13: 97-104.
- Papastefanaki F, Chen J, Lavdas AA, Thomaidou D, Schachner M, Matsas R. *Grafts of Schwann cells engineered to express PSA-NCAM promote functional recovery after spinal cord injury*. Brain 2007; 130: 2159-74.
- Piquilloud G, Christen T, Pfister LA, Gander B, Papaloizos MY. *Variations in glial cell line-derived neurotrophic factor release from biodegradable nerve conduits modify the rate of functional motor recovery after rat primary nerve repairs*. Eur J Neurosci 2007; 26: 1109-17.
- Privat A. *Treatment of the future for spinal cord injuries*. Rev Prat 1995; 45: 2051-6.
- Ramón y Cajal S, Azoulay L, Duval M (in French). *Les nouvelles idées sur la structure du système nerveux chez l'homme et chez les vertébrés*. Published by C. Reinwald, 1894.
- Ramón y Cajal S (in German). *Studien über die Hirnrinde des Menschen v.5*. Published by Johann Ambrosius Barth, 1906.
- Ramón y Cajal S. *Degeneration and regeneration of the nervous system*. Oxford University Press 1928, London, New York.
- Rich KM, Disch SP, Eichler ME. *The influence of regeneration and nerve growth factor on the neuronal cell body reaction to injury*. J Neurocytol 1989; 18: 569-76.
- Robinson GA, Madison RD. *Preferential motor reinnervation in the mouse: comparison of femoral nerve repair using a fibrin sealant or suture*. Muscle Nerve 2003; 28: 227-31.
- Rossi F, Buffo A, Strata P. *Regulation of intrinsic regenerative properties and axonal plasticity in cerebellar Purkinje cells*. Restor Neurol Neurosci 2001; 19: 85-94.

- Rutishauser U, Acheson A, Hall AK, Mann DM, Sunshine J. *The neural cell adhesion molecule (NCAM) as a regulator of cell-cell interactions*. Science 1988; 240: 53-7.
- Rutishauser U, Landmesser L. *Polysialic acid in the vertebrate nervous system: a promoter of plasticity in cell-cell interactions*. Trends Neurosci 1996; 19: 422-427.
- Rutishauser U. *Polysialic acid in the plasticity of the developing and adult vertebrate nervous system*. Nat Rev Neurosci 2008; 9: 26-35.
- Schachner M, Martini R. *Glycans and the modulation of neural-recognition molecule function*. Trends Neurosci 1995; 18: 183-91.
- Schulze C. In: *Recent research developments in comparative biochemistry & physiology*; S. G. Pandalai, Ed.; Transworld research network: Trivandrum, India, 2000; Vol. 1, pp 77-90.
- Schwab ME. *Repairing the injured spinal cord*. Science 2002; 295: 1029-31.
- Shapiro S. *Neurotransmission by neurons that use serotonin, noradrenaline, glutamate, glycine and gamma-aminobutyric acid in the normal and injured spinal cord*. Neurosurgery 1997; 40: 168-177.
- Shearman JD, Franks AJ. *S-100 protein in Schwann cells of the developing human peripheral nerve. An immunohistochemical study*. Cell Tissue Res 1987 Aug; 249:459-63.
- Simon-Haldi M, Mantei N, Franke J, Voshol H, Schachner M. *Identification of a peptide mimic of the L2/HNK-1 carbohydrate epitope*. J Neurochem 2002; 83: 1380-1388.
- Simova O, Irintchev A, Mehanna A, Liu J, Dihne M, Bächle D, Sewald N, Loers G, Schachner M. *Carbohydrate mimics promote functional recovery after peripheral nerve repair*. Ann Neurol 2006; 60: 430-437.
- Smith KJ, Hall SM. *Nerve conduction during peripheral demyelination and remyelination*. J Neurol Sci 1980; 48: 201-19.
- Stoenica L, Senkov O, Gerardy-Schahn R, Weinhold B, Schachner M, Dityatev A. *In vivo synaptic plasticity in the dentate gyrus of mice deficient in the neural cell*

- adhesion molecule NCAM or its polysialic acid.* Eur J Neurosci 2006; 23: 2255-64.
- Streppel M, Azzolin N, Dohm S, Guntinas-Lichius O, Haas C, Grothe C, et al. *Focal application of neutralizing antibodies to soluble neurotrophic factors reduces collateral axonal branching after peripheral nerve lesion.* Eur J Neurosci 2002; 15: 1327-42.
- Tang J, Landmesser L. *Reduction of intramuscular nerve branching and synaptogenesis is correlated with decreased motoneuron survival.* The Journal of Neuroscience 1993; 13: 3095-103.
- Terenghi G. *Peripheral nerve regeneration and neurotrophic factors.* J Anat. 1999; 194: 1-14.
- Tiesler Blos V. *Cranial Surgery in Ancient Mesoamerica, 2003.*
<http://www.mesoweb.com/features/tiesler/Cranial.pdf>.
- Tohill M, Terenghi G. *Stem-cell plasticity and therapy for injuries of the peripheral nervous system.* Biotechnol Appl Biochem 2004; 40: 17-24.
- Torregrossa P, Buhl L, Bancila M, Durbec P, Schafer C, Schachner M, et al. *Selection of poly-alpha 2,8-sialic acid mimotopes from a random phage peptide library and analysis of their bioactivity.* J Biol Chem 2004; 279: 30707-14.
- Walsh FS, Doherty P. *Neural cell adhesion molecules of the immunoglobulin superfamily: role in axon growth and guidance.* Annu Rev Cell Dev Biol 1997; 13: 425-56.
- Waters HJ, Barnett G, O'Hanlon GM, Lowrie MB. *Motoneuron survival after neonatal peroneal nerve injury in the rat-evidence for the sparing effect of reciprocal inhibition.* Exp Neurol 1998; 152: 95-100.
- Wong BJ, Mattox DE. *Experimental nerve regeneration. A review.* Otolaryngol Clin North Am. 1991; 24: 739-52.
- Yamamoto N, Inui K, Matsuyama Y, Harada A, Hanamura K, Murakami F, Ruthazer ES, Rutishauser U, Seki T. *Inhibitory mechanism by polysialic acid for laminaspecific branch formation of thalamocortical axons.* J Neurosci 2000; 20: 9145-9151.

Zhang Y, Zhang X, Wu D, Verhaagen J, Richardson PM, Yeh J, Bo X. *Lentiviral-mediated expression of polysialic acid in spinal cord and conditioning lesion promote regeneration of sensory axons into spinal cord.* Mol Ther 2007; 15: 1796-1804.

8. Abbreviations

BrdU = Bromodeoxyuridine

ChAT = Choline acetyltransferase

DRG = Dorsal root ganglia

FGFR = Fibroblast growth factor receptor

FBA = Foot-base angle

HNK-1 = Human natural killer antigen-1

HTA = Heels-tail angle

LTP = Long term potentiation

NCAM = Neural cell adhesion molecule

PFA = Paraformaldehyde

PSA = Polysialic acid

PLL = Poly-L-lysine

PMR = Preferential motor reinnervation

PLR = Protraction length ratio

TH = Tyrosine hydroxylase

VGLUT = Vesicular glutamate transporter

9. Acknowledgements

A PhD thesis, like life, has its ups and downs. Over the years of my work in ZMNH (2005-2009) there have been many nice days, but also many exhausting and stressful days. In addition, being alone in a foreign country did not make my life easy.

I would like to acknowledge my family who despite the distance has always been there for me. Without their support I wouldn't have been able to achieve this work.

As a work of science, I am grateful to my supervisors, Prof. Melitta Schachner who gave me a great chance to work in her laboratory and Dr. Andrey Irintchev who introduced me to a very interesting clinical related research and from whom I learnt lots of morphological techniques.

I wish to thank Prof. Konrad Wiese for his help getting the equivalence of my master degree, and his time to read and evaluate this work.

Special thanks go to Dr. Gabriele Loers and Dr. Igor Jakovcevski who also supervised different parts of this work. I will always remember their availability to answer my questions and give me suggestions and solutions for my problems.

Of course during 4 years of PhD I met some nice colleagues and few good friends who helped and encouraged me. Particularly I like to thank Bibhudatta Mishra, Iris Oezen, Nicole Karl, Meifang Xiao, Vasudharani Devanathan, Shan Bian, Gunnar Hargus, Christian Berneuther, Nuray Akyüz, Peggy Putthoff and Achim Dahlmann.

Profound thanks go to Emanuela Szpotowicz for excellent technical assistance.

I should also thank some old friends from Lebanon and France who have wished me luck all the time. I like to mention Hicham Richa, Amine Ghanem, Roula Moussa,

Mireille Merhy, Hanad Farah, Dr. Oussama el Far, Dr. Monique Laval, Dr. François Féron and Dr. Evelyne Tremblay.

Lastly I would like to thank Dr. med. Kersten Peldschus from the Universitätsklinikum Hamburg-Eppendorf for performing the MRI scan, and Frau Angelika Sült-Wüpping the secretary of the Biology department for her help and her kindness.

This work was supported by the Deutsche Forschungsgemeinschaft.